A Comprehensive Study of Antiproliferative Effects of *Artemisia carvifolia* Buch against Liver Cancer

by

Sabahat Javid

A dissertation submitted in partial fulfillment for the degree of Doctor of Philosophy

in the

Faculty of Health and Life Sciences

Department of Bioinformatics and Biosciences

2024

A Comprehensive Study of Antiproliferative Effects of *Artemisia carvifolia* Buch against Liver Cancer

By

Sabahat Javid

(DBS211004)

Dr. Mercedes Bonfill Baldrich, Professor

The University of Barcelona, Catalonia, Spain

(Foreign Evaluator 1)

Dr. Sultan Mehtap, Associate Professor

Üsküdar University, Üsküdar, Istanbul, Türkiye

(Foreign Evaluator 2)

Dr. Erum Dilshad

(Research Supervisor)

Dr. Syeda Marriam Bakhtiar

(Head, Department of Bioinformatics and Biosciences)

Dr. Sahar Fazal

(Dean, Faculty of Health and Life Sciences)

DEPARTMENT OF BIOINFORMATICS AND BIOSCIENCES

CAPITAL UNIVERSITY OF SCIENCE AND TECHNOLOGY

ISLAMABAD

2024

Copyright © 2024 by Sabahat Javid

Dedicated to my beloved parents

who sacrifice their comfort for my PhD

CERTIFICATE OF APPROVAL

This is to certify that the research work presented in the dissertation, entitled "**A Comprehensive Study of Antiproliferative Effects of *Artemisia carvifolia* Buch against Liver Cancer**" was conducted under the supervision of **Dr. Erum Dilshad**. No part of this dissertation has been submitted anywhere else for any other degree. This dissertation is submitted to the **Department of Bioinformatics & Biosciences, Capital University of Science and Technology** in partial fulfillment of the requirements for the degree of Doctor of Philosophy in the field of **Biosciences**. The open defence of the dissertation was conducted on **November 04, 2024.**

Student Name :   Sabahat Javid (DBS211004)

The Examination Committee unanimously agrees to award PhD degree in the mentioned field.

Examination Committee :

(a)   External Examiner 1:   Dr. Muhammad Sheeraz Ahmad
                               Associate Professor
                               PMAS-AAU, Rawalpindi

(b)   External Examiner 2:   Dr. Nosheen Akhtar
                               Associate Professor
                               NUMS, Islamabad

(c)   Internal Examiner :   Dr. Sohail Ahmed Jan
                               Associate Professor
                               CUST, Islamabad

Supervisor Name :   Dr. Erum Dilshad
                              Associate Professor
                              CUST, Islamabad

Name of HoD :   Syeda Marriam Bakhtiar
                              Associate Professor
                              CUST, Islamabad

Name of Dean :   Dr. Sahar Fazal
                              Professor
                              CUST, Islamabad

AUTHOR'S DECLARATION

I, **Sabahat Javid** (Registration No. **DBS211004)**, hereby state that my dissertation titled, '**A Comprehensive Study of Antiproliferative Effects of *Artemisia carvifolia* Buch against Liver Cancer**' is my own work and has not been submitted previously by me for taking any degree from Capital University of Science and Technology, Islamabad or anywhere else in the country/ world.

At any time, if my statement is found to be incorrect even after my graduation, the University has the right to withdraw my PhD Degree.

(Sabahat Javid)

Dated: **04** November, 2024

Registration No : DBS211004

PLAGIARISM UNDERTAKING

I solemnly declare that research work presented in the dissertation titled "**A Comprehensive Study of Antiproliferative Effects of *Artemisia carvifolia* Buch against Liver Cancer**" is solely my research work with no significant contribution from any other person. Small contribution/ help wherever taken has been duly acknowledged and that complete dissertation has been written by me.

I understand the zero-tolerance policy of the HEC and Capital University of Science and Technology towards plagiarism. Therefore, I as an author of the above titled dissertation declare that no portion of my dissertation has been plagiarized and any material used as reference is properly referred/ cited.

I undertake that if I am found guilty of any formal plagiarism in the above titled dissertation even after award of PhD Degree, the University reserves the right to withdraw/ revoke my PhD degree and that HEC and the University have the right to publish my name on the HEC/ University Website on which names of students are placed who submitted plagiarized dissertation.

(Sabahat Javid)

Dated: 04 November, 2024   Registration No : DBS211004

List of Publications

It is certified that following publication(s) have been made out of the research work that has been carried out for this dissertation:-

1. Sabahat Javid and Erum Dilshad (2023). *Artemisia carvifolia* Buch silver nanoparticles downregulate the Rap2A gene in liver cancer. *Scientific Reports*. 13(1): p. 21553.

(Sabahat Javid)

DBS211004

Acknowledgement

All acclamations are for **Allah Almighty**, who bestowed mankind with knowledge and wisdom. All the respect and honors to **Hazrat Mohammad Sallallah-o-Alai-e-Wasallam**, a star brightening the path of faith and knowledge. Who enabled us to recognize our creator and declared it to be the obligatory duty of every Muslim to acquire knowledge.

I owe my deep thanks to the kind and soft-hearted, my respectable supervisor **Dr. Erum Dilshad** Associate Professor, Department of Bioinformatics and Biosciences, CUST Islamabad for her continuous support during my research work. Her wide knowledge and logical way of thinking have provided a strong foundation for my PhD research work. Her understanding, encouragement, and guidance have been of great value to me. I would like to thank **Dr. Erum Dilshad** for her considerable effort and patience with my endless questions. I am grateful for her time and patience.

I also express my special thanks to the **Capital University of Science and Technology Islamabad** for providing me with a platform for my PhD work. Moreover, I would like to say thanks to **Dr. Sahar Fazal**, Dean Faculty of Health and Life Sciences, **Dr. Marriam Bakhtiar** HoD, Department of Bioinformatics and Biosciences, FHLS CUST Islamabad and **Dr. Sohail Ahmad Jan**, Associate Professor, BI & Biosciences, CUST for their throughout support during my research work.

Besides, I would like to thank **Mr. Muhammad Maaz** for his assistance in computational work. Apart from that, I would like to say thanks to my brothers **Muhammad Arslan Javid Choudhary** and **Muhammad Faizan Javid Choudhry** who supported me during this tough time. Furthermore, I would like to especially thank my younger brother **Muhammad Faizan Javid** from the start to end of my PhD for his most accountable support. I also pay gratitude to my respected parents who supported me and sacrificed their comforts for my PhD.

(Sabahat Javid)

Abstract

Cancer is the main reason of death worldwide and liver cancer is the second main reason of death globally. In Pakistan, liver cancer is increasing and may become the most widespread tumor in adult men. In the current study, the *Rap2A* gene a member of Ras Gtpase was selected as a drug target for liver cancer which has been identified as an oncogene in different types of tumors. Medicinal plants play a useful part in the treatment of cancers and other illnesses. Artemisia species have efficient therapeutic implications which can be enhanced by nanotechnology applications against various diseases including cancer. The current research was aimed to evaluate *Artemisia carvifolia* Buch extract and its Ag Nps against liver cancer targeting the *Rap2A* gene. For this purpose, the plant was identified by DNA barcoding through sequencing of the *psbA-trnH* region of chloroplast DNA. Synthesis of nanoparticles and characterization was done by adopting a green chemistry approach and already established techniques. Synthesized nanoparticles showed an absorbance peak at 450 nm by UV-Vis spectrometer. SEM showed that polyhedral AgNps had a size ranging from 80± 6nm. By fourier-transform infrared spectroscopy amines, aldehydes, ketones, and alcohols of *A. carvifolia* Buch were found to be involved in the reduction and stabilization of nanoparticles. Moreover, X-ray diffraction and energy dispersive X-ray spectroscopy confirmed the cubic crystalline nature and nanoparticle's elemental composition, respectively. Furthermore, the cytotoxicity against HePG2 cancer cell lines was also found significant with an IC50 value of 2.57 μM for silver nanoparticles and 11.57 μM for plant extract. The gene expression and protein level of Rap2A were also decreased in plant extract and nanoparticle-treated cells compared to control groups. The apoptotic potential of extract and nanoparticles was also determined by evaluating the apoptotic pathway genes and protein including Bax, caspase 3, caspase 8 and caspase 9. Significantly elevated levels of expression of these genes by real-time qPCR along with increased protein levels by ELISA were found. Furthermore, in this work, *A. carvifolia* Buch bioactive compounds specifically polyphenols were identified through HPLC-DAD analysis and then subjected to evaluation of their anticancer potential through molecular docking and molecular dynamic simulations,

against Rap2A protein to discover their potential as novel drug candidates and drug targets for liver cancer. In this work, all the interaction visualization analysis studies were performed via PyMol and LIGPLOT+. In total 9 polyphenols including ferulic acid, apigenin, caffeic acid, syringic acid, rutin, gallic acid, vanillic acid, rhamnetin and quercetin were identified in the extract of *A. carvifolia* Buch. Four lead compounds including apigenin, caffeic acid, gallic acid and rhamnetin were selected out of 9 identified compounds based on the best vina score, cavity size, and grid map score, and were subjected to molecular docking, MD simulations, drug likeliness studies by ADMET properties and Lipinski 's rule of five. Comparison with the standard drug lenvatinib was made for all the studied parameters and apigenin was identified as the best compound with the best docking score, RMSD and RMSF values, and ADMET properties. In this work, the model quality of the *Rap2A* protein was also evaluated via a Swiss model structure assessment server by Ramachandran plot analysis. QMEAN, an online server was used to analyze the quantitative model energy of the protein structure and the quality of *Rap2A* protein. The ProSA program calculated the overall quality of the protein structure and also identified the identification method of the protein structure.

To the best of our knowledge, there is no report is available describing the synthesis and efficacy of silver nanoparticles of *A. carvifolia* Buch against liver cancer and screening of *A. carvifolia* Buch compounds against the *Rap2A* gene concerning liver cancer. However, further clinical trials should be done to introduce apigenin as a potential anticancer drug and the *Rap2A* gene as a potential drug target for liver cancer.

Keywords: *Artemisia carvifolia buch*, Anti-cancer properties, apoptotic gene, liver cancer, Rap2A gene, Sliver nanoparticles, molecular docking, molecular dynamics stimulation.

Contents

List of Figures

List of Tables

Abbreviations

ADMET	Absorption, distribution, Metabolism, excretion, toxicity
AgNPS	Sliver nano particles
APAF-1	apoptotic protease activating factor-1
BCLC	Barcelona Clinic Liver Cancer
CADD	Computer-Aided Drug Design
CT	Computed tomography
CTAB	Cetyltri methyl ammonium bromide
DNA	Deoxyribonucleic acid
ELISA	Enzyme linked immunosorbent assay
FDA	Food drug administration
FTIR	Fourier Transform infrared Spectroscopy
GEFs	Guanine nucleotide exchange factors
HCC	Hepatocellular carcinoma
HPLC	High performance liquid chromatography
MD	Molecular dynamics
MMP-2	Matrix Metalloproteinase-2
MMP-9	Matrix Metalloproteinase-9
mTOR	Mammalian target of rapamycine
MTT	3-(4,5-dimethylthiazol-2-yl)-2,5-diphenyltetrazolium bromide
NASH	Non alcoholic steato hepatitis
PCR	Polymerase chain reaction
PDB	Protein data bank
PKCSM	Small molecule pharmacokinetics prediction
Pro-SA	Protein structure analysis

QMEAN   Qualitative model Energy Analysis

Rap2A   Receptor associated proten

RMSD   Root mean square deviation

RMSF   Root mean square fluctuation

SDR   Spinning disc reactor

SE   Stranded error

SEM   Scanning Electron Microscopy

TNF   Tumor necrosis factor

UV-vis   Ultra Violet Visible Spectroscopy

VEGF   Vascular endothelial growth factor

WHO   World health organization

XRD   X-ray Diffraction

Symbols

$>$	greater than
$<$	Smaller than
$=$	Equal
%	Percentage
cm	Centimeter
α, β and γ	Alpha ,Beta ,Gamma
$\circ$C	Centigrade
Υ	psi
ϕ	phi
:	Ratio

Chapter 1

Introduction

Cancer is a global threat to human lives that occurs due to the uncontrolled growth of abnormally organized tissues [1]. Recently, based on the reported data, the number of newly diagnosed cancer cases reached more than 19 million, which led to 10 million deaths in 2020 [2]. Hepatocellular carcinoma (HCC) is the most common type of primary liver cancer which is the 6th foremost cancer in prevalence and the 4th most common cause of cancer-related deaths globally [3]. There are many causes of hepatocellular carcinoma, including chronic liver disease, HBV and HCV infection, and nonalcoholic steatohepatitis [4]. In Pakistan, there is generally little awareness of the risk factors of hepatocellular carcinoma and the occurrence of hepatitis cancer has risen. Furthermore, less frequent risk factors have also been increased. The vast majority of patients have complex HCC and are ineligible for the best cure. The main perilous etiological factors for this type of cancer are infections through HCV and HBV and continual drug usage in the past. Although fatness, use of cigarettes, sugar, and overloading of iron are also the reasons that are involved in causing liver cancer. HCC is more common in males in comparison to females with a ratio of 2.4:1 having more cases in Eastern and Southern Asia, Middle and Western Africa, Melanesia and Micronesia/Polynesia [5].

Persistent liver cancer and cirrhosis are the very imperative risk factors for the growth of hepatocellular carcinoma of which viral hepatitis and more alcohol use are the main threat factors globally. Worldwide, the major reasons for persistent

hepatitis are HBV and HCV. HBV is a double-stranded rounded deoxyribonucleic acid molecule with 8 genotypes A to H. A and D are very common in Europe and the Middle East although B and C genotypes are very common in Asia [6]. HBV is spreading through infected blood exchange, intravenous syringing and sexual relations. Direct spreading from mother to baby is the most important reason for hepatitis B illness globally by which 5% of people are affected globally. Numerous epidemiological researches have confirmed major hepatic carcinogenicity with chronic hepatitis B disease. HBV patients have 10% to 25% lifetime chances of rising hepatocellular carcinoma. Various infections with hepatitis B having an autonomous risk of hepatocellular carcinoma were found to be linked with a 2.5 to 3 times higher threat of developing hepatocellular carcinoma [7]. The usage of HBV immunization has resulted in a major decrease in the occurrence of hepatocellular carcinoma from hepatitis B. The East Asian infant immunization agenda is anticipated to result in a 70% to 85% decline in the number of HBVs associated with hepatocellular carcinoma. Despite perinatal vaccination, 5% to 10% of neonates stay at risk of acquiring HBV infectivity. The usage of nucleoside analogues in curing chronic HBV-infected women in their third trimester of pregnancy has confirmed the dominance of immunization only in preventing the spreading in the infant. Various cellular methods like deregulations of the cell cycle, programmed cell death and molecular pathways related to inflammation and fibrogenesis are implicated in the progression of liver cancer. Sorafenib is the first treatment for sophisticated hepatocellular carcinoma which is a multi-kinase inhibitor accepted for the cure of liver cancer, but not yet able to work against the cancer progression because of lack of advancement of fighting to anti-proliferative therapies [8]. So, it is necessary to design novel drug molecules with pharmacological usefulness and protection from side effects.

Numerous possible biomarkers have been identified by the latest development of high throughput sequencing data for determining the prognosis of patients [9]. Rap proteins belonging to the Ras GTPase binding family share 50 to 60 % sequence similarity with RAS protein. The variety and accuracy of both proteins are determined through various parts of GEFs and GAP. In human genes, five special genes of the Rap family such as Rap (1A, 1B, 2A, 2B, and 2C have been

recognized. Rap proteins mainly play a role in cell adhesion, movement, and polarity. The result of Rap gene commencement relies on the context-precise contact of this gene with its monitors and downstream effectors in the cell/matrix [10]. The cancerous role of the Rap gene has been fine recognized in various forms of tumors for instance breast, lung, ovary stomach, cervix, prostate, and brain tumors [11]. Estimated indication advocates that Rap proteins also take part in serious functions in HCC and cancer development. Single nucleotide polymorphism in the Rap1A gene (rs494453) has been represented to be linked among high occurrence and reappearance after transplantation of the liver. More advanced action of the NF-κB/RAP1 signaling channel is linked to tumorigenicity in hepatocellular carcinoma [12].

Few works have also presented powerful associations between Rap1A appearance and liver swelling as a perilous feature for cancer of the liver. For Rap1A and RapGEF1 the GEF has also been presented to be more expressed in hepatocellular carcinoma. Prior research described that hepatitis B virus multiplication causes liver cancer by upregulation of Rap1B. High expression of Rap1B increases the production and movement of hepatocellular carcinoma cells by variable Twist-1 gene appearance [13]. Overexpression of Rap2B has also been depicted in hepatocellular carcinoma and its reticence diminishes cell explosion and expropriation. It is reported currently that hepatocellular carcinoma tissues show considerably high *Rap2A* protein levels that are linked with cancer size, metastasis, pathological separation, and vascular incursion [14].

The curative perspective of plants may be searched back more than 5000 times since there is confirmation of plant exploitation for the healing of illness and for stimulating body functions in Indian, Egyptian, Chinese, Greek, and Roman cultures. In India, plants of curative perspective are extensively used by every part of citizens together like folk remedies in various aboriginal organizations of drugs like Siddha, Ayurveda, and Unani and like product progression of the pharmaceutical industry [15]. Medicinal Plants are one of the valuable and great sources for the well-being of individuals and populations. The therapeutic significance of plants lies in a few chemically active materials that have a definite physiological effect on

human health. There are different plants that are considered a wealthy resource of bioactive chemicals and they may be another cause of disease managing agents. SMs or phytochemicals that are derived from plants have famous pharmacological actions for example anti-oxidative, anti-allergic, antibiotic, hypoglycaemic and anti-carcinogenic. These SMs defend the cells from the harmful effects caused by the imbalance of molecules identified as free radicals [16].

The genus *Artemisia* L. belonging to the Asteraceae family exhibits efficient therapeutic implications. Plants of this group are frequently found in the moderate sectors of the northern hemisphere with an inadequate number of species in the southern hemisphere of the globe. It contains approximately 500 species of both herbs and shrubs and is a different genus of the Anthemideae tribe. The financial significance of numerous plants of *Artemisia* species is because of their consumption as aesthetics, feedstuff, fodder, therapeutics, and soil binder, although, some species are allergic and toxic weeds. The artemisia genus is reported to have medicinal properties including antioxidant, anti-inflammatory, antimicrobial, and numerous anti-cancer compounds present in it [17]. *Artemisia carvifolia* Buch has been reported to have antidiabetic, antimalarial, and anticancer properties. It has also been reported to have phytoconstituents including flavonoids, artemisinin and derivatives with anticancer properties [18–20].

Nanotechnology is one of the newest scientific achievements leading to rising industries with public and financial interest. This felid is a modern form of material manufacturing by handling and operating material structures on a nanoscale efficiently [21]. The major purpose of most nanoscience studies is to manufacture novel resources or to formulate accessible materials. The manufacturing of Nps which has broad functions in various scientific areas is a major purpose of nanoscience. The nanoparticle preparation and self-assembly may be considered like very major principles of nanotechnology and their associated study. In the NPs, silver, zinc and IO NPs are marvelous scientific successes in nanotechnology and consist of broad functions in various sciences. Now these are the main topics of various current research projects in the area of nanoscience and nanotechnology. Metallic

nanoparticles have been broadly used in medicine delivery systems, magnetic targeting, hyperthermia cancer therapy, thermal ablation, stem cell sorting technology and manipulation, gene therapy, negative magnetic resonance imaging contrast enhancement, food-related applications bioprocess, intensification, antimicrobial agents, tissue repair engineering and bioseparation [22].

The strategies of Computer-Aided Drug Design (CADD) are now considered vital gears in recent drug discovery and advancements. Nowadays, apart from academia, industrial companies including pharmaceutical and biotechnology are using these tools for the discovery of novel drug molecules. Numerous medicines or drugs have been discovered using this technology technologies in different phases including Aliskiren, Boceprevir, Captopril, Dorzolamide, Nolatrexed, Oseltamivir, Rupintrivir, Saquinavir and Zanamivir [23].

The structural properties of various macromolecules and compounds under study are determined by using different algorithms. On the other hand, interactions of nuclei of the compounds with the electrons of macromolecules or drug targets are studied in small systems based on quantum mechanics calculations. In most of the cases, an amalgamation of numerous techniques is used and methods are recurrently accustomed for diverse drug design projects [24].

1.1 Gap Analysis

- Absence of prior studies on *A. carvifolia* Buch extract's evaluation against liver cancer targeting the *Rap2A* gene.

- Restricted knowledge of the *A. carvifolia* Buch extract's apoptotic role in cancer prevention.

- Lack of studies on the preparation and evaluation of silver nanoparticles of *A. carvifolia* Buch extract.

- Uncertainty concerning ideal conditions for the preparation of silver nanoparticles of *A. carvifolia* Buch.

- Limited knowledge about the detection and quantification of flavonoids of *A. carvifolia* Buch.

- Absence of prior studies on the computational analysis of metabolites especially flavonoids detected in the extract of *A. carvifolia* Buch.

1.2 Problem Statement

Cancer has been set as a main global threat to mankind by the World Health Organization due to high death and high incidence rates and low cure. The are available therapies like chemotherapy, radiotherapy immunotherapy and hormonal therapy but they have various side effects and there is a problem of developing drug resistance which is being faced by cancer patients against available drugs.

1.3 Research Questions

Research Question 1

What impact does *A. carvifolia* has as an anticancer agent against liver cancer cells?

Research Question 2

Does the silver nanoparticles of *A. carvifolia* are more effective than the respective plant extract?

Research Question 3

Does the *Rap2A* gene has an antiproliferative role in the liver cancer cells?

Research Question 4

Does the downregulation of *Rap2A* is linked with the upregulation of apoptotic pathway genes and proteins?

Research Question 5

Which metabolites (flavonoids) of *A. carvifolia* are effective in targeting *Rap2A* protein when checked computationally?

1.4   Research Objectives

The objectives of this research include

Research Objective 1

To identify the anti-proliferative role of *A. carvifolia* Buch plant extract and its respective metallic (Ag) nanoparticles against liver cancer cell lines and their impact on the expression of liver cancer target gene, apoptotic pathway genes and protein.

Research Objective 2

To identify and analyze the role of bioactive compounds of *A. carvifolia* Buch against liver cancer target gene through computational approaches and to perform molecular dynamics simulation against selected ligands.

1.5   Scope and Significance

It is important to tremendously develop targeted therapies as a possible treatment for hepatocellular carcinoma and other liver diseases by targeting diverse members of the Rap subfamily like receptor-associated proteins 1 and 2 as in the liver context they may have different results. However, Rap has not yet been inhibited specifically or selectively. Only pan inhibitors which target small GTPases or indirect strategies using inhibitors of GEF or GAP activators are available. However, due to their nonspecific effects, none of these techniques are suitable for the treatment of patients. In reality, the same factor that prevented the development of particular Rap inhibitors also prevented its success due to the lack of specificity of the compounds. The current study would serve the purpose of the detection of the inhibitory compounds against receptor associated protein (*Rap2A*) that could be useful in drug development and improvements to fight the challenges of liver cancer. The present research work focuses on the evaluation of *A. carvifolia* Buch plant extract against liver cancer by anti-proliferative assays and computational approaches. It also involves the preparation of metallic nanoparticles (AgNPs) of *A. carvifolia* Buch plant extract along with their characterization in order to focus on identifying their inhibitory role against liver cancer.

1.6 Applications and Innovations

The current study emphasizes unveiling the natural anti-cancer mechanisms in liver cancer cell line HepG2 after treatment with a plant extract and respective metallic nanoparticles. As a long-term goal, the identification of natural bioactive compounds for the management and cure of liver cancer might help to pave the way for the development of novel diagnostics or treatment strategies against liver cancer with the following outcomes.

- Anti-cancerous potential of *A. carvifolia* Buch and its metallic nanoparticles against liver cancer.

- Gene targets of metallic nanoparticles.

- New possible inhibitor for Rap gene signaling cascade.

- Finding new cancer biomarkers in human liver cancer.

The pharmaceutical industry and health care sector can be the possible end user, depending upon the positive outcome of our proposed hypothesis. Current research can help in finding a possible biomarker for liver cancer diagnosis and treatment as well as lead towards clinical trials.

Chapter 2

Literature Review

Hepatocellular carcinoma is the sixth most widespread liver cancer globally, attributing to 6 % of new cancer cases per annum. It is also the third most prevalent reason for cancer-related deaths globally with a general existence ratio of only 3-5 %. The main load of hepatocellular carcinoma lies in developing countries where more than 8 % of hepatocellular carcinoma cases are identified as well as 35 % from China alone. However, comparatively higher prevalence rates are there in Sub-Saharan Africa and Southeast Asia. The occurrence of hepatitis B and C is intermediate in South Asia where Pakistan is situated. Considering the load of hepatitis B and hepatitis C, it is anticipated that the prevalence of hepatocellular carcinoma will rise more in the future, particularly in China and Taiwan. Therefore, hepatocellular carcinoma will be the main load on their healthcare organizations [25]. The worldwide impact of liver cancer is significant. Liver cancer occurrence and death ratio have declined in certain Eastern Asian nations including Japan, and the Republic of Korea while death and occurrence ratio have increased in several earlier low-incidence countries throughout the globe as well as the United States, Australia and numerous European countries. According to the World Health Organization, about 905,677 new cases of liver cancer were diagnosed in 2020 and about 830,180 people died of liver cancer in the world [26].

Hepatocellular carcinoma progression outcomes from the contact of ecological and hereditary features. Hepatitis B and C infection, liver cirrhosis, consumption

of more alcohol, B1 aflatoxins use and nonalcoholic steatohepatitis are all risk factors for hepatocellular carcinoma progression. Patients' survival expectation with hepatocellular carcinoma relies on the phase of the tumor at analysis. In the higher phase, a few months are anticipated though if the analysis is done before time and an efficient cure is carried out [7].

At the initial point of hepatocellular carcinoma therapeutic cures like surgical resection transplantation of liver and local ablation can recover the existence of the patients. So, over time recognition with sufficient treatments is vital to enhance existence as well as to recover the existence value of hepatocellular carcinoma patients. When grouped like phase C (higher stage) by the occurrence or deficiency of vascular invasion and the conserved liver role, the employ of sorafenib has been efficient in recovering these patients' life span [8].

2.1 Risk Factors and Epidemiology

There are some recognized reasons for hepatocellular carcinoma which include consumption of alcohol, chronic infection along hepatitis B and C, NASH and liver cirrhosis (Figure 2.1).
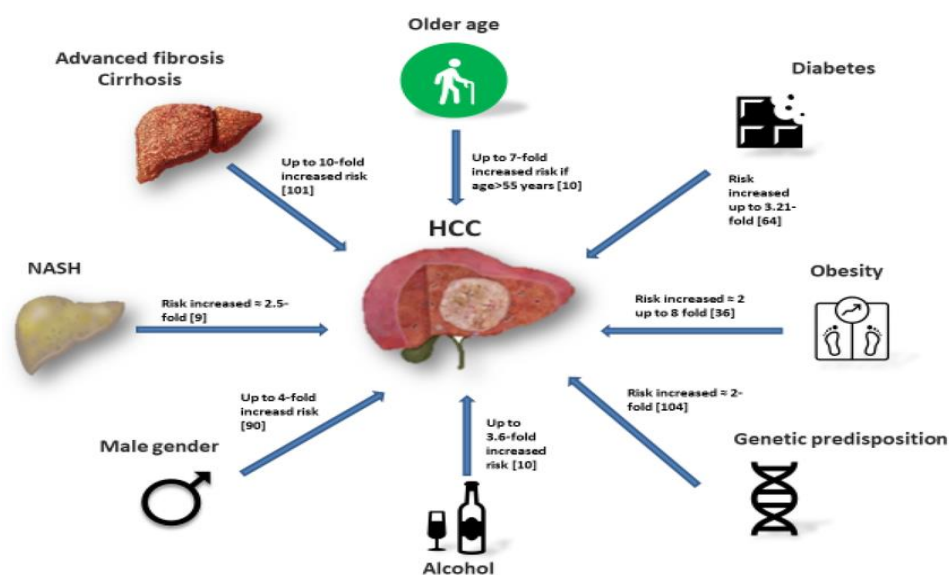
FIGURE 2.1: Some of the major risk factors of hepatocellular carcinoma [27]

There are ample facts of links between sugar and obesity to hepatocellular carcinoma. More factors include the use of cigarettes, sugar, overloading of iron which are also the reasons that are involved for causing liver cancer. Hepatocellular carcinoma is more common in males as comparison to females with 2.4:1 having more cases in Eastern and Southern Asia, Middle and Western Africa, Melanesia and Micronesia/Polynesia [28].

Persistent liver cancer and cirrhosis are the very imperative peril reason for the growth of hepatocellular carcinoma of which viral hepatitis and more alcohol uses are main threat factors globally. Persistent viral hepatitis may be reason of cirrhosis or hepatocellular carcinoma. Worldwide, the major reason of persistent hepatitis is hepatitis B and hepatitis C [29]. Hepatitis B virus is a double-stranded rounded deoxyribonucleic acid molecule with 8 genotypes A to H. A and D are very common in Europe and the Middle East although B and C genotypes are very common in Asia. Numerous epidemiological researches have confirmed major hepatic carcinogenicity with chronic Hepatitis B and C disease [30]. The information about people with increased risk of HCC is given in Table 2.1.

TABLE 2.1: Risk factors for HCC patients [31]

Population Group	Incidence Threshold (>0.25 LYG; % per year)	HCC Incidence
Surveillance benefit		
Asian male hepatitis B carriers over age 40	0.2	0.4%-0.6% per year
Asian female hepatitis B carriers over age 50	0.2	0.3%-0.6% per year
Hepatitis B carrier with a family history of HCC	0.2	Incidence is higher than without a family history
African and/or North American blacks with hepatitis B	0.2	HCC occurs at a younger age

TABLE 2.1: Risk factors for HCC patients [31]

Population Group	Incidence Threshold (>0.25 LYG; % per year)	HCC Incidence
Hepatitis B carriers with cirrhosis	0.2-1.5	3%-8% per year
Hepatitis C cirrhosis	1.5	3%-5% per year
Stage 4 PBC	1.5	3%-5% per year
Genetic hemochromatosis and cirrhosis	1.5	Unknown, but probably >1.5% per year
Alpha-1 antitrypsin deficiency and cirrhosis	1.5	Unknown, but probably >1.5% per year
Other cirrhosis	1.5	Unknown
Surveillance benefit uncertain		
Hepatitis B carriers younger than 40 (males) or 50 (females)	0.2	<0.2% per year
Hepatitis C and stage 3 fibrosis	1.5	<1.5% per year
NAFLD without cirrhosis	1.5	<1.5% per year

Furthermore, cholaginocarcinoma a lethal neoplasm of the biliary duct system estimated for 3% of gastrointestinal cancer is the second major widespread primary hepatic tumor representing 10 % to 25 % of primary hepatic malignancies globally. Cholangiocarcinoma usually does not often take place prior to the age of 40, but the usual age of appearance is the seventh decade of life. Males have a higher number of cholanginocarcinoma than do females with ratios of 1:1.2-1.5. The occurrence of cholanginocarcinoma change significantly by geographic regions, which is secondary to variations in risk factors. The prognosis of cholangiocarcinoma is reduced so mortality and incidence rates are the same. Though there are recognized risk factors for the growth of cholaginocarcinoma, the majority of patients do not have a particular peril aside from age [32].

The carcinogenesis of HCC is frequently linked with cirrhosis of the liver resulting from chronic diseases of the liver like chronic HBV or HCV and auto-resistant hepatitis. More risk factors include extreme use of alcohol, Nonalcoholic steatohepatitis, non-alcoholic fatty liver disease, contact and intake of aflatoxin, diabetes mellitus, tobacco, and sporadically hereditary ailments such as alpha-1 antitrypsin deficiency hemochromatosis, tyrosinemia, porphyria and Wilsons disease [28].

2.2   Prevalence in Pakistan

According to published data, the stranded ratio of hepatocellular carcinoma in Pakistan is 7.6 % annually for men and 2.8 % for women. Such findings are consisting of hospital-based information and cannot accurately reflect the real population based occurrence of hepatocellular carcinoma in recent years [5]. National records of cancer statistics for cancer cases are generally derived from single center experiences or fragmented regional registries. Up to 58% of patients have hepatitis C which is considered to be the most frequent cause, while there are 25.3% reported cases of hepatitis B. Outcomes from larger studies numbers greater than or equal to 100 on hepatocellular carcinoma are differing, where anti-hepatitis C virus antibody positivity range from 24 to 72.5 % while hepatitis C surface antigen positivity varies among 13.1 to 51 %. If we analyze molecular evolution it suggests that the hepatitis C virus IIIa formed a well-defined phylogenetic cluster in the Pakistan region around the 1920s which was then quickly amplified in the 1950s. As a result, Pakistan experienced a pandemic increase of the HCV IIIa very high than other nations. Here, 66 % of the population exists in villages, where illiteracy, unscreened blood products, and injectable drug abuse are all perilous reasons for the occurrence of the hepatitis C virus [5].

This disease has been investigated in nations such as Pakistan, Zimbabwe, Colombia and Costa Rica but it is presently changing. The prevalence of this illness is growing in Pakistan which correlates with increased exposure to peril factors for hepatocellular carcinoma in this community. According to recent findings, hepatobiliary malignancies can arise in mature men in this population. A total

of 233 cases were reported among males and 382 cases among females. Recently a study was conducted estimating the occurrence of different types of cancers in the population of Islamabad Pakistan. Prostate cancer (9.9%) was found to be the most prevalent cancer among males followed by liver cancer (7.7%), oral cavity cancer (7.7%), colorectal cancer (7.3%), and lung cancer (5.3%) (Figure 2.2). Among females in Islamabad, breast cancer was the most prevalent (46.3%), followed by uterine cancer (9.4%), ovarian cancer (7.1%), colorectal cancer (5.5%), and less than 5.0%, with other types of cancer [33].
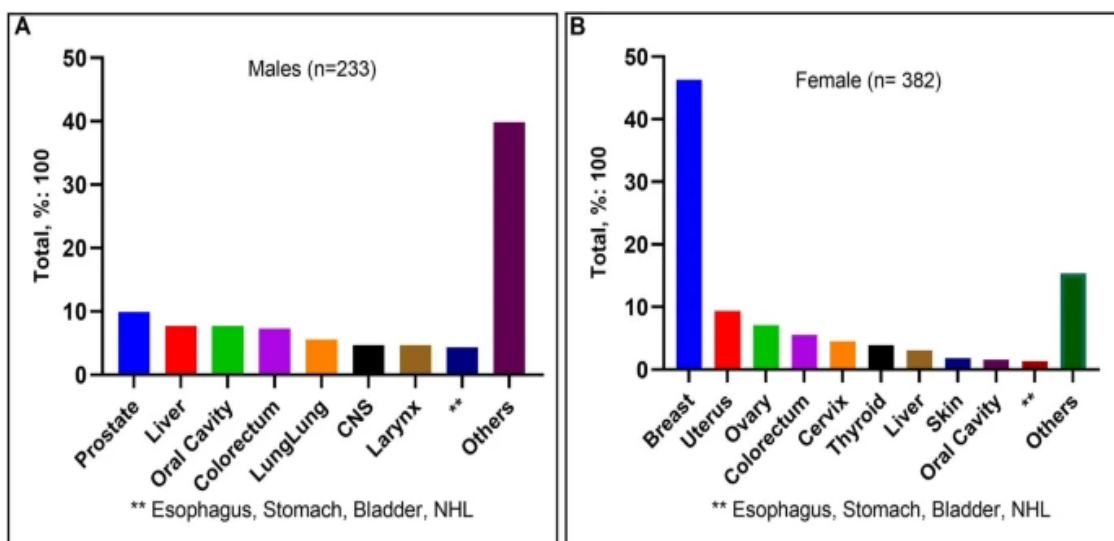
FIGURE 2.2: Prevalence of different cancers including HCC in Islamabad [33]

2.3 Screening of HCC

It is highly recommended to perform regular screening tests in patients with liver cirrhosis if they would benefit from an early tumor diagnosis (Figure 2.3). The median subclinical time for hepatocellular cancer is three years and two months. At such time screening has the greatest impact in terms of early diagnosis and cancers as small as 1.6 ± 0.6 centimeters can be identified by ultrasound. While ultrasound has a sensitivity and specificity of more than 90% for identifying hepatocellular cancer, its sensitivity and specificity are decreased in liver cirrhosis. Its output is heavily reliant on the competence of the ultra-sonographer. Regional standards for hepatocellular carcinoma viewing and diagnosis differ significantly. The usage of

serum AFP is advised for routine viewing because of its little expense and increased specificity for every initial stage of liver cancer diagnosis. The Asian Oncology Summit advises the US with serum AFP three to six times each year. Due to the high occurrence of risk factors of hepatitis B, C and HCC in Asia, the criteria are least restrictive. Moreover, AOS advises high risk individuals having an AFP level greater than 400 ng/mL to go for a diagnosis of hepatocellular carcinoma. The majority of people who have hepatocellular carcinoma risk factors for the disease do not get screened. Moreover, there has been an increase in non-hepatitis B and C hepatocellular cancer. The prevalence of diabetes, obesity and aflatoxin use is a rising factor [34]. Screening in the United States is frequently undertaken by unskilled sonographers. Cirrhosis complicates the interpretation of results. In Pakistan, less than 10% of individuals are identified with hepatocellular carcinoma during screening which may explain the late appearance and poor diagnosis in most hepatocellular carcinoma patients. The relationship between high alpha-fetoprotein levels and hepatocellular carcinoma diagnosis varies. Hepatocellular carcinoma may occur in 7.5% to 100% of individuals with elevated alpha-fetoprotein. This variation is mostly due to the different cut-offs used to indicate increased alpha-fetoprotein levels [35].
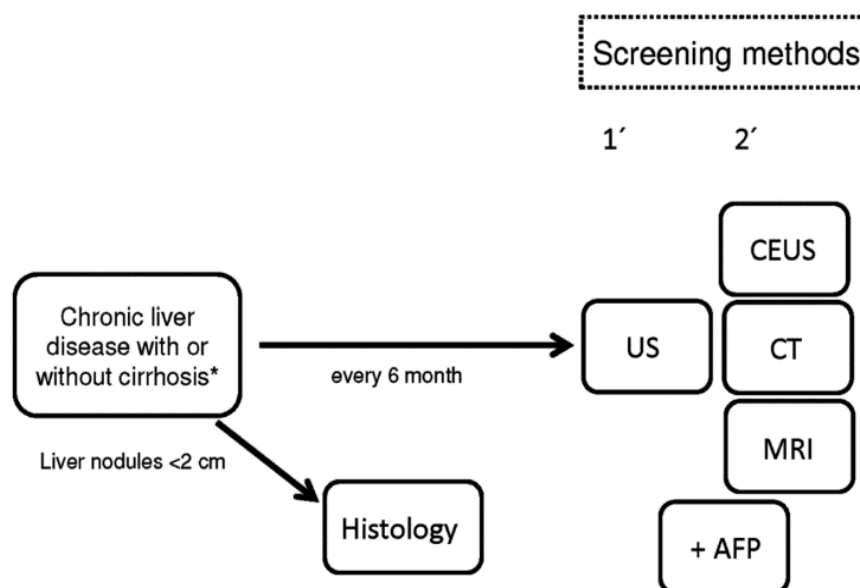
FIGURE 2.3: HCC screening tests. US=ultrasound, AFP= alpha-fetoprotein test, MRI= magnetic resonance imaging, CT=computed tomography, CEUS=Contrast Enhanced Ultrasound (CEUS) [36]

2.4   Diagnosis and Staging of HCC

In hepatocellular carcinoma, investigative criteria remain controversial. The usual features of Computed Tomography or Magnetic Resonance Imaging are sufficient for making an analysis for lesions larger than 1cm (Figure 2.4). If lesions smaller than 1 cm in size do not show characteristic enhancement of arties and venous washout on CT or MRI the NCCN and EASL-EORTC propose four to six monthly monitoring using US, CT or MRI. A biopsy is likely to change the course of treatment for lesions larger than 1 cm but with unusual imaging characteristics, it is advised [37].

In the Asian continent where, hepatocellular cancer is highly prevalent, and hepatitis B and C are common, proper surveillance is challenging and seems to be a better fit for the Adams Oliver syndrome criteria. More than 400 alpha-fetoproteins are also being researched for hepatocellular cancer. Patients with uncertain diagnoses should get a biopsy. According to a recent interpretation of the BRIDGE research, BCLC stage C remained the most prevalent stage at appearance for patients with hepatocellular carcinoma with the exception of Japan and Taiwan. National observation programs which are still missing in North America, Europe, and China, have begun in Japan and Taiwan [34].

Just 1.7 % of patients are identified on CT scan findings alone although different combinations of CT scan alpha-fetoprotein and histopathology are applied in 62 % of patients. Late appearance and complex cirrhosis in more patients are contributory. Since fewer than ten per cent of patients are selected for imaging. In Pakistan, patients mostly have more tumor which is greater than eight centimeters or equal to eight centimeters at the time of diagnosis. Tumors greater than five centimeters are seen in 44.3% of patients and at appearance fifty-two to sixty-two cases have greater than 1 tumor nodule. In addition, 46 to 87 % of patients have Child-Pugh stage B or C. Approximately, eighty six per cent of patients are related to Okuda class II or III and less than 15% of patients are willing to get any form of perfect cure [5].
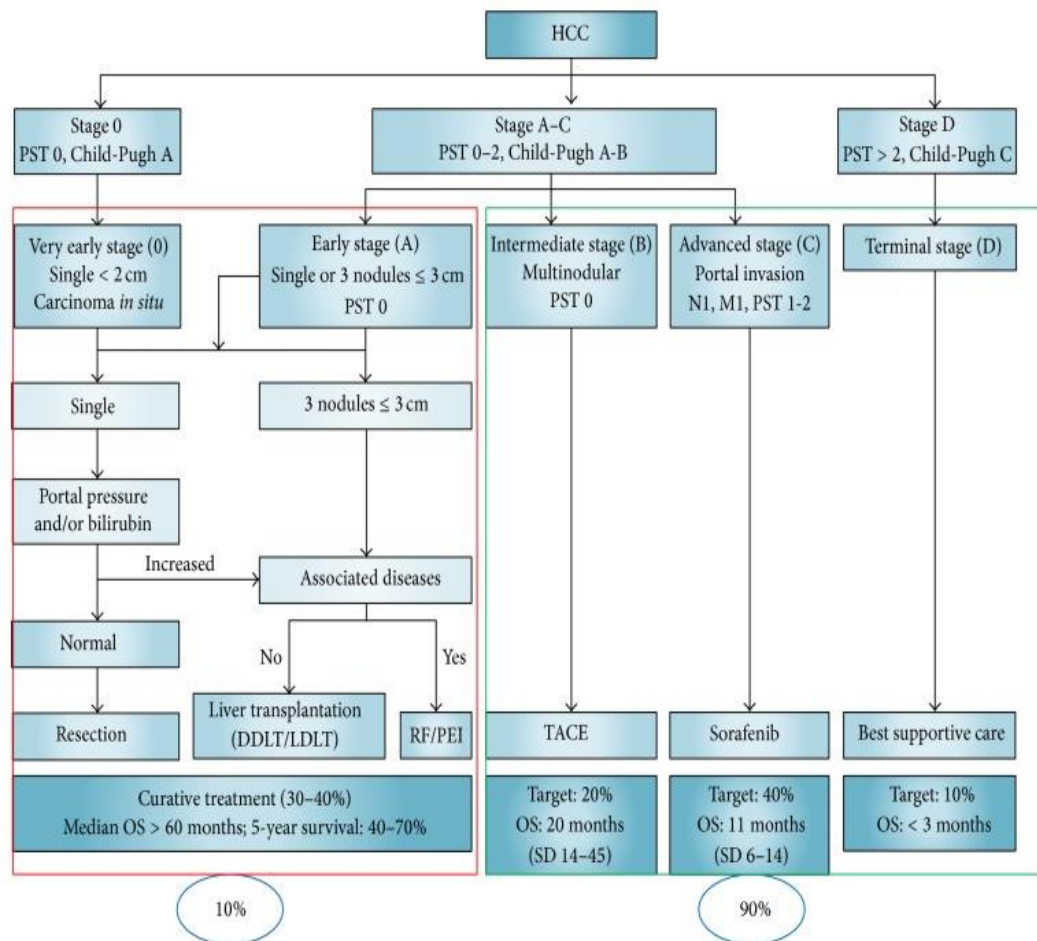
FIGURE 2.4: Different stages of hepatocellular carcinoma [5]

2.5 Treatment of HCC by Targeting VEGF Pathway

Hepatocellular carcinoma is the main vascular solid tumor identified and VEGF seems to be a prime mediator of new blood vessels in hepatocellular carcinoma. There are some treatments available for HCC (Figure 2.5) but angiogenesis inhibitor drugs like bevacizumab (which is a vascular endothelial growth factor antibody) and sorafenib participate to inhibit the vascular endothelial tyrosine kinase receptor (Figure 2.6). They have already expressed important clinical action in hepatocellular carcinoma and sorafenib is currently the Food Drug Administration accepted cure for patients with newly diagnosed hepatocellular carcinoma [38].
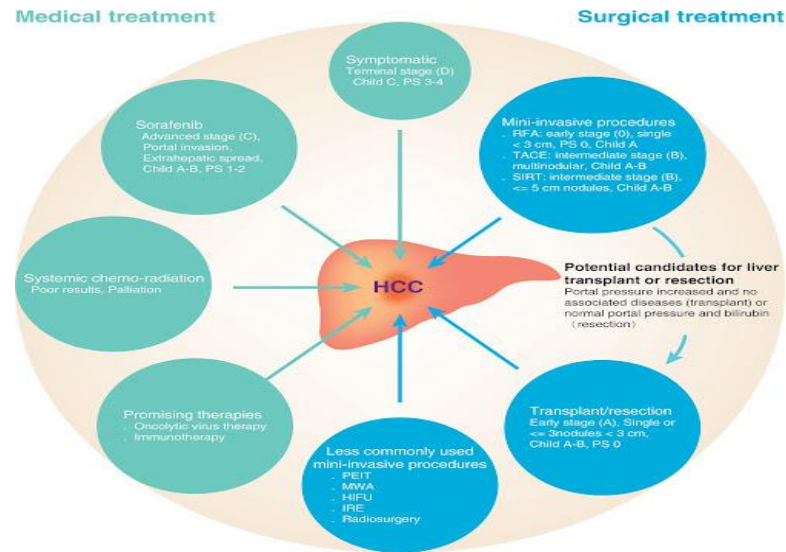
FIGURE 2.5: Available treatments of HCC [39]

Epidermal growth factor receptor action is also implicated in hepatocellular carcinoma carcinogenesis. The pathway of the Ras gene is activated by vascular endothelial growth factor/epidermal growth factor receptor. Ras pathway activation outcomes in the transcription of numerous genes in the activating protein-1familylike c-fos and c-jun. Activating protein-1 is a transcription factor complex considered to be intricated in the wicked change of cells with activation of other cancers, especially those in the Ras pathway [40].
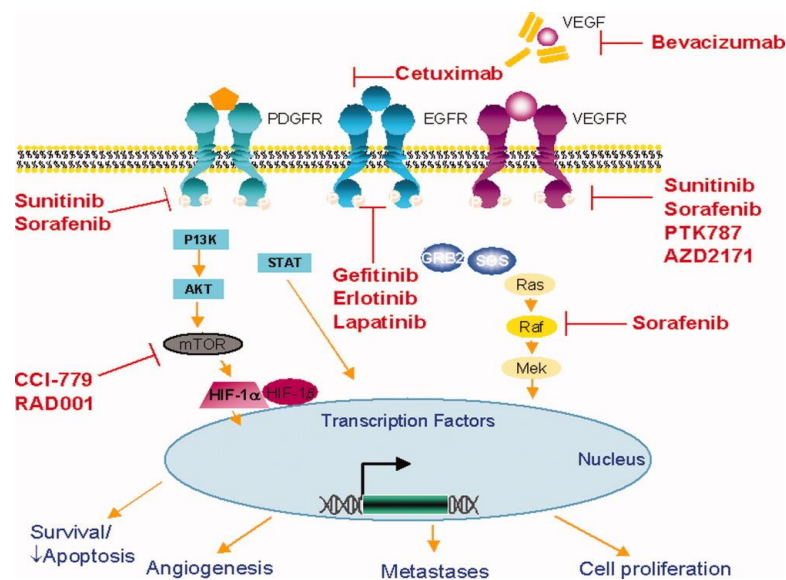
FIGURE 2.6: Molecular targeted treatment in hepatocellular carcinoma [40]

2.5.1 Bevacizumab

It is an anti-vascular endothelial growth factor and recombinant humanized monoclonal antibody. In the United States, this medicine is permitted for the cure of various forms of cancers like cancer of the lungs, breast and larger intestine. This medicine has been explored as a single agent for the cure of hepatocellular carcinoma. In a multicenter phase 2 study of 46 patients with compensated disease of liver and unrespectable hepatocellular carcinoma this drug resulted in 180 days progression free survival in 65 % of patients with 13% reporting a partial response to cure. At one year, the median progression of free survival was 209 days and on the whole, the rate of existence was 53%. Bleeding is a common adverse effect of this medication, the bleeding ratio during this study was eleven per cent. This drug has also been proposed in addition to oxaliplatin and gemcitabine [41].

2.5.2 Erlotinib

This is a small molecule inhibitor which targets the epidermal growth factor receptor tyrosine kinase. This drug has also been considered a single agent in hepatocellular carcinoma in the United States with phase 2 trials at a dose of 150 mg every day. In that study, 32 % of patients were progression free at 182.5 days and on the whole survival was 190 days. Currently, a combination of erlotinib with bevacizumab in a stage two study of forty patients was estimated by Thomas and colleagues. A combination of these two drugs yielded a median on the whole survival of sixty-eight weeks. The outcomes of this treatment are stomach bleeding and tiredness [42].

2.5.3 Cetuximab

In comparison to erlotinib, this is a monoclonal antibody against the epidermal growth factor receptor targeting the extracellular receptor binding site. Cetuximab has been considered separately and along with other therapies in hepatocellular carcinoma. In one stage two trial, it was provided to thirty patients of hepatocellular carcinoma for a time of six weeks. Although the treatment was very enduring in comparison to erlotinib,

no objective anticancer actions were seen. In forty-five cure-naive patients with new hepatocellular carcinoma, a combination of cetuximab along with gemcitabine and oxaliplatin was linked with a progression free existence of 142 days. On whole survival of 288 days a forty percent survival rate was observed. Given the effectiveness of the GEMOX combination without the other agent and the lack of persuasive facts like immunotherapy, the effectiveness of cetuximab remains unsure [43].

2.6 Phosphatidylinositol - 3 - Kinase - Akt - Mammalian Target of *Rapamycin*

The signalling pathway of the epidermal growth factor receptor (EGFR) and insulin-like growth factors involved in the activation of a protein recognized as phosphatidylinositol-3-kinase which stimulates Akt ultimately activates mTOR (Figure 2.7). A growth factor (e.g., EGF, HGF) binding to a receptor tyrosine kinase (RTK) activates the receptor. Active PI3K binds to phosphatidylinositol 4, 5-bisphosphate (PIP2) in the cell membrane. PI3K initiates transphosphorylation from PIP2 to create PIP3. Phosphorylated PIP3 or PDK1 activates AKT1. The activation of AKT1 triggers downstream activation of protein complexes mTORC1 and mTORC2 complexes that activate gene transcription and promote cell growth and survival. PIP2, or phosphatidylinositol 4, 5-bisphosphate, is bound by active PI3K in the cell membrane. PIP2 is transphosphorylated by PI3K to produce PIP3. AKT1 is activated by phosphorylated PIP3 or PDK1. The protein complexes mTORC1 and mTORC2, which drive gene transcription and support cell growth and survival, are activated downstream by the activation of AKT1. It is an imperative cell growth regulator [44]. *Rap2Amycin* is a mammalian target of rapamycin inhibitor with anticancer characteristics that can also be used as an immune suppressant, post-transplant. In a previous study of seventy-three patients who underwent orthotropic liver transplantation, those patients who received *Rap2Amycin* had better survival than those patients who were provided tacrolimus-based immune suppression [45].

Clearly, more research is required to be completed to evaluate the character of *Rap2Amycin* for the cure of HCC for the setting of pre and post-transplant. Everolimus is a mammalian target of rapamycin inhibitor that has been shown to work as anti-hepatocellular carcinoma in xenografts and is at present being studied in phase 2 trials in metastatic disease. Everolimus has also been studied with sorafenib treatment with hopeful early outcomes [46].

2.7 Receptor Associated Gene-2A (*Rap2A*)

Receptor associated protein-2A belongs to the RAS oncogenic family. Complementary nucleotide sequences of the *Rap2A* gene are present on 13q34 and have an origin of replication of 549 bp encoding 183 amino acids [47]. Previous work has revealed that the *Rap2A* gene plays an imperative part in processing special cellular processes like the re-organization of the cytoskeleton and the development of brush border (developed by enterocytes and kidney tubule epithelial cells) and cell relocation. It is described that the *Rap2A* gene is unregulated in numerous forms of cancers like prostate cancer, follicular thyroid cancer and nasopharyngeal carcinoma [47]. However, no data relates to *Rap2A* gene expression in hepatocellular carcinogenesis other than one research which observed the high *Rap2A* gene expression in liver cell lines (HepG2). According to that research, *Rap2A* enhances hepatocellular carcinogenesis and metastasis [11]. Therefore, more studies related to the*Rap2A* gene in hepatocellular carcinoma are required. For example, researchers can study the *Rap2A* gene effects on hepatocellular carcinoma, cell migration, and invasion in nude mice using a heterotopic xenograft model.
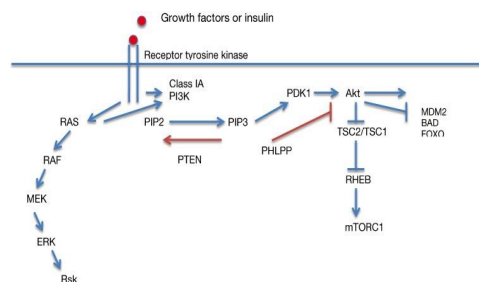
FIGURE 2.7: Phosphatidylinositol-3-kinase-Akt- mTOR signaling pathway [48]

2.8   Signaling pathway of *Rap2A* gene

Receptor associated proteins such as *Rap1a, Rap1b and Rap2A, Rap2b, Rap2c* are members of Ras related superfamily of small guanosine tri-phosphate binding proteins that have mostly been involved in various cellular processes. However, there is a high structural similarity between the Rap subfamily and with Ras protein family but both protein families have different signaling pathways in space and time representing exclusive biological effects. Very remarkably Rap proteins show a vital part in regulating the function of cell adhesion and integrin in that way handling the motility of cell and interaction of cell/matrix [10]. Beyond the crucial work of cell biology, various research in history has focused on the special part of receptor associated protein signalling for particular functioning of controlling tissue systems as well as in cancer. Rap gene affects the invasiveness of tissue and metastasis of different human cancers as previously reported. Many researchers have exposed that the p53 tumor suppressor gene effects on the motility of cells are mainly mediated by the Rho gene signalling regulation by controlling actin cytoskeletal reorganization [49].

2.9   Akt Phosphorylation Involved in *Rap2A* - Mediated Cancer Cell Migration and Invasion

Highly incorporated multi step cellular activities mediated via multiple signalling molecules like phosphatidylinositol 3-kinase/Akt and matrix metalloproteinases induce cell metastasis. Akt recognized as protein kinase B controls the proliferation, existence, and cell metabolism. Akt dysregulation causes substantial unavailing health necessitates like cancer, diabetes, cardiovascular disease, and neurological disorders [50]. *Rap2A* gene expression boosted Akt phosphorylation substantially according to Western blot analysis. *Rap2A* inhibition, on the other hand, reduced Akt phosphorylation (Figure 2.8). Immunoblotting revealed that the *Rap2A* gene is

upregulated in numerous tumor types. *Rap2A* downregulation, on the other hand, decreases cancer cells' migratory and invasive abilities. In order to understand more about the mechanisms that lead to *Rap2A* mediated elevation of MMP2 and MMP9, it was investigated that whether *Rap2A* expression might influence PI3-kinase activity. It was discovered that increased *Rap2A* appearance increased Akt signal while decreased *Rap2A* expression participated in a decrease in p-Akt [51].

These results specify the role of the PI3K/Akt pathway in *Rap2A* induced matrix metallopeptidase 2 and matrix metallopeptidase 9 expressions and invasion of tumor cells. Taken collectively these results advocate that p53 induces *Rap2A* gene which activates PI3K/Akt signalling pathways leading to enhanced matrix metallopeptidase 2 and matrix metallopeptidase 9 expressions and heightened invasiveness of cancer cells. Metastasis and invasion management are key therapeutic targets because the failure to regulate metastasis and malignant invasion remains the most difficult barrier to effective therapy. The recognition of the *Rap2A* gene as a key participant in p53 signalling gives potentially critical indications for managing human disorders [51].
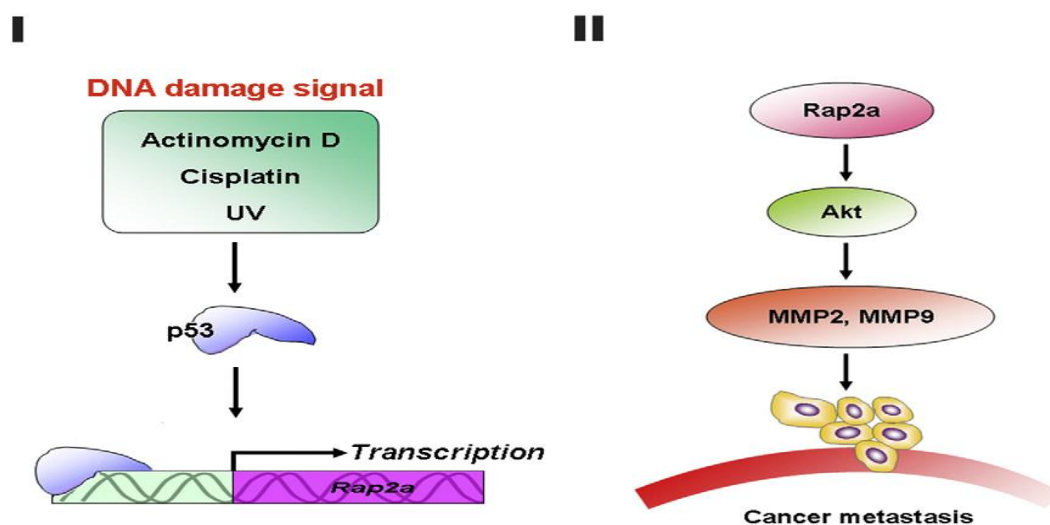
FIGURE 2.8: Diagram of p53 and *Rap2A* relationship upon deoxyribose nucleic acid damaging and the function of *Rap2A* in tumor genesis. (1) Upon deoxy ribose damage, p53 combines with the *Rap2A* promoter and triggers its transcription. (2) *Receptor associated proteins* enhance the actions of MMP2 and MMP9 and increase the movement and bad aptitude of tumor cells via up-regulating p-Akt [51]

2.10   Apoptosis

Apoptosis is broadly depicted as an important method of death regulation that participates not merely as an outcome of cell damage or external stress, even though, this also occurs in normal growth, and morphogenesis (Figure 2.9). Via various groups of the executioner and regulatory molecules, apoptosis is strongly regulated. Apoptotic cell death action is characterized by chromatin material condensation, deoxyribonucleic acid fragmentation taking place in the nucleus, cell shrinkage, and membrane blebbing with extracellular matrix adhesion loss. Moreover, biochemical variations are phosphatidylserine externalization with the action of cysteine aspartyl proteases described as caspases that cause cell death [52].
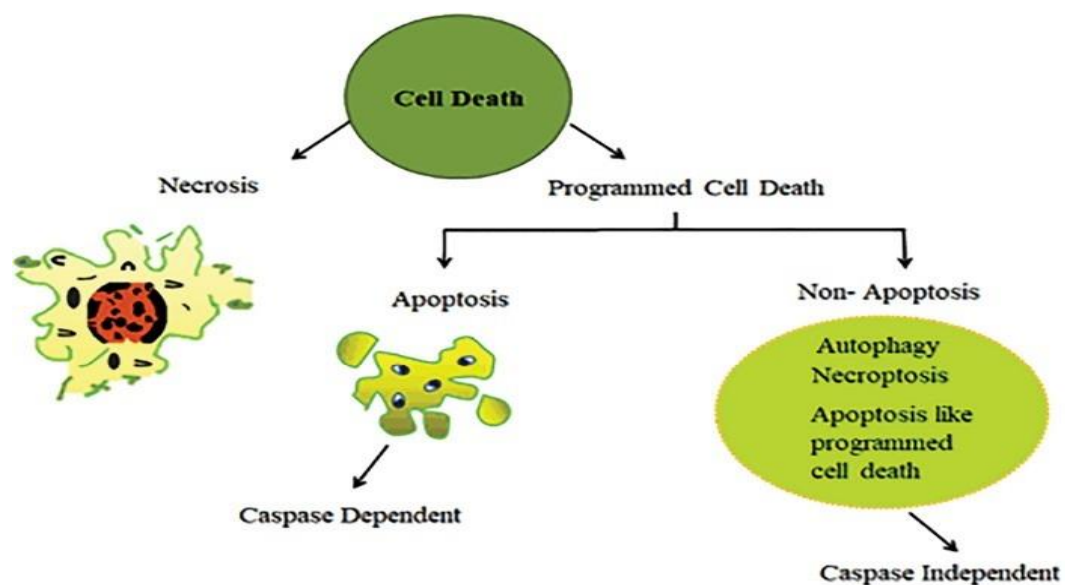
FIGURE 2.9: Common method of cancerous cell death. Cancer cell death consists of 2 largely described methods. Apoptosis is a programmed cell death mostly and non-apoptosis includes autophagy, necrosis, and programmed death [53]

2.10.1   Considerate Apoptotic Pathways for Tumor Treatments

Current progress in cancer studies is focused on the progression of novel treatments that stop the escape of cancerous cells by the execution of apoptosis. For such

conditions, new inducers or sensitizers of apoptosis have been consumed along with the amalgamation of novel medicines. Deficiency in the apoptosis-inducing pathways may ultimately cause the development of neoplastic cells (Figure 2.10). The apoptosis resistance enhances abnormal cellular growth that ultimately causes tumorigenesis and is an important difficulty in energetic tumor cure [53].
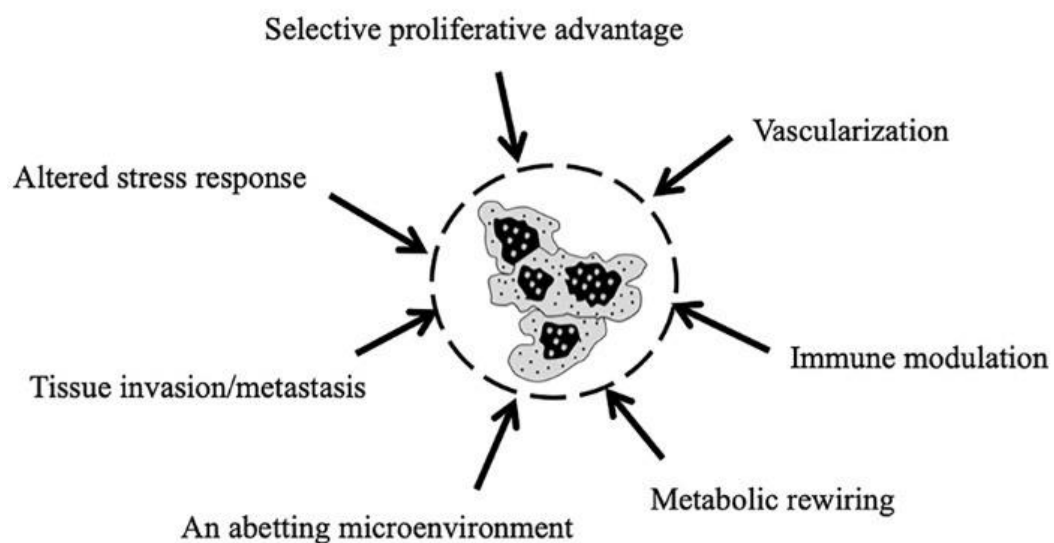
FIGURE 2.10: Cancer hallmark. Different acquired characteristics of tumor cells [53]

Apoptosis initiation in cancer cells and limited concurrent death of normal cells is the main purpose of cancer treatment. A number of proteins have been considered to exert pro and anti-apoptotic actions in the cell and the amount of such proteins show an important role in cell death regulation. During cancer, gene therapy, or immunotherapy, cancer cells' apoptosis initiation is among the major processes. The apoptosis process primarily consists of two main pathways that participate in the apoptosis; extrinsic and intrinsic pathways (Figure 2.11). The extrinsic pathway refers to the death receptor mediated pathway, and the intrinsic pathway is a mitochondrial mediated pathway. Both apoptotic pathways can lead to similar executing pathways [54].

2.10.2   Extrinsic Pathway

By extrinsic pathway, apoptosis signalling starts when TNF, Fas ligand, and TRAIL (extracellular ligands) are associated with the extracellular domain of the death receptor. In the apoptosis extrinsic phase, the order of events involved is characterized by TNFR1 /TNF-alpha and FasL/FasR models. Such death receptor activation by definite death ligands results in the arrangement of a DISC. Experimental verification expresses the extreme function of caspases in apoptosis. Caspases are vital originators and apoptosis executioners. Various caspases consist of long pro domains that participate in a particular pattern like the DED and CARD that permit interaction with more proteins. Death effector domain contains caspases 8 and 10 while CARD consists of caspases 1, 2, 4, 5, 9, 11 and 12. Originator and effector or executioner caspases are conventionally grouped via their place in apoptotic signalling cascades [54].

2.10.3   Intrinsic Pathway

This pathway refers to the primarily mitochondrial mediated apoptotic pathway. By many extracellular and intra-cellular stresses that are oxidative stress, irradiation, and cure through cytotoxic medicines this intrinsic pathway is activated. The cytochrome c unites with apoptotic protease activating factor-1 (apaf 1) and procaspase 9 to create apoptosome. Apoptosome is a quaternary protein structure that consists of a sevens poke ring-shaped complex and activates caspase 9 followed by the activation of caspase 3 signaling cascade that causes the destruction of cells leading to programmed cell death [55].
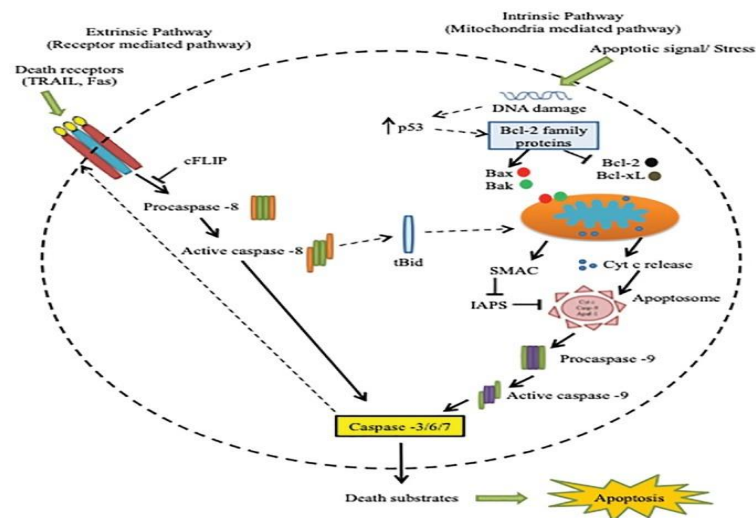
FIGURE 2.11: Apoptosis pathway showing both extrinsic and intrinsic pathways
[53]

2.10.4   Execution Pathway

Intrinsic and extrinsic pathways join at the execution pathway. The execution phase is called the last apoptotic pathway. Caspases 8 and 9 are initiator caspases that activate caspase 3 leading to activation of Caspase-activated DNase. Originator caspases are triggered like an outcome of auto cleavage, which triggers executioner caspases that later on proteolyze several substrates causing apoptosis. All have lengthy pro domains that attach big adapter particles to enhance multimerization which results in further activation of caspases [56]. Though effector caspases have a short prodomain, they carry out programmed death while triggered via caspases called originators. Cytoplasmic endonuclease triggered via executioner caspases leads to chromatin condensation, the arrangement of cytoplasmic blebbing, and apoptotic bodies. Caspases adjust apoptotic cell death by cleavage of many target proteins. The pathway starts when execution caspases stimulate cytoplasmic endonuclease. Cytoplasmic endonuclease causes the protease and nuclear material nuclease degradation followed by nuclear and cytoskeletal protein degradations. In all caspases, executioner caspase 3 is very significant and any of the originator caspases may stimulate them. Execution caspases play a vital part in the

reorganization of cytoskeletal, cytoplasmic blebs formation, and apoptotic bodies [57].

2.11 Medicinal Plants

Globally, about 80 percent public of developing countries relies on conventional medicine for their prime health care necessities reported by WHO. There are significant financial profits in the enhancement of native medicines and the consumption of medical flora for the cure of many sicknesses. Because of little contact, poverty, unawareness, and unavailability of novel medical services many communities particularly villagers are still obligated to perform conventional medications for their common day ailments. Plants are a great source of bioactive compounds. Secondary metabolites are those chemicals which are derived from these plants having anticancer, anti-oxidative, anti-allergic, and many other medicinal properties. These secondary metabolites protect the cells from free radicals, which are unstable chemicals. Natural antimicrobial compounds particularly those extracted from plants are gaining popularity for food protection. As a result, it is necessary to look for plants with therapeutic properties [58].

2.11.1 *Artemisia* Genus

The Artemisia genus is a shrub and member of the family Asteraceae. It has more consumption in China as a therapeutic plant which has been extensively considered as an antimalarial, antitumor, and antioxidant plant. *Artemisia* has artemisinin and derivatives and a variety of components of essential oils. It is reported by Tang and Eisenbrand that chemical compounds in *Artemisia* are the member of sesquiterpene group and the flavonoid group (like coumarin, scopoletin, artemetin, esculetin, and tetramethoxy flavones). Furthermore, it also has fatty acids, coumarins, phenols, artemisinic acids, and essential oils. Almost 85 % of health concerns like tumor, microbial infections, and immunological diseases are cured with naturally occurring compounds and their related medicines. It is represented that approximately twenty

five per cent of accepted medicines around the globe are acquired from plant origin [59]. These *Artemisia* species have extensive biological action against malaria, bacteria, and tumors along with antirheumatic and antiseptic activities. Extracts acquired by this plant are also utilized for nervousness, neurological disorders, sadness, sleeplessness, irritability, psychoneurosis, and stress cure. Malaria is a worldwide and life peril illness that causes an annual death toll of approximately 1,000,000. *Artemisinin* a sesquiterpenoids/lactone compound acquired from the trichomes of annual *Artemisia* species like *Artemisia annua* is used for the treatment of malaria. The chemical composition of artemisinin proves the presence of an endoperoxide bridge in the 1, 2, and 3-trioxane structures. This endoperoxide bridge works as a pharmacophore and gives antimalarial activities against *Plasmodium falciparum*. Currently, the World Health Organization advocates artemisinin-based combination therapy to stop the transmission of the malarial parasite *Plasmodium falciparum*. *Artemisia* species extracts are also used against cancer and work by causing apoptosis by ER pathways [60, 61].

2.11.2 *Artemisia carvifolia* Buch

The genus *Artemisia* of the Asteraceae family includes the species *Artemisia carvifolia* Buch. Commonly the plant is known as sweet wood and had already been described by Francis Buchanan-Hamilton, though William Roxburgh had first used the name [62]. *Artemisia carvifolia* resembles *Artemisia annua* in morphology having light-yellow, multi-stellate blooms with alternate leaves (Figure 2.12). They have modest wide-ranging leaves. The length of the plant grows to 30 to 150 cm in length and it is an annual or biennial herb. The cultivation of this plant is done in the wild region with water zones around for medicinal use. This plant is native to India, the Himalayas, Assam, Burma, and China. Conditions for the growth of this plant include dry to moderately damp soil and a sunny location [62].

Figure 2.12: *Artemisia carvifolia* Buch

2.12 Nanotechnology

Nanoparticles show better or considerably enhanced properties based on definite characteristics for example morphology, size and distribution. Bulk and atomic structures vary in their characteristics and metal nanoparticles bridge the gap among them with their exclusive physicochemical properties, which are increased surface area, more reactivity, large surface to volume ratio, spatial confinement, tunable pore size and particle morphology. The nanoparticles made up through inert metals mainly gold, silver, platinum is investigated efficiently [22].

2.12.1 Synthesis of Nanoparticles

The NPs preparation procedure can be classified into 2 major categories like bottom-up and top-down approaches (Figure 2.13). Generally, the NPs preparation process is divided into 3 major preparation methods i.e. physical, chemical and biological methods and ways [22].
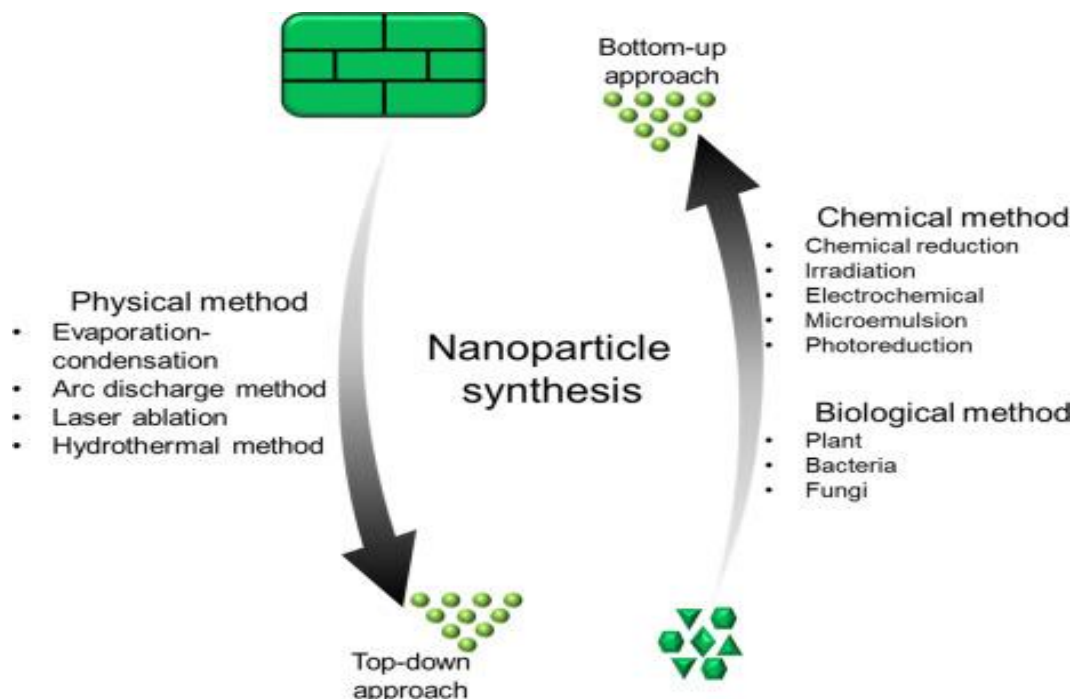
FIGURE 2.13: Main approaches of synthesis of nanoparticles [63]

2.12.2 Bottom-Up Method

The construction of material from smaller molecules to specific clusters of nano-materials is known as a bottom-up construction system. This method involves combining different compounds to synthesize various NPs. Hydrothermal, sol-gel, pyrolysis, biosynthesis, chemical vapor deposition and spinning are the most often used bottom-up methods for producing NPs. The hydrothermal method is the most widely used and is being taken into consideration in the processing of NPs preparation. Bottom-up methods rely on the self-assemblage of molecules, phenomena linked with nanoscale physiochemical interactions that put together basic components into macroscopic structures [64].

2.12.3 Chemical Vapor Deposition Method

This is the process of depositing a slight coating of gaseous reactant on the substrate. A reaction chamber is used to deposit the thin film. A chemical reaction occurs when a gas comes into contact with a heated substrate. As a result of this response a thin layer of things is present on the substrate surface. This thin layer is retained and reused. The chemical vapor deposition process produces rigid, well-built, standardized and very pure NPs. The disadvantages of this chemical vapor approach include the need for specific apparatus and the creation of very hazardous gases by the products [64].

2.12.4 Sol Gel Method

This process is a made up of two words sol and gel. Sol is a colloid produced from hard particles suspended in constant liquid. Gel is a solid larger molecule which is liquefied in solvent. Because of effortlessness this technique is more chosen bottom-up strategy for the preparation of NPs. This is a technique where appropriate chemical solution work like a precursor. The metal oxide and chloride are used as precursors in this process [65].

2.12.5 Spinning

NPs are also prepared via spinning (Figure 2.14). The NPs are designed by using SDR which is involved in the rotation of disc where physical parameters can be tackled at that temperature. To avoid chemical reactions and eliminate O_2 the reactor is filled with N, He or Ne. The water and precursor are pumped within the reactor. The characteristics of NPs prepared from spinning disc processing are determined by different features like a surface disc, precursor ratio, speed of the rotating disc, ratio of liquid and locality of feed. Smith, Nigel, *et al* prepared Magnetic NPs by SDP. The size of particles ranged from 3 to 12 nm [65].
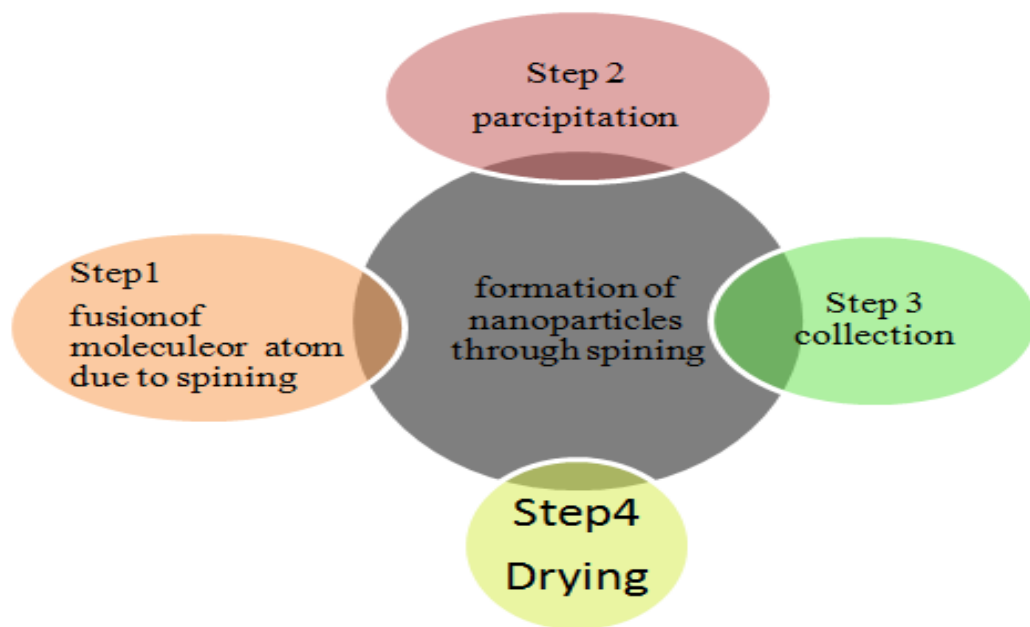
FIGURE 2.14: Nanoparticle preparation steps through spinning. It involves the fusion of atoms due to spinning followed by the precipitation of atoms leading to the collection and drying of synthesized nanoparticles.

2.12.6 Pyrolysis

This is an industrial strategy for the preparation of NPs. The precursor is burned with flame in this process. The precursor can be in a condition of fluid or steam. The precursor is transferred into the furnace at high pressure and recovers NPs. Sometimes laser or plasma are employed in place of fire to create more temperature. More temperature makes easy evaporation and synthesis of nanoparticles [65].

2.12.7 Top-Down Preparation

In this preparation, a destructive technique is applied. The bulk material is broken into a smaller molecule and then such smaller molecules convert into the NPs. Grinding or milling, physical vapor deposition and other destructive strategies are the models of top-down preparation [65]. Some of the types of top-down approach are given below.

2.12.8 Thermal Decomposition Method

Chemical breakdown is created by heat in the endothermic process known as thermal decomposition. By the use of heat, a compound's chemical bond is broken. The temperature at which an element decomposes chemically is known as the decomposition temperature. The NPs are consequences of broken chemical bonds at specific temperatures. Ahab, Atika *et al.* prepared gold oxide NPs functionalized by paramagnetic this way [65].

2.12.9 Lithographic Strategies

Lithographic procedures are top-down processes capable of producing most micron sized aspects. However, they are energy intensive and need expensive tools. For many decades, lithography has been employed to create printed circuit boards and computers. Nano imprint lithography is a kind of lithography which is distinct from typical lithography. Photo lithography, electron beam lithography, soft lithography, focused ion lithography, nano-imprint lithography and dip pin lithography are examples of lithography processes. Photo lithography involves contact and proximity printing and projection printing [65].

2.12.10 Mechanical Method/Ball-Milling Method

This technique is a cheap strategy to make NPs from bulk. It is a simple mechanical process. Mechanical method by which Kinetic Energy (KE) is transmitted from the grinding medium to the material being reduced. Consolidation and compaction, are industrial scale processes where NPs are put back together to produce material with better qualities. The preparation of various metal alloys is done mechanically [65].

2.12.11 Laser Ablation

In a solution, laser ablation is a simple method for the preparation of NPs from diverse solvents. The irradiation of diverse metals immersed in a solution by a laser beam condenses plasma to make NPs. Laser ablation is an incredibly valuable top-down technique that is diverse from usual chemical ways for the reduction of metal to NPs [65].

2.12.12 Sputtering

This is the process of NPs deposition by discharge of particles from it. In NPs deposition, annealing of thin layer is especially valuable. NPs formulation and size are determined from features including temperature, layer thickness, annealing period, substrate and so on [65].

2.12.13 Bio Based Methods of Preparation of Nanoparticles

2.12.13.1 Nanoparticles' Preparation Using Microbes

Bio based preparation of NPs consists of preparation via the extract of microbes like bacteria, fungi and yeast. Bacteria have the capability to reduce the metal ions and are therefore used in the preparation of NPs. Diversity of microbial groups is applied in the preparation of metallic and other new NPs. Bio-based preparation of metallic NPs by fungus is also an especially well-organized strategy with more cleared morphology. Because of the internal cellular enzyme, fungi behave like biological agent for the preparation of NPs. Bacteria produce fewer amounts of NPs compared to fungus. The preparation of NPs by yeast has also been explored by many scientists. Countless NPs are synthesized via yeast [66].

2.12.13.2 Preparation of Nanoparticles Using Plants

Bio-based preparation of NPs consists of preparation via the extract of plants and microbes like bacteria and fungi. Plant nanotechnology has appeared as a modern area for the preparation of NPs which is ecofriendly, simple and low cost. Scalability, biocompatibility and preparation of NPs by universal solvents as reducing agents are benefits of plant nanotechnology. Plant nanotechnology exploits plants for the preparation of NPs. NPs are synthesized by diverse plant parts like roots, fruit, shoots, kernel and leaves. The accurate method for the preparation of NPs by plant remains to be explained. It has been depicted that organic acid, proteins, vitamins and SMs like alkaloids, flavonoids, terpenoids, polysaccharides and heterocyclic compounds are liable for the preparation of different kinds of NPs [67].

2.13 Different Metallic Nanoparticles

Metallic nanoparticles have diverse biomedical applications (Figure 2.15). Silver nanoparticles have numerous significant effects as well as medical applications like anti-oxidant, anti-bacterial and cytotoxic properties. Sliver nanoparticles can be prepared by physiochemical and bio-based techniques. Ag in bulk form has less efficacy, but when it is changed into Nps it shows different results. A sliver nanoparticle has enhanced characteristics against microbes and influences the metabolic, respiratory and reproductive process of microbes. AgNP's different antibacterial characteristics are employed in different manufacturing appliances [68]. The biocompatibility, steadiness and protection of zinc oxide nanoparticles present them as an outstanding option for therapeutic purposes. FDA has agreed zinc oxide nanoparticles as a medical excipient which are extensively consumed in treatment methods and beauty products. Zn oxides have biomedical applications as anti-bacterial, antiviral, antifungal and also as parasites against cancer and as medicinal mediators. Moreover, zinc oxide is consumed for preparing concrete, for photo catalysis, in electronics and electro technology as well as in various industrial appliances [69].
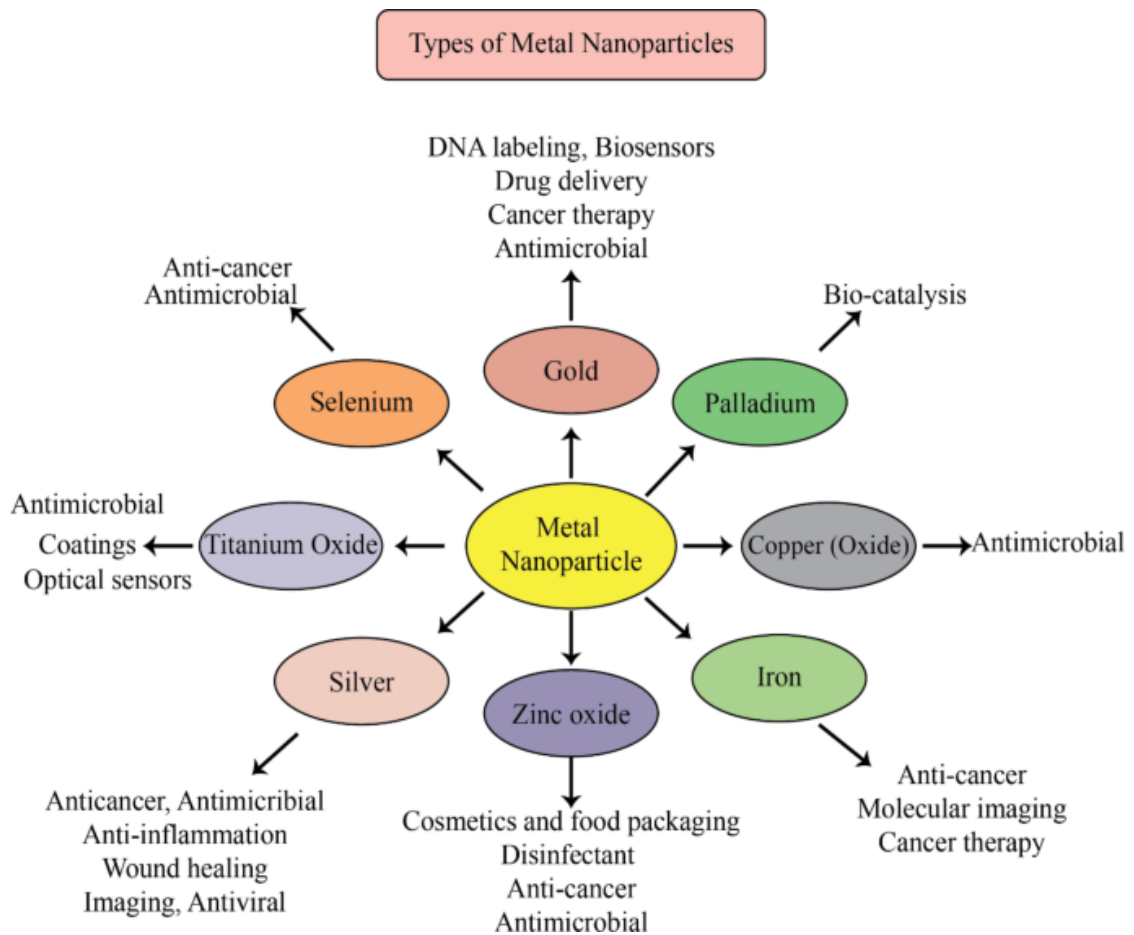
FIGURE 2.15: Applications of metallic nanoparticles [70]

Iron nanoparticles are just now achieving large significance in the environmental remediation sphere. The major function in this sight is the elimination of organic and inorganic contaminants from aqueous solutions. Non-organic nano tools comprise silica Nps Carbon nano resources, nano graphene, Au and Ag Nps, magnetic Nps and quantum dots which are extensively in use for cancer cure. Iron nanoparticles have been broadly consumed to identify and eradicate cancer cells with high warmth, for example, hyperthermia of breast tumors. These inorganic elements may connect to tumor cells and get magnetized when connected to the magnetic field [71].

2.14   Role of Metallic Nanoparticles Against Cancer

Silver nanoparticles have been a much-explored material in cancer treatment. They have been broadly investigated because of their physical, chemical and bio-based properties with a large surface to volume ratio, biocompatibility, usefulness against microbes, excellent Surface Plasmon Resonance, ease of functionalization and cytotoxicity against cancer cells. Sliver nanoparticles have gained rising interest in the tumor domain having an intrinsic activity against cancer and being confirmed as valuable agents against cancer drug delivery systems [68].

In terms of the anticancer activity mechanism, nanoparticles were shown to influence the fluidity of the membrane, allowing for easy entrance and gathering in tumor cells, a reason for tumor cells to die or limiting their uncontrolled proliferation. Furthermore, nanoparticles can liberate Ag+ that gain electrons, enhance intracellular oxidative stress, enhance reactive oxygen species production, decrease adenosine triphosphate levels of tumor cells and decrease the rates of cell proliferation [72].
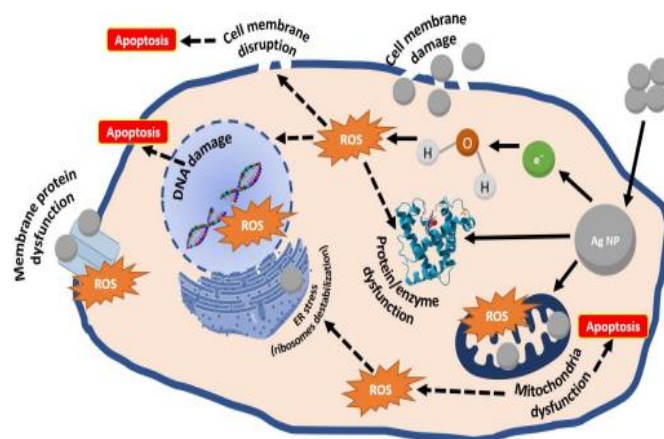
FIGURE 2.16: Representation of sliver nanoparticles mechanisms against cancer [73]

Released sliver ions mostly in the nuclei and mitochondria and their interaction with deoxyribonucleic acid results in its fragmentation and resulting in cell death. The depicted sliver nanoparticles' process of working is visually symbolized in

Figure 2.16. The same ways have also been planned for other noble metal-based NPs like gold, platinum and palladium NPs. Major outcomes concerning sliver nanoparticles anticancer action were identified against numerous human tumor cell lines that are hepatocellular carcinoma, breast cancer, ovarian cancer, prostate cancer and larger intestinal cancer [73].

In nature, diverse kinds of iron oxide nanoparticles have been started to be investigated for preparation like Fe_3O_4, α, β and γ Fe_2O_3. Non-toxicity, biocompatibility, super para magnetism, chemical inertness and an easily adjustable surface are just a few of the benefits of IONPs for biomedical applications. In terms of cancer treatment, iron oxide nanoparticles have been FDA approved in tumor diagnostics, imaging and magnetic hyperthermia therapy as well as in displaying preclinical settings potentials for photothermal and photodynamic treatments. One Ferro fluid formulation produced by Mag Force AG has been approved for the cure of brain cancer with their NanoTherm therapy being certified for use on patients from European Union member states. Iron nanoparticles have also been studied broadly for screening purposes. IONPs have been identified as potential contrast agents for many imaging modalities including fluorescence imaging, SPECT and multimodal imaging [74].

Iron nanoparticles have also generated strong awareness in the preparation of magnetic nanoparticles-based drug delivery systems. This is mostly due to the remarkable targeting capabilities of drug-loaded iron nanoparticles when guided by external magnetic fields (Figure 2.17) [75].
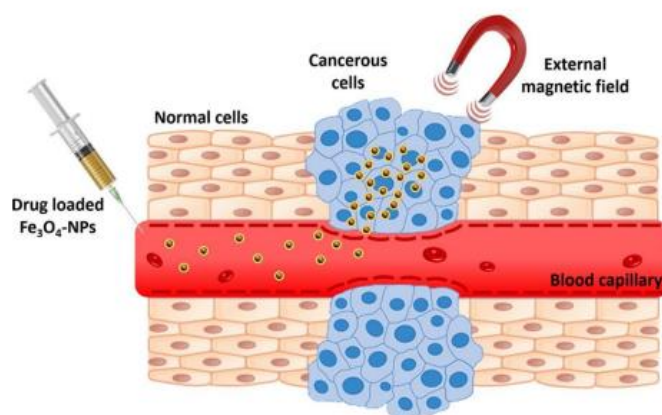
FIGURE 2.17: Diagram of targeted drug delivery by IO nanoparticles [75]

In particular iron nanoparticles-based delivery systems that are injected, travel via capillaries of blood to the preferred site releasing the drug in cancer cells and rising treatment usefulness without harming the nearby normal cells. This is accomplished by using an external magnetic field. Also, after applying this local external magnetic field their magnetic characteristics enable the radiant energy exchange into heat or reactive oxygen species, decreasing the side effects of tumor therapy. Several of these iron nanoparticles-based nano systems have undergone *in vitro* and *in vivo* testing and have been found to be effective against a wide range of tumor types like the cancer of ovaries, breast, colorectal, liver, gastric and lungs. These particles show promising results when used alone or in combination with other nano materials such as Cu, chitosan, amino silane and polyethylene glycol or like carriers of other chemotherapeutic agents, for example, doxorubicin, docetaxel and curcumin [75].

Numerous other metals and metal derivatives in addition to nanoparticles already mentioned, have begun to be studied in their nano form as potential candidates for use in the treatment of tumors. For instance, due to their advantageous chemical characteristics, zinc oxide nanoparticles are currently used in biomedical and tumor applications [75]. Zinc oxide nanoparticles have strong biocompatibility, prevent cancer and work against bacteria, and are becoming more and more popular in nanomedicine. In addition, because zinc oxide nanoparticles may generate micronuclei inside cells, it has been suggested that they behave similarly to genotoxic drugs. Its impact was shown to be minimal on normal cells, medium on epithelial carcinoma cells and highest on glioblastoma multiforme cancer cells. Green synthesized ZnO NPs have been shown to have anticancer properties against a variety of additional human cancer cell lines like those for osteosarcoma, large intestine cancer, cervical cancer, breast cancer, lung cancer and laryngeal cancer [69].

2.15 Computational Approaches of Computer - Aided Drug Design (CADD)

The CADD tools are now an essential component of drug discovery which is making an important contribution in the field of drug development and discovery.

Computational techniques play a vital role in the drug design and development process [76]. The most important task in the CAAD is to discover lead compounds with the highest binding affinity to disease-causing proteins of interest. In recent years, molecular docking has been extensively utilized in the field of drug design and research. This technique is basically a structure-based drug design approach that shows the molecular interaction and predicts the binding mode and affinity between receptors and ligands. It provides the optimal conformation according to complementarity and pre-organization that can predict the binding affinity by the interaction methods between receptor and ligand [77]. Molecular docking simulation predicts the binding affinities and orientation when two molecules attract each other to form a stable complex [78]. As depicted in Figure 2.18 the molecular docking software can help to search the optimal conformation and direction of drug candidates according to complementary and pre-organization of drug targets by specific algorithm followed via using the scoring function for predicting affinity and analyzing the interactive method [79].
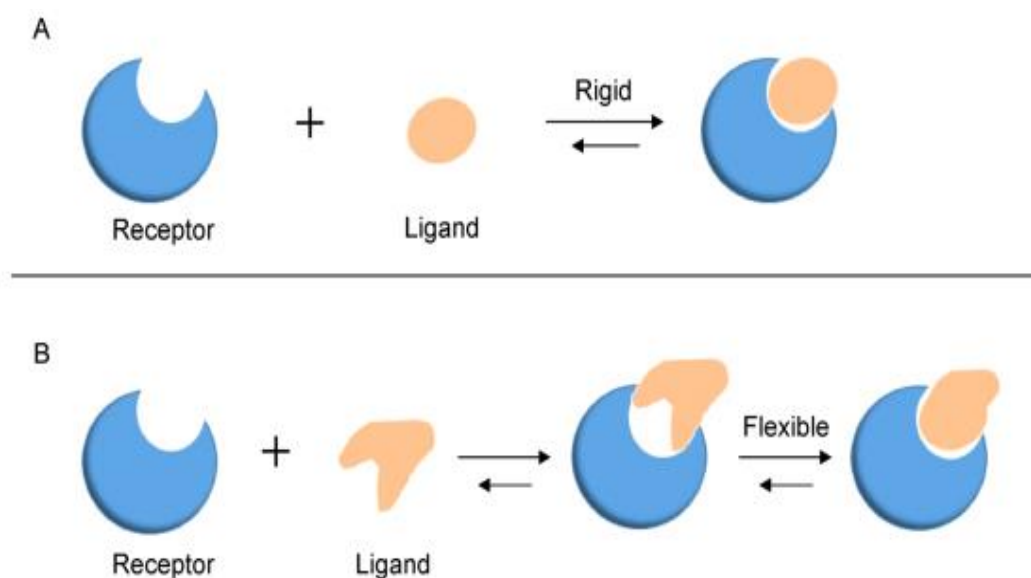
FIGURE 2.18: The molecular docking models. (a) A lock-and-key model. (b) Induced fit model [79]

In Figure 2.18 the 1st proposed lock and key model (A) refers to the rigid docking of receptors and ligand to search the right orientation for the key to open up the lock [80]. This model emphasizes the importance of geometric complementarity.

Part "B" presents that the real docking method is very flexible in the sense that ligands and receptors have to change their conformation to fit to gather and design an induce fit model [81]. The important databases being used in the process of drug design and development include the most popular protein structure database known as Protein Data Bank (PDB). Moreover, there are some other public databases such as PubChem Compound Database and ZINC are free to use. Besides, there are many important commercial databases, such as Compound Database (AcD), and Cambridge Structural Database (CSD) [79].

There are three types of methods and software that are being used for molecular docking whose details are described in Figure 2.19 and Figure 2.20. From these software, flexible rigid docking has been a more adopted approach these days. Although flexible rigid docking is commonly very efficient, relevant studies have become the hot-searching spots currently [82].
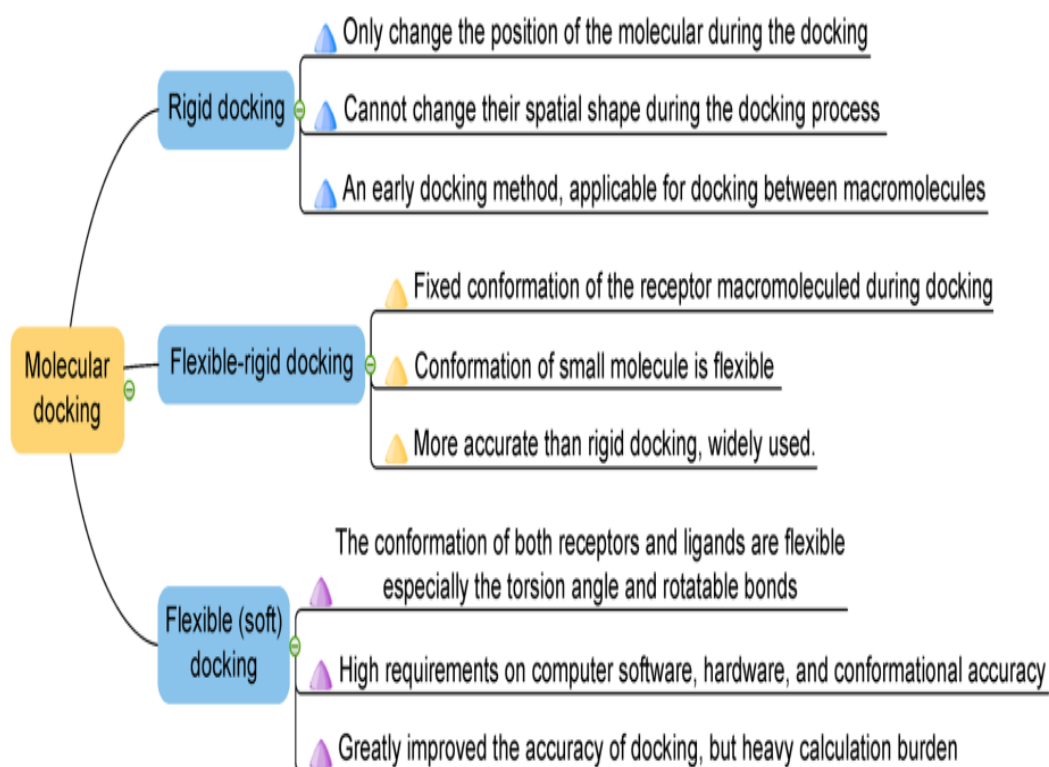
FIGURE 2.19: Docking software [79]
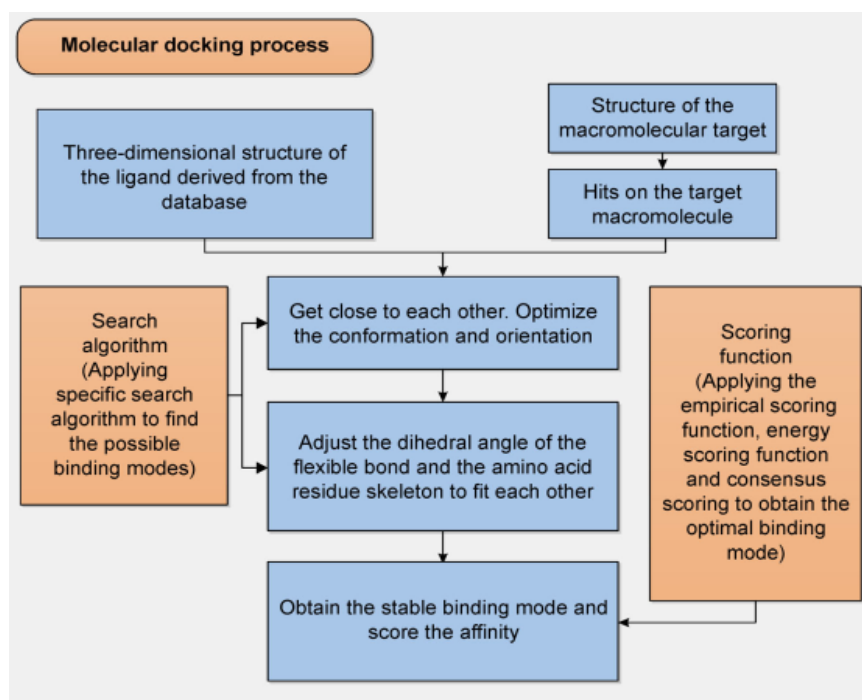
FIGURE 2.20: Overview of molecular docking process [79]

According to the scoring function, virtual screening is to find the lead compound and hit compound from the molecular database which has greatly improved the screening efficiency compared with the traditional screening method [83].
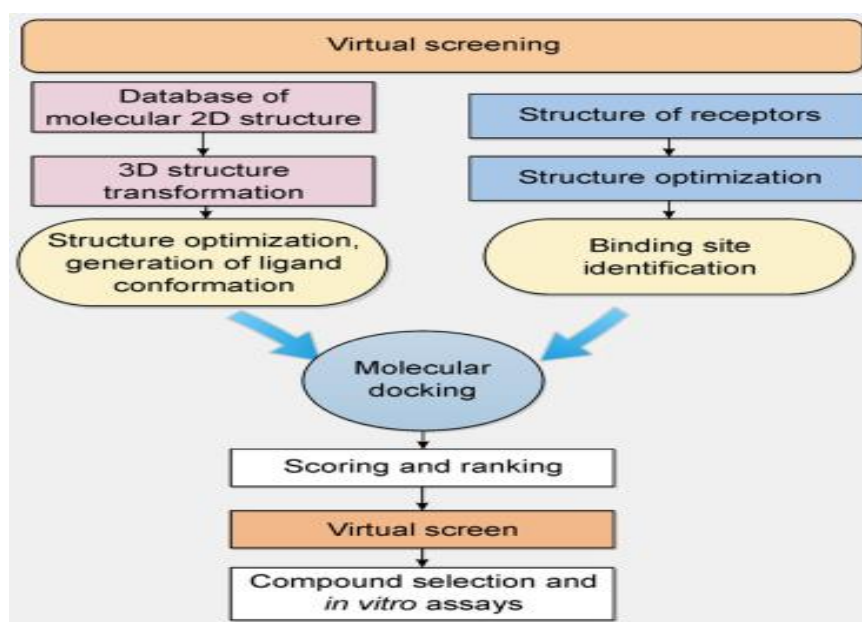
FIGURE 2.21: Virtual screening process [79]

The undesirable results of pharmacokinetics and toxicity are the main cause of failure of drug development in the late stage. It has been identified that drug ADMET properties should be considered as easily as possible to minimize the failure ratio in the clinical stage of drug designing. Simultaneously, drug recalls are increasing commonly in these years, and drug designing companies are paying more attention to the safety evaluation of preclinical drugs. Such techniques are expensive. Currently, advancement in computational techniques, and in silico approaches has been widely adopted to assess the relevant properties of drugs in the preclinical stage and has designed different software programs and in silico models, widely expanding the study of ADMET in vitro[79, 84]. Drug designing (Figure 2.21) is a very risky, difficult and time-consuming process that can be divided into different stages, including disease-related genomics, target reorganization and conformation, lead discovery and optimization, preclinical studies and clinical trials [85].
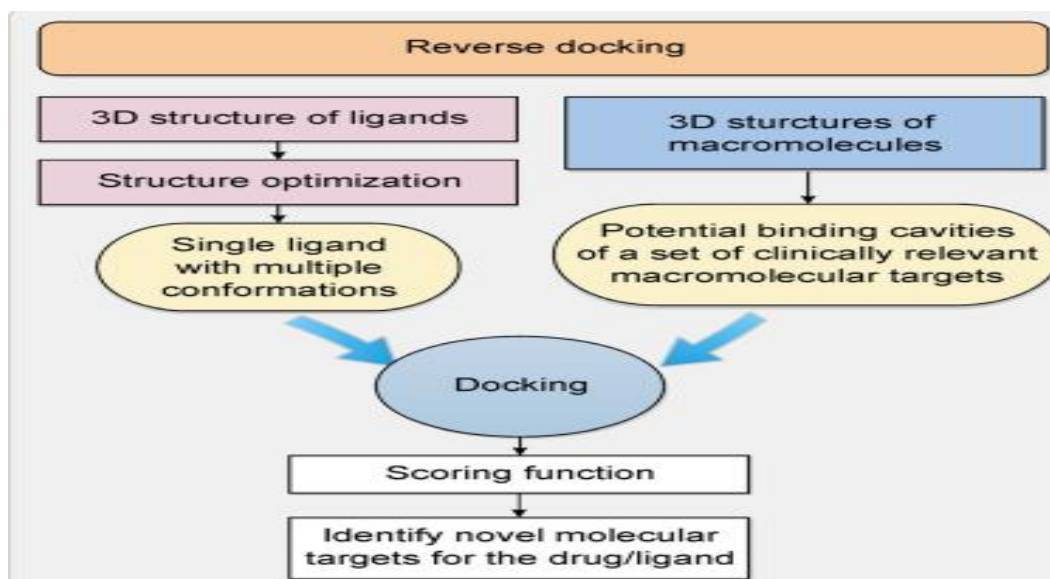
FIGURE 2.22: The process of reverse docking [79]

The flow chart in Figure 2.22 presents the drug designing by reverse docking and the major preclinical study content. Preclinical studies consist of in silico ADMET prediction and PBPK simulation, which play a major character in the selection and optimization of drug candidates [85].

2.15.1 Molecular Dynamic Simulation

Molecular dynamics simulation is important in understanding the conformational changes and dynamic processes of enzymes and is mostly used in drug design [86]. By molecular dynamic simulation, the macroscopic properties of matter can reflect the microscopic system in time and space [87]. MD simulation's impacts in drug designing and molecular biology have been explored dramatically recently. Such simulation captures the protein's actions and other biomolecules in full atomic detail and more fine temporal resolution. MD predicts how every atom in protein or other molecular system will show movement over time, based on a general model of physics governing interatomic interactions [88]. Molecular dynamic simulation is more valuable in lead optimization where one modifies a ligand for enhancing its properties and efficacy. Molecular dynamic simulations can also be beneficial for virtual screening, where one selects a set of ligands to predict binding to a target. The more use of MDS as a major tool in Insilco study of proteins as well as complementary machinery in experimental work has propelled actions for advancing different ways of MDS, justifying the good predictive power and very reliable computational analysis of protein structures, dynamics and functions [89]. The molecular dynamic simulation overview and enhanced sampling technique are shown in Figure 2.23 which is used in protein–protein study and protein-ligand complexes. The Figure is designed by the crystal structure of human PIM1 kinase in complexes along imidazopyridazin inhibitor and peptide substrate [90].
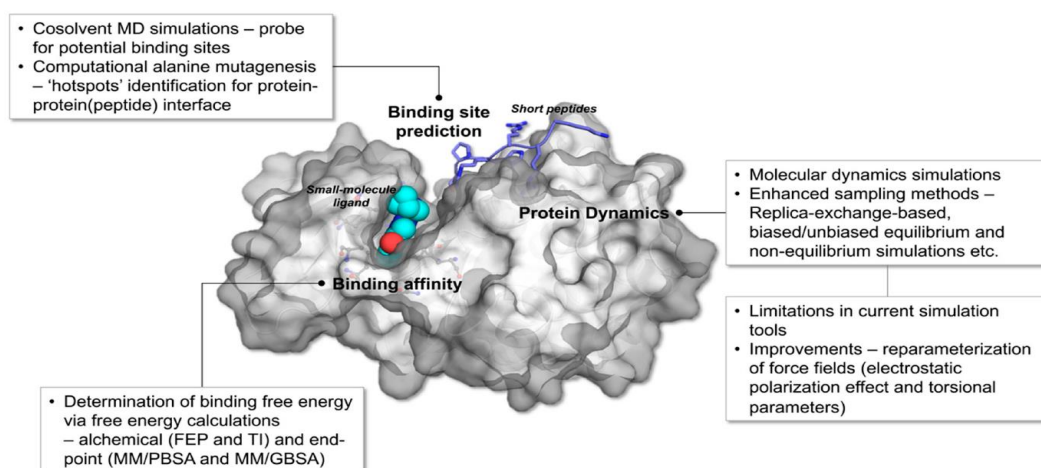
FIGURE 2.23: Molecular Dynamic Simulation [90]

Chapter 3

Materials and Methods

3.1   Laboratory Glassware and Chemicals

All the materials used in the adopted methodology are briefly mentioned here. In all of the experiments, borosilicate glassware was used which was purchased from Pyrex®. At the start of this process, all the glassware was wiped with detergents followed by immersion in a 10% bleach solution. After that at 200 ^{o}C, the glass apparatus was dried in the air-dry heating oven. Then it was subjected to sterilization for 20 minutes at 120 ^{o}C and 15 psi. During the whole experiment, molecular biological grade analytical chemicals were applied (MS, sucrose, gelrite, plant growth regulators) purchased from Sigma Chemical Co.

3.2   Collection and Identification of Plant Material

A. carvifolia Buch seeds obtained commercially were germinated [91] and DNA barcoding was done for plant identification using the *psbA-trnH* region of the chloroplast genome [92]. Plant specimens were submitted to the herbarium of

Quaid-i-Azam University Islamabad, Pakistan with specimen voucher no. HMP-ART 0001. All the experiment was done according to the institutional, national and international guidelines for conducting plant research.

3.2.1 Seed Germination Medium

MS medium was preferred for the germination of seeds. Half-strength MS salt added with sucrose (3 % w/v) and gelrite (0.5 % w/v) was prepared with pH set to 5.8 by using 1 N sodium hydroxide/hydrochloric acid before the accumulation of gelrite. For 20 minutes at 15 psi and 121 °C, the medium was sterilized. The medium was called the seed germination medium [91].

3.2.2 Seeds Germination

A. carvifolia Buch seeds were surface sterilized by 70 percent CH_3CH_2OH for thirty seconds followed by 0.1 percent (w/v) $HgCl_2$ for ten seconds. The seeds were then cleaned with sterilized distilled water thrice under a laminar flow hood and dried up on sterilized filter paper. Adjusting the sterile conditions, seeds were implanted on half strength Murashige and Skoog medium in petri dishes. They were placed in chill at 4 °C for 72 hours in the dark. Afterward, Petri dishes having seeds were incubated in a growth chamber at 25 °C for sixteen hours of photoperiod, lighting of 45 μE m^{-2} s^{-1} and 60 percent RH in the aseptic state [91].

3.2.3 DNA Extraction from Germinated Plantlets

1. The entire deoxyribose nucleic acid of *in vitro* grown plantlets was extracted by using Cetyltrimethylammonium bromide following the reported methodology [93] with small amendments. In brief, these steps were followed.

2. 200 mg ice-covered leaves were ground in liquid nitrogen to well powder form.

3. After that 500μL of cetyltrimethylammonium bromide extraction buffer was inserted into it.

4. It was followed by the addition of 20% (40 μL) SDS to each bottle and vortexed for twenty seconds.

5. Incubation was done at 65 °C for half an hour in a water bath with strong shaking.

6. It was followed by the addition of 500μL of phenol, and chloroform (25:24) to all bottles and set on shaking for ten to twenty minutes.

7. At 14000 rpm, centrifugation was done for five minutes.

8. The supernatant was finally transferred into new bottles.

9. 100% chilled ethanol was inserted afterwards, and vortexed at twenty centigrade whole night for the DNA precipitation.

10. The next day, bottles at 14000 rpm were centrifuged for fifteen mins.

11. Pellets were collected and cleaned thrice with seventy percent ethanol.

12. At last, the pellets were suspended in 60μL of TE buffer.

13. Storage was done at 20 °C in a freezer.

14. The DNA concentration and quality were confirmed by taking absorbance at 260 as well as 280 nanometers. The DNA quality was well tested on agarose gel (0.8%) having 3,8-Diamino-5-ethyl-6-phenylphenanthridinium and photographed in Ultraviolet light.

3.2.4   Polymerase Chain Reaction

For the *A. carvifolia* Buch identification, the non-coding region among the *psbA* and *trnH* gene of chloroplast deoxyribonucleic acid was amplified via polymerase chain reaction using the following primers.

pdbA   5'-GTTATGCATGAACGTAATGCTC-3

tmH   5'-CGCGCATGGTGGATTCACAATCC-3

Polymerase chain reaction was performed by following the Khan and Dilshad (2023) methodology. In 200 μL tubes, 25 μL of total reaction volume was prepared. Reagents that were added included concentration of DNA (50 ng), forward primer (0.25 ng), reverse primer (0.25 ng), deoxynucleotide triphosphate 0.2 ng, magnesium chloride 2 mM, Taq pol 0.2 U and polymerase chain buffer 1X [19].

3.2.5   Agarose Gel Electrophoresis

For observing the polymerase chain reaction products, agarose gel electrophoresis was used. For that purpose, agarose gel (1.5 percent w/v) was prepared as follows:

Reagent	Concentration
Agarose gel	1.5 g
TBE buffer (1X)	100 mL
ETBR0.2 microgram/milliliter	2 uL (microgram/milliliter stock)
DNA loading dyes (3μL)	0.25 % bromophenol blue 40 % sucrose

100 voltage was applied in 1X TBE running buffer for one hour. The gel picture was taken via a UV transilluminator.

3.2.6   Decontamination of Polymerase Chain Reaction Product and Sequencing

Polymerase chain reaction product purification was carried out by the quick polymerase chain reaction purification method. After that, the purified products were sequenced by using the dideoxy-chain termination method in ABI Prism 310 Automated DNA. Sequences attained were recognized and examined via using BioEdit software/sequence alignment tool (version 7.2.5.0) [19].

3.3 Silver Nanoparticles Preparation and Characterization

The overview of steps involved in the synthesis and characterization of silver nanoparticles of *A. carvifolia* Buch is given in Figure 3.1.
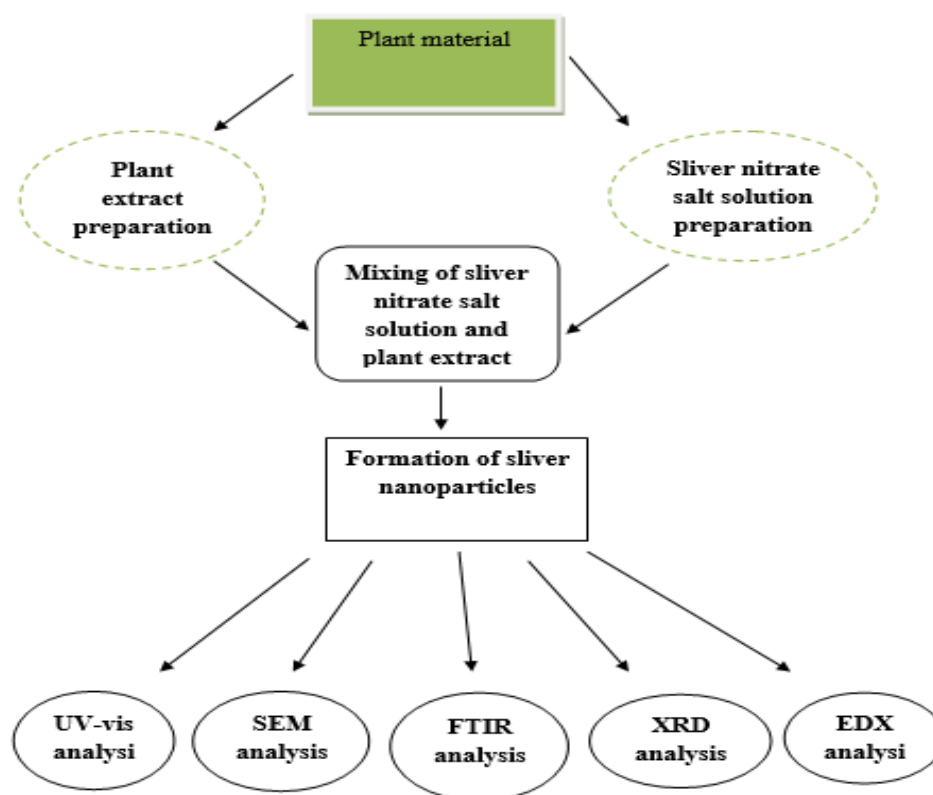
FIGURE 3.1: Overview of nanoparticle synthesis and characterization

3.3.1 Preparation of *A. carvifolia* Buch extract

A. carvifolia Buch plant extract of different concentrations was prepared (10, 20, 40, 80, 160 mg/mL) in a conical flask of 250 mL and boiled for almost 10-15 minutes. The prepared extract was filtered utilizing a Whatman filter paper and stored at 40 °C for further use in nanoparticle synthesis [94].

3.3.2   Synthesis of Silver Nitrate (AgNO$_3$) Salt Solution

The silver nitrate salt solution was prepared (5 mM) by dissolving 425 mg AgNO$_3$ in 500 mL of distilled water under vigorous stirring for about 30 minutes at room temperature [94].

3.3.2.1   Synthesis of Silver Nanoparticles of *A. carvifolia* Buch

A. carvifolia Buch plant extract of different concentrations (10, 20, 40, 80, 160 mg/mL) and 5 mM solution of AgNO$_3$ were mixed in a ratio of 1:9 and put under sunlight for 12 hrs which led to changing the solution color to blackish brown [94]. After centrifugation of the nanoparticle synthesis mixture, the supernatant was removed and pellets were accumulated for sample preparation. The sample was prepared by adding distilled water in the pellets making the concentration of suspension1mg/mL.

3.4   Characterization of Silver Nanoparticles

In the current research work, the characterization of synthesized silver nanoparticles by UV–Vis, SEM, EDX, XRD and FTIR was done according to the reported method [95, 96].

3.4.1   UV–Vis Spectrophotometry

UV–Vis analysis was done by using UV 1602 BMS, UV–Visible spectrophotometer. This was done by placing the reaction mixture in a quartz cuvette, and the absorbance was measured from 300 to 600 nm [97].

3.4.2 Scanning Electron Microscopy (SEM)

In the current research work, the size and morphological details of synthesized nanoparticles were attained by SEM analysis (JEOL-JSM-6490LATM) functioning at 20 kV of the voltage with a counting frequency of 2368 cps. The chemical-based configuration was long-established by EDX (Oxford instruments) coupled with the SEM as plugin hardware. For that purpose, dried AgNPs were mounted on carbon tape and coated with gold sputtering for 2 min and then analyzed. The micrographs at the magnified scale of 10 μm resolution were captured. SEM slides were set up by forming a solution smear on the slides. A coat of platinum thin layer was made so that the samples become conductive [97].

3.4.3 FTIR Analysis

Fourier Transform Infrared spectroscopy is a method adopted to attain an infrared spectrum of absorption or discharge of a gas, solid, or liquid. A Fourier Transform Infrared spectrometer intensely accumulates high-resolution spectral data over a broad spectral range [98]. The bioactive compounds of *A. carvifolia* Buch are involved in the synthesis of nanoparticles and to know the surface chemistry of synthesized nanoparticles FTIR analysis was performed. The AgNPs solution was dried at the temperature of 75 °C and the dried powder of AgNPs was subjected to characterization in the range of 4000–400 cm^{-1} utilizing a KBr pellet strategy [95].

3.4.4 X-Ray Diffraction Analysis

The XRD is a verified, influential method used for identifying the composition phase, arrangement, also crystalline material microstructural features [99]. In this work, the sample preparation for the XRD procedure was done by picking a slight sample solution from the bottle and drying it on a quartz plate [95, 97].

3.5 MTT Assay for Cytotoxicity Analysis

The cytotoxic potential of synthesized nanoparticles was tested by MTT assay against liver cancer HePG2 cell line (obtained from ATCC with ATCC number HB-8065^{TM}) according to the reported procedure [19, 96, 100]. MTT (3-(4,5-dimethylthiazol-2-yl)-2,5-diphenyltetrazolium bromide) is a yellow tetrazolium salt mostly adopted for checking the viability, proliferation, and cytotoxicity of cells. In metabolically active cells, water soluble MTT is reduced in mitochondria by succinate dehydrogenase to insoluble purple formazan crystals. The formazan produced could be quantified spectrophotometrically upon solubilization and is directly proportional to the number of cells viable in culture [101].

3.5.1 Assay procedure

Briefly, DMEM was used for cell culturing which was added to 96 well fat bottom plates in triplicate. The wells were added with the different concentrations (50, 40, 30, 20, and 10 μM) of prepared nanoparticles and plant extract. Afterward, incubation was done for 24 hrs at 37 °C with 5% CO_2. This was followed by the addition of 10 μL MTT (5 mg/mL) incubated at 37 °C for 3 hrs. Finally, solubilization solution (100 μL) was added to the wells and incubated for 2–4 hrs in the dark. Lastly, the sample's absorbance was measured in a microplate reader (at 570 nm) and IC$_{50}$ was calculated.

3.6 Determination of Expression of Target Genes by Real-Time qPCR

Real-time qPCR is a polymerase chain reaction that facilitates the more consistent identification and measurement of product generated in every round of polymerase chain reaction. This method is performed with an oligonucleotide probe that hybridizes to a targeted sequence introduced [102].

Real-time quantitative polymerase chain reaction is a more established process of nucleic acid identification and quantification in biosamples. In a conventional polymerase chain reaction, amplified Deoxyribonucleic Acid products are visualized by end-point analysis. In a quantitative polymerase chain reaction, fluorescence detection methodology is used as the product accumulation could be determined in real-time as the reaction steps forward along the product quantification after each polymerase chain reaction cycle [103].

3.6.1 Procedure of Real-Time qPCR

The determination of expression of target gene *Rap2A* and apoptosis regulatory gene Bax along with the genes of caspases (caspase 3, caspase 8 and caspase 9) were done by real-time qPCR by following the reported methodology [12]. RNA was extracted from control and all the treated/untreated cells, which was used for the synthesis of complementary DNA (cDNA). All untreated/treated cells were washed with phosphate buffer saline (pH 7.2) then RNA extraction was done by using GeneJET RNA Purification Kit (Thermo Fischer Scientific) according to the kit user instruments. Complementary DNA (cDNA) was synthesized using the High-Capacity RNA-to-cDNA™ Kit (Applied Biosystems™) following kit instructions. The confirmation of the cDNA synthesis was done by usual agarose gel electrophoresis, then it was stored at -20 °C for RT qPCR analysis. The qPCR was performed using iTAqTM Universal SYBR Green Supermix (BioRad, Hercules, CA, USA) in a 384-well platform system (ABI Prism® 7900HT sequence detection system, Applied Biosystems, Foster, CA, USA). The gene-specific sets of primers for *Rap2A*, Bax, caspase 3, caspase 8, caspase 9 and housekeeping gene GAPDH30 were used as reported earlier (Table 3.1) [12, 21].

TABLE 3.1: Sequences of primers for the studied genes

Gene Name	Primer Sequences
Rap2A	F: ACAATGGTGGACGAACTCTTT
	R: CAGAACAGCATGGGTCATCT T
Bax	F: CCCGAGAGGTCTTTTTCCGAG
	R: CCAGACCATAGCACACTCGG

TABLE 3.1: Sequences of primers for the studied genes

Gene Name	Primer Sequences
Caspase 3	F: TGCCTGTAACTTGAGAGTAGATGG
	R: CTTCACTTTCTTACTTGGCGATGG
Caspase 8	F: GACAGAGCTTCTTCGAGACAC
	R: GCTCGGGCATACAGGCAAAT
Caspase 9	F: CTCAGACCAGAGATTCGCAAAC
	R: CTCAGACCAGAGATTCGCAAAC
GAPDH	F: AAGCTCATTTCCTGGTATGACAACG
	R: TCTTCCTCTTGTGCTCTTGCTGG

3.7 Determination of the Level of Proteins by ELISA

The ELISA technique uses the catalytic properties of enzymes for the detection and quantification of immunologic reactions. Enzyme-linked immunosorbent assay is a heterogeneous EIA system adopted in clinical analysis [104]. In such a form of the assay, one of the components of the reaction is not specifically adsorbed or bound covalently to the surface of a solid phase, like a microtiter well, a plastic bead, or a magnetic particle. Such a connection makes the separation of bound and free-labeled reactants easy [105]. Final detection is carried out by inserting a substrate that could show a colour. Different substrates are available that are adopted in ELISA detection. Though, the substrates most frequently adopted are horseradish peroxidase and alkaline phosphatase [106].

In the current research work, ELISA kits were used to study the level of proteins of target genes *Rap2A*, Bax and caspase enzymes based on the manufacturer's protocol for *Rap2A* (Abbexa), BAX (Invitrogen) and caspases (Termo-Fisher). Shortly, the lysates of cells were made ready according to the instructions of the ELISA kit. Cell lysate proteins explicitly bound to the primary antibody were spotted by a secondary antibody conjugated with Horseradish peroxidase. Afterward, a microplate reader was used to measure protein levels at the absorbance of 450 nm.

3.8 Determination of Flavonoids Through an HPLC - DAD System

HPLC (High-Performance Liquid Chromatography) technique is a form of column chromatography that is mostly adopted in biochemistry to examine the separation, reorganization, and quantifying of the active chemicals of biological samples. It is mostly adopted as separation technology for separating, detecting and for quantification of drugs [107]. The high-performance liquid chromatography-based flavonoid quantification method is the best way in the chromatographic methods adopted for the analysis of flavonoids because of the different positive features offered, as it requires no derivatization as a result decreases the consumption of time compared to gas chromatography. In addition, this is secure for flavonoid analysis, because to avoid the risk of decomposition of flavonoids at higher temperatures, it could be functioned at room temperature [108].

3.8.1 Chemicals and Reagents

All the chemicals and reagents that were used were of HPLC grade which included methanol, n-hexane, ethyl acetate and acetonitrile. It also included the standards used for flavonoid analysis (ferulic acid, apigenin, caffeic acid, syringic acid, rutin, gallic acid, vanillic acid, rhamnetin and quercetin).

3.8.2 Standard's Stock Solution Preparation

Stock solutions of all standard flavonoids (ferulic acid, apigenin, caffeic acid, syringic acid, rutin, gallic acid, vanillic acid, rhamnetin and quercetin) at the conc. of 1000 ppm were synthesized in methanol and reserved at -20 °C till use. Moreover, serial dilutions including 40, 20, 10 and 5 ppm were prepared from this stock solution. This was done to generate a calibration graph for the examination of studied flavonoids qualitatively and quantitatively in crude extracts [19].

3.8.3 Preparation of Plant Extract

Extracted flavonoids from the young plant of *A. carvifolia* Buch were done according to the reported method [19]. In brief, 10 milligrams of dry powder plant material was extracted at a concentration of 1000 μg/mL methanol at room temperature in a sonication bath (40 KHz, Branson) for fifteen minutes. After that the extract was centrifuged at 13000 rpm for 5 min and the supernatant was shifted to a fresh vial. Three times this process was repeated and subsequently, supernatant was taken. After that, the drying of the extract was done in a vacuum cell at 50 ^{o}C and then liquified in 200 μL solvent mixture of methanol: water (2:1). After that, filtration was done by using a PTFE 0.45 μm membrane filter and transferred to vials for HPLC analysis.

3.8.4 Analysis of Flavonoids by HPLC

In the current study, flavonoids in extracts of *A. carvifolia* plants were measured using HPLC-DAD analysis following the reported protocol [19]. For this purpose, 1000 μg/mL methanolic extracts of dry *A. carvifolia* shoots were used. Moreover, standard stock solution, including ferulic acid, apigenin, caffeic acid, syringic acid, rutin, gallic acid, vanillic acid, rhamnetin and quercetin were prepared in methanol at 1000 μg/mL concentration. The injection volume was 20 μL at a flow rate of 1 mL/min. Polyphenols in the extract were discovered by comparing their wavelength and retention rates with those of reference standards (Table 3.2).

TABLE 3.2: Detail of identified flavonoids with retention time and wavelength

S.No.	Standards	Wavelength (nm)	RT (retention time)(min)
1	Vanillic Acid	257	9.1
2	Rutin	257	12.7
3	Gallic Acid	279	3.7
4	Catechin	279	7
5	Syringic Acid	279	9.8
6	Coumaric Acid	279	13.8
7	Geutisic Acid	325	7.5
8	Caffeic Acid	325	9.3
9	Quercetin	370	15.2

3.9 Statistical Analysis

All the data was obtained in replicates of three, and the values are presented as the mean $\pm$ standard error (SE) of the mean. Two-way ANOVA was used to analyze the collected data statistically using the V.5 software of Graph Pad Prism. The p-value which was less than 0.05 was well thought out and statistically significant.

3.10 In silico Analysis of Detected Flavonoids
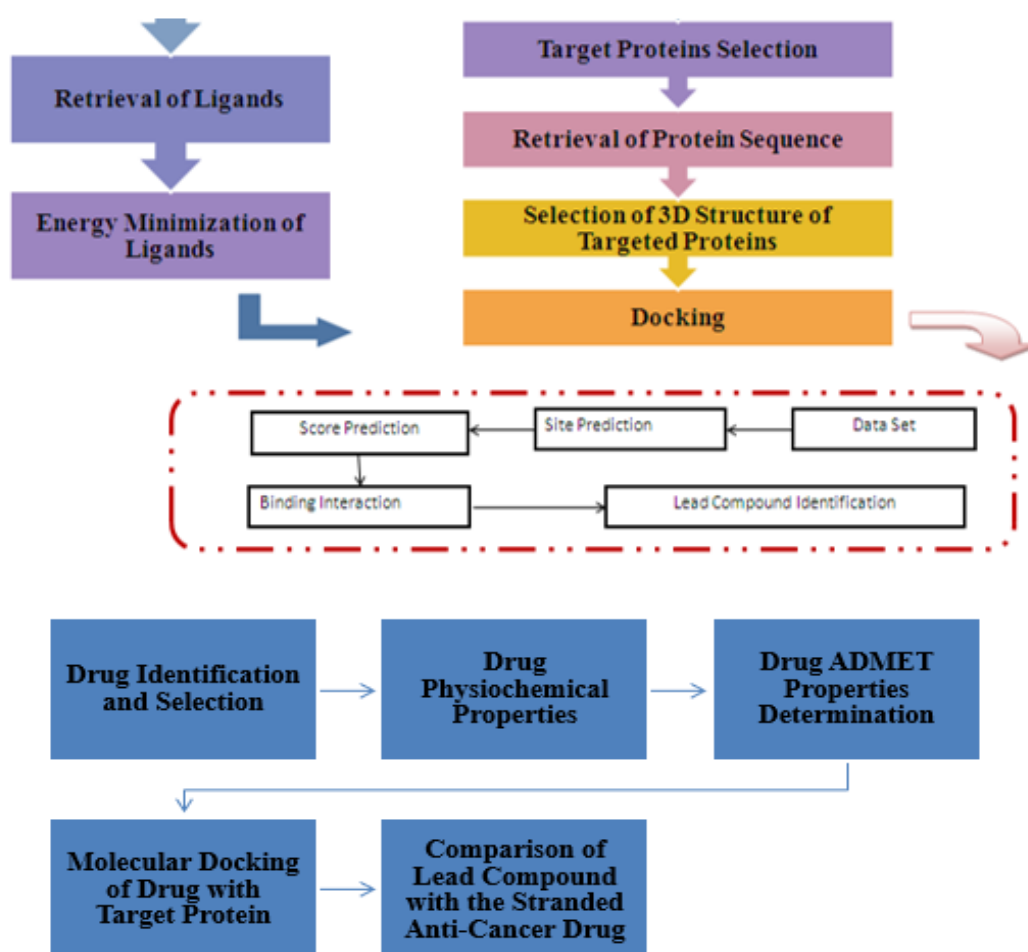
FIGURE 3.2: Methodology scheme of Insilco study of flavonoids
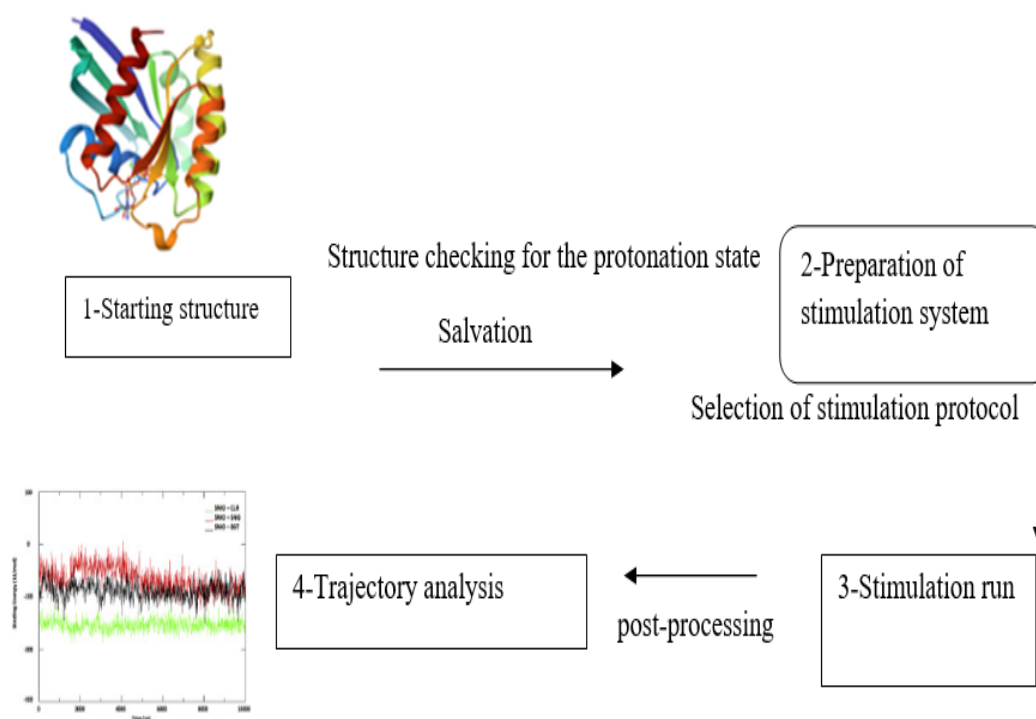
FIGURE 3.3: Overall methodology of molecular dynamic (MD) simulation

3.10.1 Selection of Ligands

PubChem database is an open-access database, which is mostly used to collect chemical information regarding ligands or bioactive compounds and the pharmacological activities of these chemical substances [109]. These databases are used to retrieve different ligand's 2D structures. The structures of polyphenols of *A. carvifolia*, identified through HPLC were downloaded from the PubChem database. Minimization of ligand's energy was carried out by Chempro software chem12 [109].

3.10.2 Ligands Preparation for Molecular Docking

Selected ligands from the PubChem database and standard drug lenvatinib (currently being used against liver cancer) from the drug bank database were tested for their drug likeliness following the Lipinski rule of five which is a rule to evaluate drug-likeness or determination of chemical compounds with certain pharmacological and biological activities that would make it a likely orally active drug. The

potential success of compounds depends on their ADMET properties. PKCSM an online tool was used to find ADMET properties of ligands [110]. For the molecular docking process, the CB dock online docking tool was used for the molecular docking process [111].

Analysis of the docked complex was done by Ligplot+, a protein-ligand interaction software that automatically generated a diagram of protein-ligand interactions. These interactions were modified through hydrophobic and hydrogen bonds. Ligplot+ generated a 2D representation of the protein-ligand complex. The complex file, in PDB format, was opened in Ligplot+ and the H-bonds and hydrophobic interactions of docked molecules were examined. The RMSD and RMSF values were calculated [112].

3.10.3   Retrieval and Analysis of Protein Structures

Rap2A protein with pdb id 2rap was selected from the protein data bank (PDB) and the 3D structure of *Rap2A* was downloaded in pdb format [113]. The primary sequence of the selected protein *Rap2A* was retrieved from the uniport database with accession number P10114 and a residue length of 183 amino acids. ProtParam Expasy was used to determine and analyze physical and chemical properties of proteins such as molecular weight, instability index, Extension Coefficient, theoretical PI, positively and negatively charged particles and grand average of hydrophobicity [114]. The refining of protein 3D structure is a very important step for the molecular docking process. All spare water molecules and complex molecules were detached from the protein structure. For visualization and refining of 3D structures, Pymol software was used [115]. To find the functional domain of the selected protein, the Interpro database was used [116].

3.10.4   Molecular Docking

Molecular docking is a type of computational modeling that allows for the prediction of the binding orientation of one chemical compound (ligand) to another molecular

compound (receptor) to create a stable complex. The molecular docking process is frequently used to predict the binding alignment of small molecules. For the molecular docking process, the CB dock online docking tool was used [111].

In CB-Dock, the ligand and protein docking process identifies the binding sites automatically and estimates the size and center also, the docking box is customized by query ligand after it performs the molecular docking with AutoDock Vina [117]. This cavity-focused docking could increase the accuracy of blind docking and hit ratio. So, for that reason, CB-Dock could make the process of docking easy by improving the accuracy of the binding site prediction of target proteins by adopting the curvature-based cavity detection approach. Similarly, also predicts the query ligand's binding pose by adopting AutoDock Vina [118].

3.10.5   Analysis of Docked Complex Via LigPlot plus

LigPlot is a computational program that makes the 2D schematic presentation of protein and ligand complexes from PDB file input [119]. In current research work, analysis of the docked complex was done by ligplot plus protein-ligand interaction software which automatically generated a diagram of protein ligand interactions. These interactions were modified through hydrophobic and hydrogen bonds. The ligplot plus generated a 2D representation of the protein-ligand complex [120].

The complex file, in PDB format, was opened in Ligplot and the H-bonds and hydrophobic interactions of docked molecules were examined. The RMSD and RMSF values were calculated [112].

3.10.6   Molecular Dynamic (MD) Simulation

Molecular dynamic simulation has evolved as the most powerful method to investigate and analyze biomolecules. MD simulation technique was developed in the late 70s and it has been applied over a range of atoms including membrane embedded proteins, nucleosomes, ribosomes and large complexes [121]. The aim of this work was to carry out molecular dynamic simulations considering the characteristics of

molecular assemblies in terms of their structures along with connections among them. It was performed to check the interactions of selected proteins with different ligands to examine which ligand was showing the best interaction with selected protein *Rap2A*. In this work, the interaction of *Rap2A* was examined with the four best docked and analyzed ligands. It also examined selected protein's interaction with synthetically designed standard drug.

To perform simulations high performance computers were used and simulation was done with the help of the GROMACS software package [122]. This software used OPLS-AA as a force field. There were specific commands for running the simulation and they were given by using the PuTTY software. The supercomputer domains were accessed by using WinSCP [123]. Before running the molecular simulation, a specific supercomputer screen was selected on the basis of its load. Next, the screen number was added and the protein complex folder was accessed. Later, the MD simulations were started to run. The first command was run for solvating the protein complex in a cubic box with the water molecules. The Na^+ and Cl^- ions were incorporated too. Next, the energy minimization commands were run and the energy values were saved for 50,000 steps. After this, the commands for pressure and volume were run too. The last command subjected the protein complex to 20 ns molecular simulation. After the entire trajectory was completed, the analysis commands for RMSD (root mean square deviation), RMSF (root mean square fluctuations), the radius of gyration, surface accessibility and no. of hydrogen bonds were run. These commands were put up for analyzing the compactness, flexibility, stability and interaction of the protein complex in the cellular environment.

Chapter 4

Results

This chapter describes the results of all the steps taken to achieve the objectives of the study including preparation of plant extract, synthesis and characterization of silver nanoparticles via UV-vis spectrophotometer analysis, Scanning Electron Microscopy, X-ray Diffraction spectroscopy, Energy Dispersive X-ray spectroscopy and Fourier Transform Infrared spectroscopy, MTT assay, real-time qPCR, determination level of protein by ELISA, statistical analysis, determination of flavonoids content through an HPLC-DAD system and drug designing for targeted cancer causing gene *Rap2A*. All the step-wise results are described under headings sequentially.

Objective 1: To identify the anti-proliferative role of *A. carvifolia* Buch plant extract and its respective metallic (silver) nanoparticles against liver cancer cell lines and their impact on the expression of liver cancer target gene, apoptotic pathway genes and protein.

4.1 Plant Identification

After amplification of the *psbA-trnH* region (500 bp) of chloroplast genome and sequencing of an amplified region of DNA, Basic Local Alignment Search Tool (BLAST) in NCBI and CLUSTAL-W in BioEdit software (version 7.2.5.0) was

performed. Reference sequence (Gene Bank Accession number [NCBI: FJ418751]) was used for the identification of the plant under study. It was confirmed to be a *psbA-trnH* sequence of *A. carvifolia* Buch [92]. The plant specimen was submitted in the herbarium of Quaid-i-Azam University Islamabad, Pakistan with specimen voucher no. HMP-ART 0001. All the experiments were conducted following the institutional, national, and international guidelines for conducting plant research. Ethical approval was obtained from the departmental ethical review committee with reference no. CUST-2022/2 (Annexure I).

4.2 Sliver Nanoparticles Synthesis

Synthesis of silver nanoparticles was done successfully by mixing plant extract and silver nitrate salt solution. The color change from yellowish to dark brown indicated the complete formation of silver nanoparticles. The formation of AgNPs was confirmed by solution color change. The color change was observed 30 minutes after plant extract insertion in sliver nitrate salt solution. The pure color of the silver nitrate solution did not change during the whole time of incubation. The reduction of silver ions occurred when the extract of the plant was added which resulted in the formation of dark brown AgNps (Figure 4.1 & 4.2)
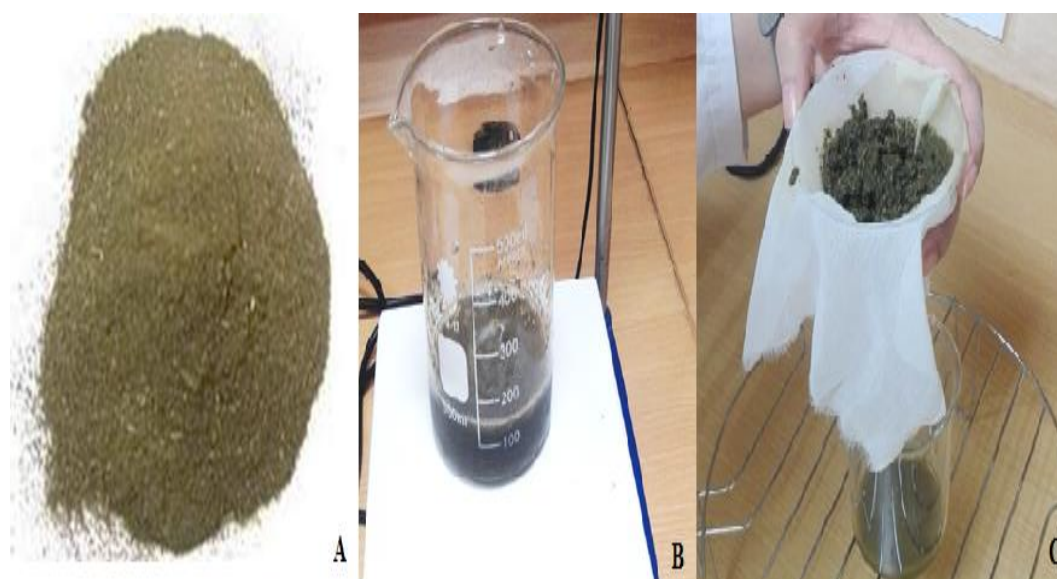
FIGURE 4.1: (A) Powdered form of *A. carvifolia*. (B) *Extract preparation*. (C) Filtration of *A. carvifolia* plant extract.

FIGURE 4.2: Silver nanoparticles after centrifugation (A and B). Synthesized silver nanoparticles in powder form (C).

4.3 AgNps Characterization

4.3.1 AgNps Analysis via UV-vis Spectrophotometer

AgNps synthesis was confirmed via UV-vis spectrophotometer which was adopted for the determination of optical properties of synthesized nanoparticles. In the current research work, confirmation of nanoparticle synthesis was done by observing a strong peak at 450 nm. SPR (surface plasma resonance) is responsible for maximum absorption in the range of 400-500 nm in UV-Vis spectrometry. Different concentrations of *A. carvifolia* extracts 10, 20, 40, 80 and 160 mg/L were adopted to optimize the synthesis of silver nanoparticles. There was observed a 1.5 times increase in the absorbance of the nanoparticle's suspension with an increase in the concentration of plant extract. The highest absorbance was observed when nanoparticles were prepared with 160 mg/L of plant extract (Figure 4.2).
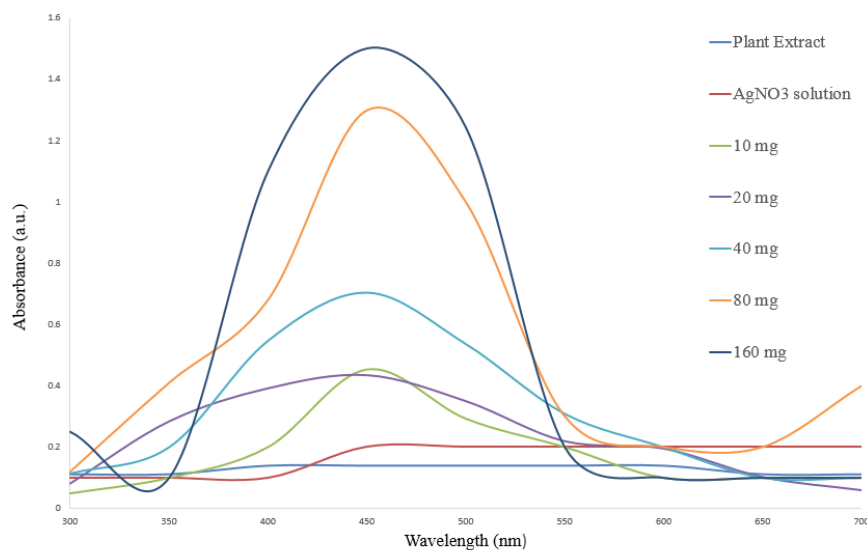
FIGURE 4.3: UV-vis spectroscopy of synthesized AgNPs. The spectra display the absorption peaks of AgNPs synthesized by different concentrations of plant extract at 450 nm wavelength.

4.3.2 AgNps Analysis via SEM

Scanning Electron Microscopy analysis was implemented to find the AgNps size and their morphological features. SEM analysis gave a comprehensive understanding of the size and morphology of the green synthesized silver nanoparticles. The nanoparticles were found with a calibrated size of 80±6 nm. Furthermore, the shape of silver nanoparticles was found to be icosahedron (polyhedral) (Figure 4.4).
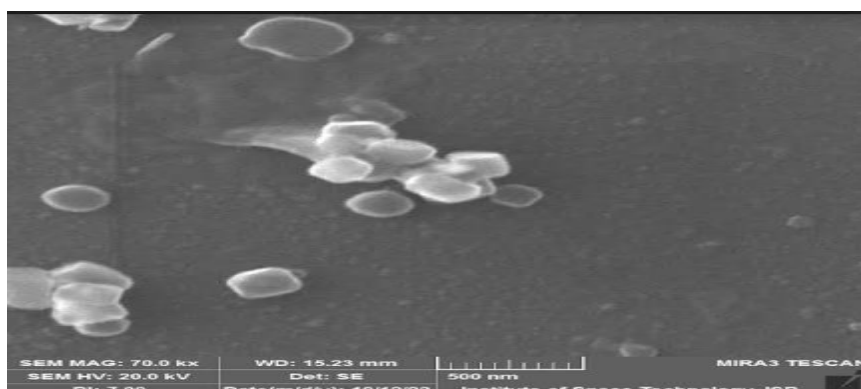
FIGURE 4.4: SEM analysis of AgNPs: The image shows the morphology of the AgNPs at 500 nm.

4.3.3 AgNps Analysis by FTIR

For determining the different biological molecules present in *A. carvifolia* Buch extract which were involved in the preparation of AgNps, FTIR analysis was adopted by using an FTIR spectrophotometer. FTIR was carried out to find the latent natural compounds in *A. carvifolia* Buch plant extract which were involved in the synthesis of nanoparticles. The spectra depicted changes between 800 and 1500 cm^{-1} which confirmed the involvement of flavonoids, phenolics and lipid-containing oils having aldehydes and ketonic bonds represented in the extract of the plant under study (Figure 4.5). Ketones with carbonyl (C–O) stretching vibration were observed at 1000–1140 cm^{-1}. It was confirmed from FTIR investigations, that the amino acid and proteins resulting in carbonyl gatherings have the extra beached capacity to bind with metal, displaying that the proteins might be involved in shaping the metal nanoparticles. Similarly, the=C–O stretching between the 1100–1350 cm^{-1} may go with the lipid's carboxyl groups. There was observed change in the range of 1331–1334 cm^{-1} showing the involvement of carboxyl groups in the synthesis of the silver nanoparticles.
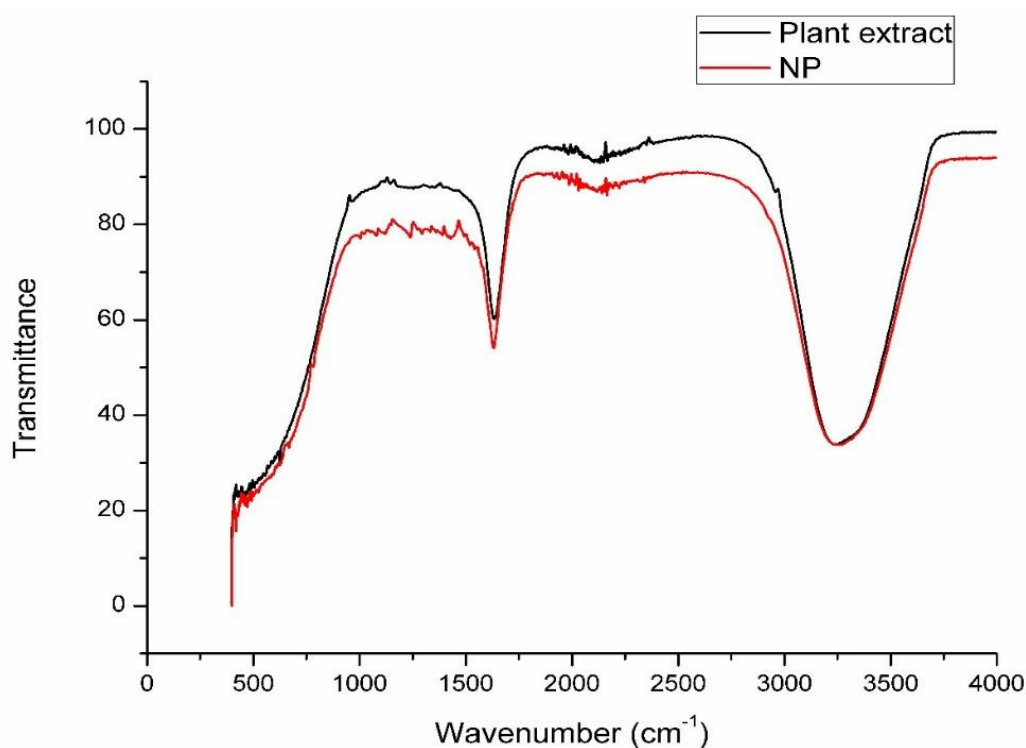
FIGURE 4.5: FTIR of synthesized silver nanoparticles and plant extract.

4.3.4 Analysis of AgNps through EDS

The chemical composition of synthesized AgNps was determined by Energy Dispersive X-Ray Spectroscopy equipped with Scanning Electron Microscopy. It was confirmed from the EDX spectrum that Ag is the main constituent found in the sample (Figure 4.6). Moreover, EDX was used to study the elemental composition of silver nanoparticles which showed silver as the major element (Table 4.1).

TABLE 4.1: Elemental composition of EDS spectrum.

Element	Weight%	Atomic%
C K	2.92	16.64
O K	5.84	24.97
S K	0.15	0.31
Fe K	0.59	0.72
Ag K	90.50	57.36
Totals	100.00	
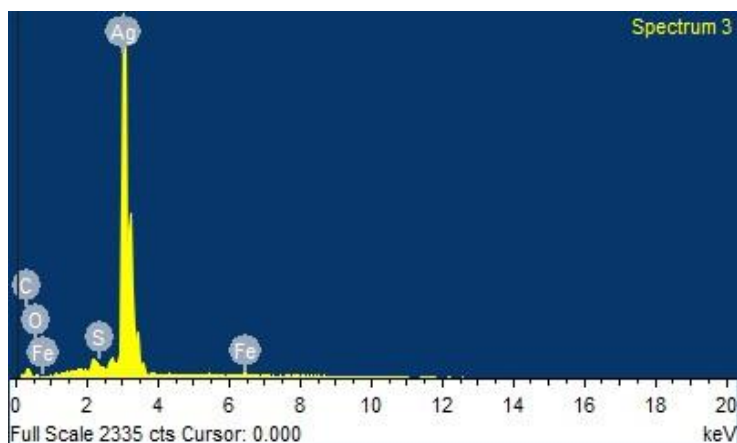
FIGURE 4.6: EDS of AgNPs displaying major peaks of silver (Ag).

4.3.5 Analysis of AgNPs through XRD

The structural nature of nanoparticles either amorphous or crystalline was confirmed by X-ray Diffraction spectroscopy. A characteristic XRD pattern was generated which gave unique fingerprints of crystal present in the sample. Interpretation was

done properly by comparison with standard reference patterns. In the current study, X-ray crystallography results showed the crystalline nature of silver nanoparticles with identified peaks [38.23 (1 1 1), 44.41 (2 0 0), 64.38 (2 2 0), 77.5 (3 1 1)] at 20^0 (Figure 4.7). These findings were found in agreement with the standard ICSD No. 98–018-0878 [96, 124].
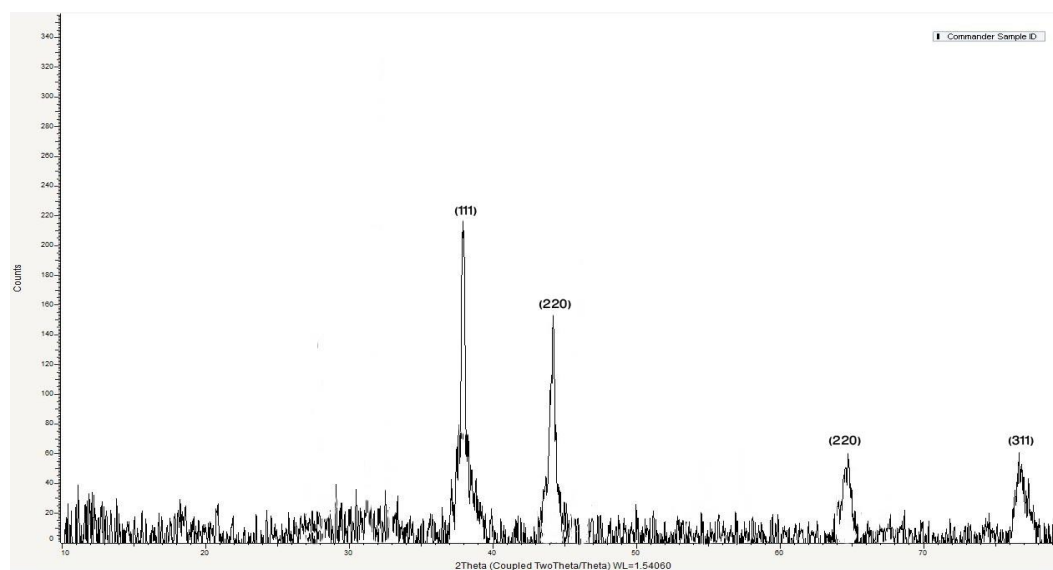
FIGURE 4.7: XRD analysis of AgNPs.

4.4 Cytotoxicity Assay

The cytotoxic potential of plant extract and synthesized silver nanoparticles was tested against liver cancer cell lines HepG2 (Figure 4.8). In this study, four different concentrations of synthesized silver nanoparticles and plant extract (10, 20, 30, 40 and 50 μM) were used to study their cytotoxicity. The percentage cell viability of HePG2 cells was found to be decreased more at the higher concentration (50 μM) than at the lower concentration (10 μM). Plant extract and silver nanoparticles showed cytotoxicity in a concentration dependent manner indicating their increased cytotoxicity at higher concentrations. Furthermore, IC$_{50}$ of silver nanoparticles was found 2.57 μM for HepG2 cells, while for plant extract it was 11.57 μM. The statistical significance of the data was also observed with p<0.0001 (Table 4.2).

Analysis of variance for factors affecting the viability of HePG2 Cells is also shown in Table 4.2.
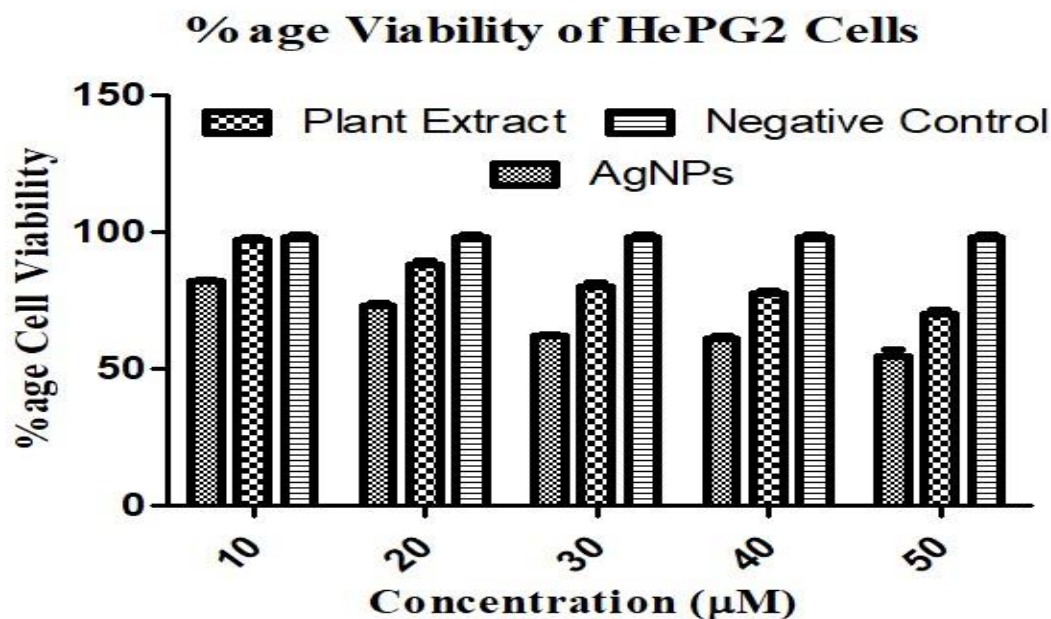
FIGURE 4.8: Antiproliferative activity of silver nanoparticles: Percentage (%) cell viability of HePG2 cell line after treatment with silver particles and plant extract.

TABLE 4.2: Analysis of variance for factors affecting the viability of HePG2 Cells

Source of Variation	Df	Sum-of-squares	Mean square	F-Value	P Value	Sig.
Interaction	8	1122	140.3	12.11	<0.0001	Yes
Types of Nanoparticles	2	10330	5163	445.9	<0.0001	Yes
Concentration	4	561.0	140.3	12.11	<0.0001	yes
Residual	30	347.3	11.58			

4.5 Gene expression Studies by Real time-qPCR

The level of expression of the target gene of liver cancer (*Rap2A*) in silver nanoparticles and plant extract treated HePG2 cells was found to be significantly decreased

as compared to untreated cells indicating its role as an oncogene in liver cancer (Figure 4.9). The experiment was run with the IC_{50} of plant extract and synthesized silver nanoparticles and it was observed that expression of *Rap2A* gene was decreased more prominently in HePG2 cells treated with synthesized silver nanoparticles than that of plant extract.

Furthermore, the stimulatory effects of synthesized silver nanoparticles and plant extract on the Bax gene up-regulation were also studied (Figure 4.10). Similarly, the experiment was run with the IC_{50} of plant extract and synthesized silver nanoparticles against HepG2 cell lines. Synthesized silver nanoparticles caused more upregulation of the Bax gene in HePG2 cells than that of plant extract. High levels of expression of the Bax gene suggested the role of silver nanoparticles in HePG2 cell apoptosis through an intrinsic apoptotic pathway.

Moreover, caspase-3, caspase-8 and caspase-9 genes were also evaluated for relative gene expression to determine the apoptotic role of synthesized silver nanoparticles against treated cells. It was found that plant extract and silver nanoparticles brought up-regulation of all studied caspase gene expression in HepG2 cells (Figures 4.11 to 4.13). Silver nanoparticles showed more efficacy than those of the plant extract. The data was also found statistically significant (p<0.0001) by 2-way ANOVA (Table 4.3)
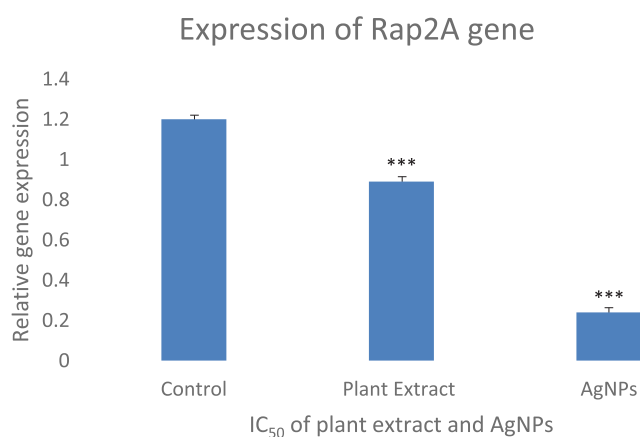
FIGURE 4.9: Gene expression studies by Real-time, showing the level of expression of *Rap2A*.

Error bars indicate the standard error (SE) of three means, asterisk represents the significant difference in data compared with control at *P less than 0.05, **P less than 0.01 and ***P less than 0.001.

Expression of Bax gene
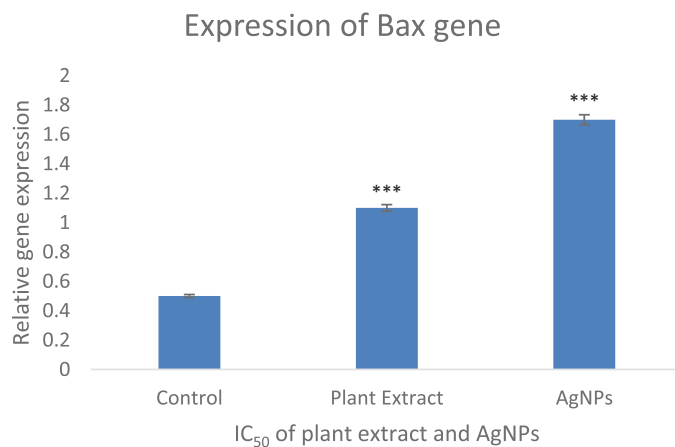
FIGURE 4.10: Gene expression studies by Real-time, showing the level of expression of the Bax gene.

Error bars indicate the standard error (SE) of three means, the asterisk represents the significant difference in data compared with control at *P less than 0.05, **P less than 0.01 and ***P less than 0.001

Expression of Casp 3 gene
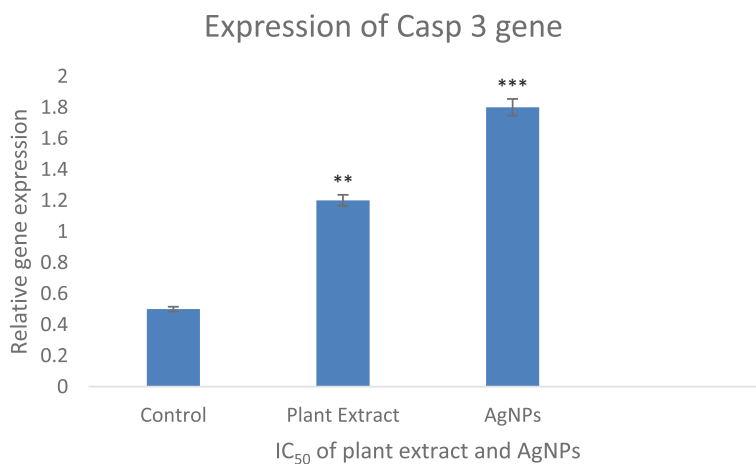
FIGURE 4.11: Gene expression studies by Realtime-qPCR, showing the level of expression of caspase 3.

Error bars indicate the standard error (SE) of three means, asterisk represents the significant difference in data compared with control at *P less than 0.05, **P less than 0.01 and ***P less than 0.001

Expression of Casp 8 gene
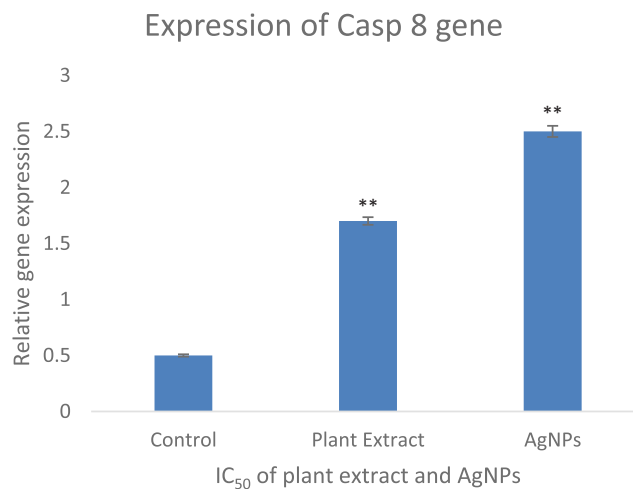
FIGURE 4.12: Gene expression studies by Realtime-qPCR, showing the level of expression of caspase 8.

Error bars indicate the standard error (SE) of three means, asterisk represents the significant difference in data compared with control at *P less than 0.05, **P less than 0.01 and ***P less than 0.001

Expression of Casp 9 gene
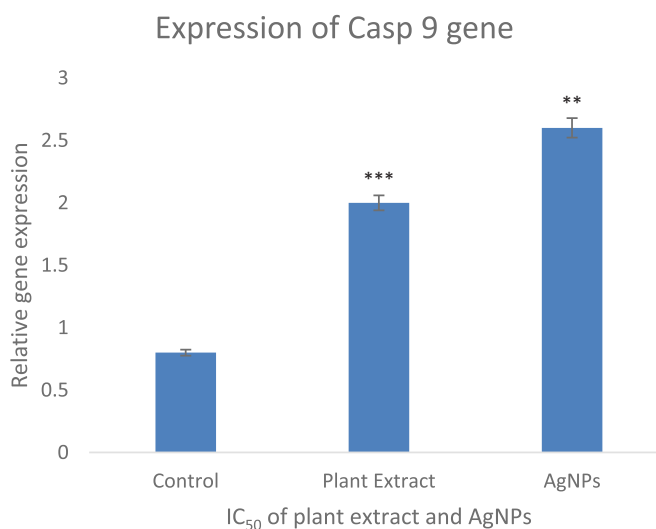
FIGURE 4.13: Gene expression studies by Realtime-qPCR, showing the level of expression of caspase 9.

Error bars indicate the standard error (SE) of three means, asterisk represents the significant difference in data compared with control at *P less than 0.05, **P less than 0.01 and ***P less than 0.001

TABLE 4.3: Analysis of variance for factors affecting the gene expression

Source of Variation	Df	Sum-of-squares	Mean square	F-Value	P Value	Sig.
Interaction	8	4.504	0.5630	16.39	<0.0001	Yes
Types of genes	4	3.589	0.8974	26.12	<0.0001	Yes
Silver nanoparticles and plant extract	2	4.763	2.382	69.34	<0.0001	yes
Residual	15	0.5153	0.03435			

4.6 Protein Levels Determination by ELISA

Furthermore, the level of proteins of all studied genes was also evaluated and similar findings were observed which confirmed the activation of programmed cell death of nanoparticles treated HepG2 cells. In this work, the *Rap2A* protein was found to be decreased in plant extract and silver nanoparticles treated cells, whereas the level of Bax and caspase-3, caspase-8 and caspase-9 proteins were found to be increased in the HePG2 cells treated with silver nanoparticles and plant extract. Likewise, synthesized silver nanoparticles caused more downregulation of *Rap2A* protein and more upregulation of apoptotic proteins than plant extract (Figures 4.14). Moreover, the protein levels of Bax (key gene in extrinsic IL-3 mediated apoptosis cascade), CASP 3 (the chief executioner of programmed cell death in extrinsic and intrinsic signaling cascade), CASP 8 (starter gene in TNF-α apoptosis cascade) and CASP 9 (starter gene in intrinsic apoptosis cascade) were found increased in HepG2 cells as compared to control group (untreated cells) signifying the cytotoxic role of synthesized silver nanoparticles in the activation of apoptotic pathway (Figure 4.15 - 4.18). Data was also found statistically significant when tested by 2-way ANOVA with p<0.0001 (Table 4.4).

Level of Rap2A protein
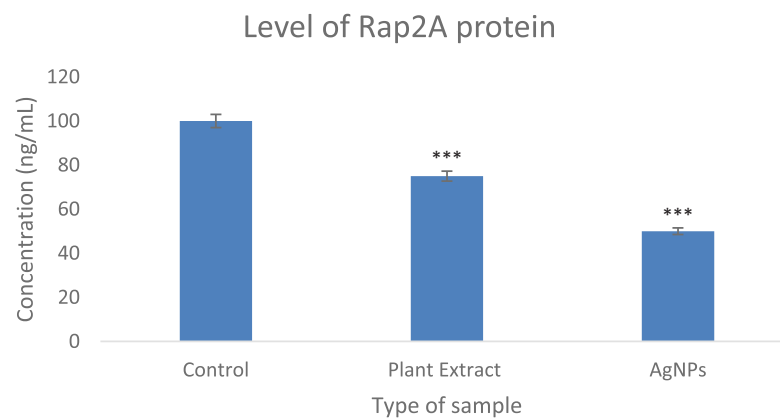
FIGURE 4.14: Protein levels determination by ELISA: showing the level of *Rap2A* protein.

Error bars indicate the standard error (SE) of three means, asterisk represents the significant difference in data compared with control at *P less than 0.05, **P less than 0.01 and ***P less than 0.001.

Level of Bax protein
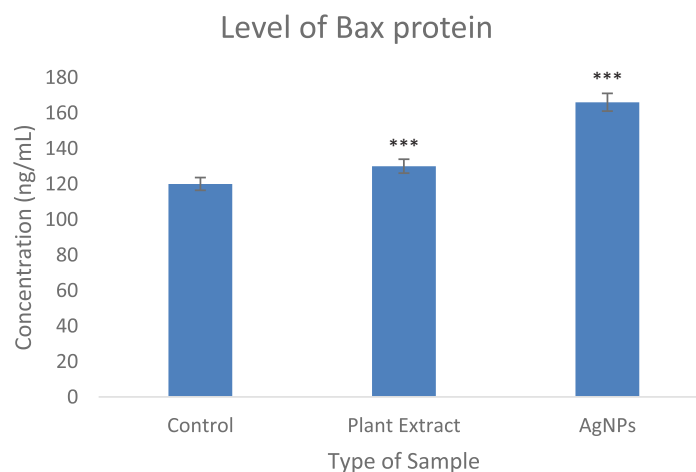
FIGURE 4.15: Protein levels determination by ELISA: showing the protein level of Bax protein.

Error bars indicate the standard error (SE) of three means, asterisk represents the significant difference in data compared with control at *P less than 0.05, **P less than 0.01 and ***P less than 0.001.

Level of caspase 3 protein
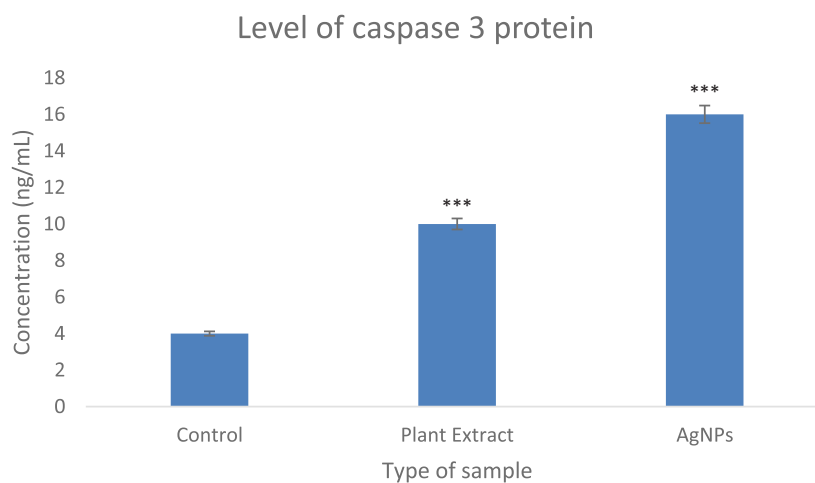
FIGURE 4.16: Protein levels determination by ELISA: showing the protein level of caspase 3 protein.

Error bars indicate the standard error (SE) of three means, asterisk represents the significant difference in data compared with control at *P less than 0.05, **P less than 0.01 and ***P less than 0.001.

Level of caspase 8 protein
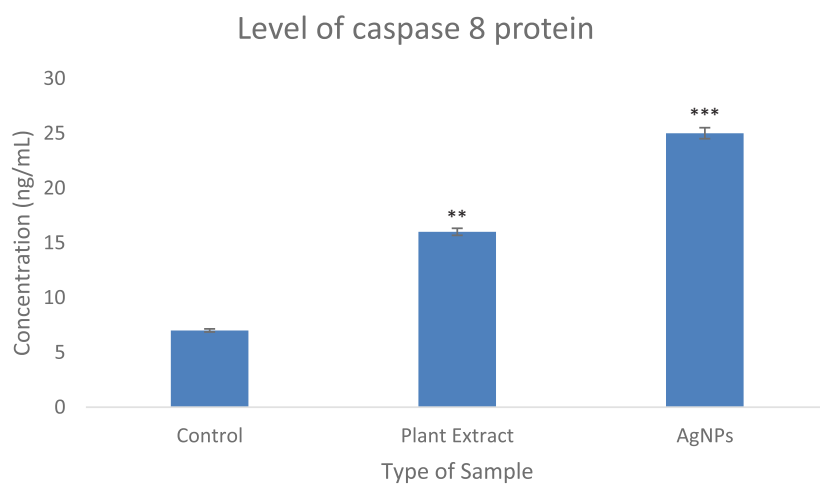
FIGURE 4.17: Protein levels determination by ELISA: showing the protein level of caspase 8 protein.

Error bars indicate the standard error (SE) of three means, asterisk represents the significant difference in data compared with control at *P less than 0.05, **P less than 0.01 and ***P less than 0.001.
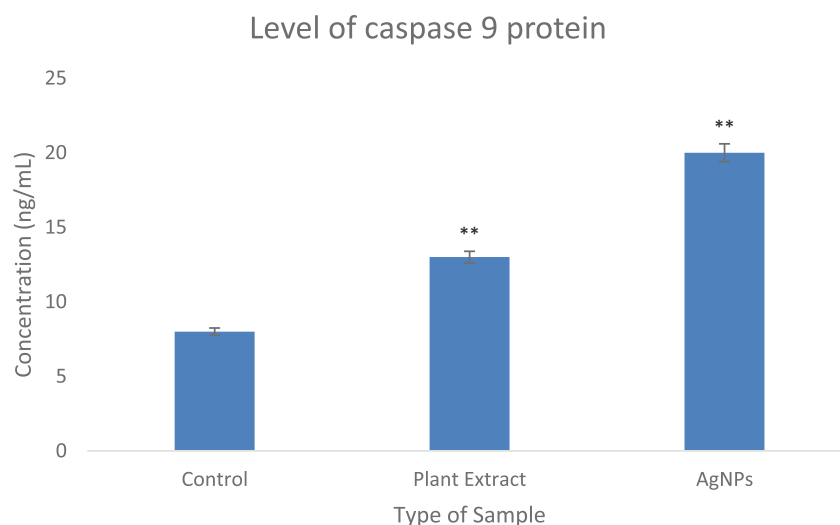
FIGURE 4.18: Protein levels determination by ELISA: showing the protein level of caspase 9 protein.

Error bars indicate the standard error (SE) of three means, asterisk represents the significant difference in data compared with control at *P less than 0.05, **P less than 0.01 and ***P less than 0.001.

TABLE 4.4: Analysis of variance for factors affecting the level of proteins

Source of Variation	Df	Sum-of-squares	Mean square	F-Value	P Value	Sig.
Interaction	8	16580	2073	68.25	<0.0001	Yes
Types of Protein	4	37870	9468	311.8	<0.0001	Yes
Silver nanoparticles and plant extract	2	19160	9579	315.4	<0.0001	yes
Residual	15	455.5	30.37			

Objective 2: To analyze the role of bioactive compounds of *A. carvifolia* Buch against liver cancer target gene (*Rap2A*) through computational approaches and to perform molecular dynamics simulation against selected ligands.

4.7 Determination of Polyphenols by HPLC

Qualitative and quantitative analysis of flavonoids of *A. carvifolia* Buch (ferulic acid, apigenin, caffeic acid, syringic acid, rutin, gallic acid, vanillic acid, rhamnetin and quercetin) was performed via HPLC. In this research work, the absorption spectra and retention time of 9 standard polyphenols including ferulic acid, apigenin, caffeic acid, syringic acid, rutin, gallic acid, vanillic acid, rhamnetin and quercetin were used to study the HPLC profile of methanolic extract of *A. carvifolia* Buch. It was observed that the highest concentration found was that of rhamnetin which was 1.65 μg/mg. The second highest concentration found was that of apigenin (1.39 μg/mg) while the lowest concentration found was that of quercetin (0.12 μg/mg) (Figure 4.19).
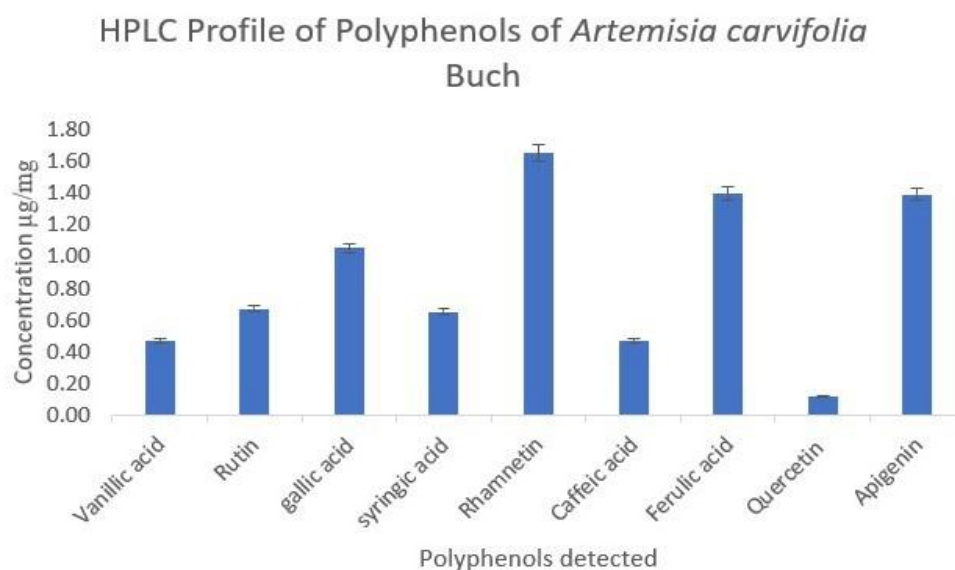
FIGURE 4.19: HPLC Profile of polyphenols of *A. carvifolia* Buch methanolic extract.

4.8 Ligands Preparation

The 2D structures and information of identified ligands of *A. carvifolia* through HPLC i.e. apigenin, caffeic acid, gallic acid, rhamnetin, rutin, ferulic acid, syringic acid, vanillic acid and quercetin and standard drug lenvatinib were downloaded

from PubChem database (Table 4.5), which is an open access database, mostly used to collect chemical information regarding ligands or bioactive compounds. This database is a public repository for information on chemical substances and their biological activities. Minimization of ligands energy was carried out by Chempro software chem12. This is a compulsory step in the designing of ligands/chemical substances before docking as without it, there would be unpredictable vina scores in the outcomes of the docking.

TABLE 4.5: Ligands of *Artemisia carvifolia* Buch.

S. No.	Ligand	Ligand CID No.	Molecular Formula	Molecular Weight	2D Structures
1	Apigenin	5280443	C15H10O5	270.24g/mol	
2	Caffeic acid	689043	$C_9H_8O_4$	180.16 g/mol	
3	Gallic acid	370	C7H6O5	170.12g/mol	
4	Rhamnetin	5281691	C16H12O7	316.26 g/mol	
5	Rutin	5280805	C27H30O16	610.5 g/mol	
6	Ferulic acid	445858	C10H10O4	194.18 g/mol	
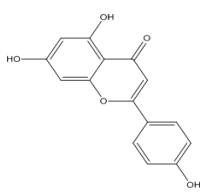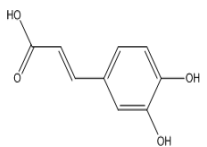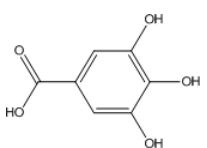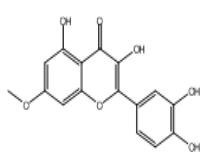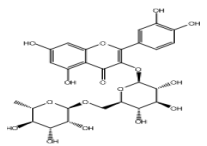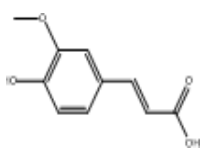
TABLE 4.5: Ligands of *Artemisia carvifolia* Buch.

S. No.	Ligand	Ligand CID No.	Molecular Formula	Molecular Weight	2D Structures
7	Syringic acid	10742	C9H10O5	198.17 g/mol	
8	Vanillic acid	8468	C8H8O4	168.15 g/mol	
9	Quercetin	5280343	C15H10O7	302.23 g/mol	
10	Lenvatinib	9823820	C21H19 ClN4O4	426.9 g/mol	
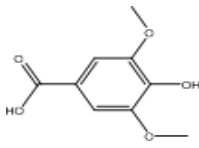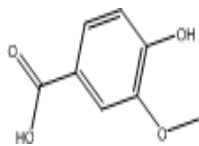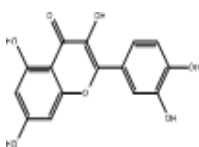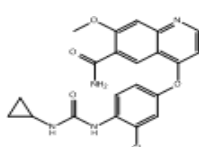
4.9 Protein's Primary Sequence Retrieval

The primary sequence of the selected protein *Rap2A* was retrieved from the uniport database with accession number P10114 and a residue length of 183 amino acids. The UniProtKB Proteomes portal provides access to more than 451000 proteomes, which are sets of protein sequences originating from completely sequenced viral, bacterial, archaeal and eukaryotic genomes. The primary sequence of the selected protein *Rap2A* is given below

>sp|P10114|*RAP2A*_HUMAN Ras-related protein Rap-2a OS=Homosapiens OX = 9606 GN = *RAP2A* PE = 1 SV = 1

MREYKVVVLGSGGVGKSALTVQFVTGTFIEKYDPTIEDFYRKEIEVDSSPSVL
EILDTAGTEQFASMRDLYIKNGQGFILVYSLVNQQSFQDIKPMRDQIIRVKRY
EKVPVILVGNKVDLESEREVSSSEGRALAEEWGCPFMETSAKSKTMVDELFA
EIVRQMNYAAQPDKDDPCCACNIQ

4.10   Physiochemical Properties Analysis

The physicochemical properties of selected protein determined by ProtParam
Expasy an online tool is given in Table 4.6. It included molecular weight, instability
index, extension coefficient, theoretical PI, positively and negatively charged
particles and grand average of hydrophobicity.

TABLE 4.6: Physicochemical properties of *Rap2A* gene.

Number of Amino Acid	Molecular Weight	Instability index (II)	Extension cofficient1	Extension coefficient 2	Theoretical PI	Positively charged particles	Negatively charged particles	GRAVY
183	20615.46	44.34	16180	15930	4.73	21	29	-0.208

4.11 Identification of Functional Domains and 3D Structure of Protein

The functional domains of *Rap2A* protein were identified through Interpro an online database (Figure 4.20). This protein was found to contain mainly IPR005225 and TIGR00231 domains which are small GTP-binding protein domains and some others as shown in Figure 4.20. *Rap2A* protein with pdb ID 2rap was selected from the Protein Data Bank (PDB) and the 3D structure of *Rap2A* was downloaded in pdb format (Figure 4.21). All extra water molecules and complexes were removed from the protein structure. The resultant 3D structure visualized by Pymol software is shown in Figure 4.22.
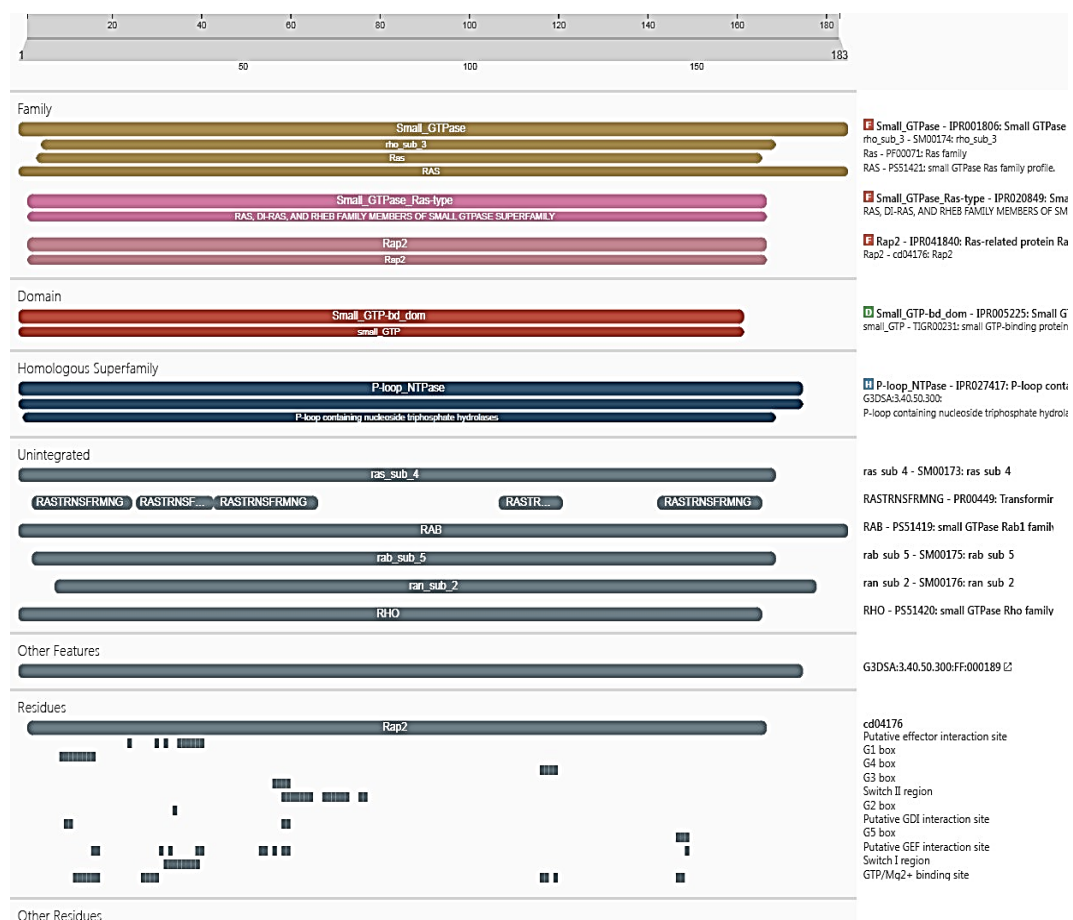
FIGURE 4.20: Functional domains and classification of protein families of *Rap2A* protein.
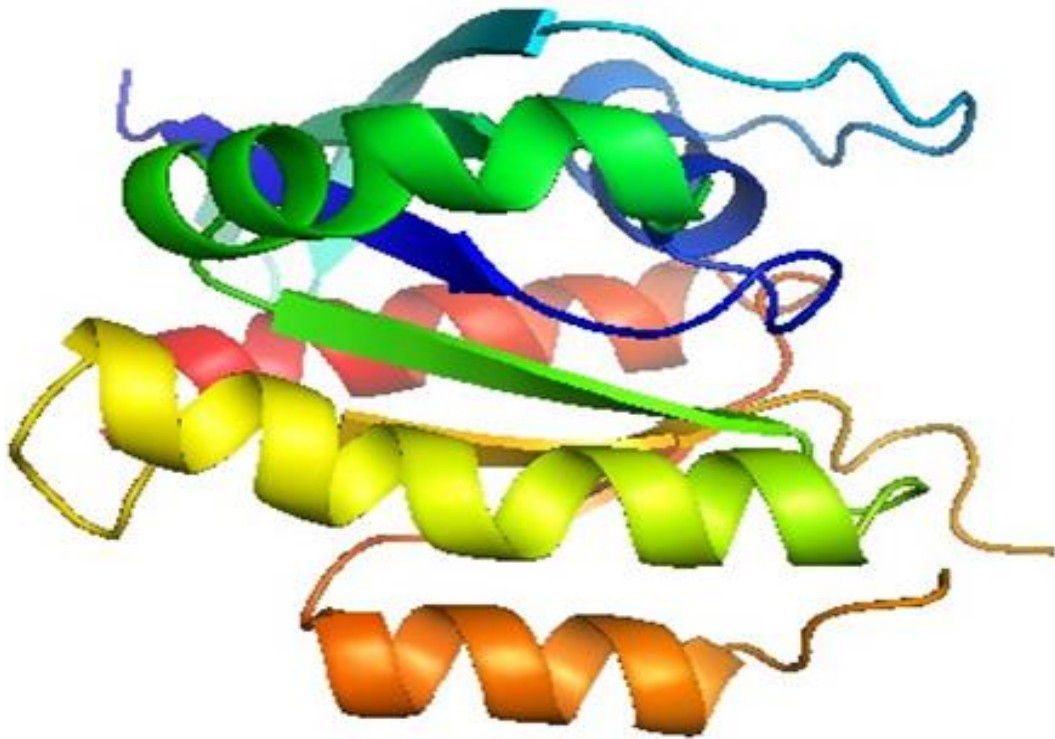
FIGURE 4.21: 3D Structure of *Rap2A* protein retrieved from protein databank.
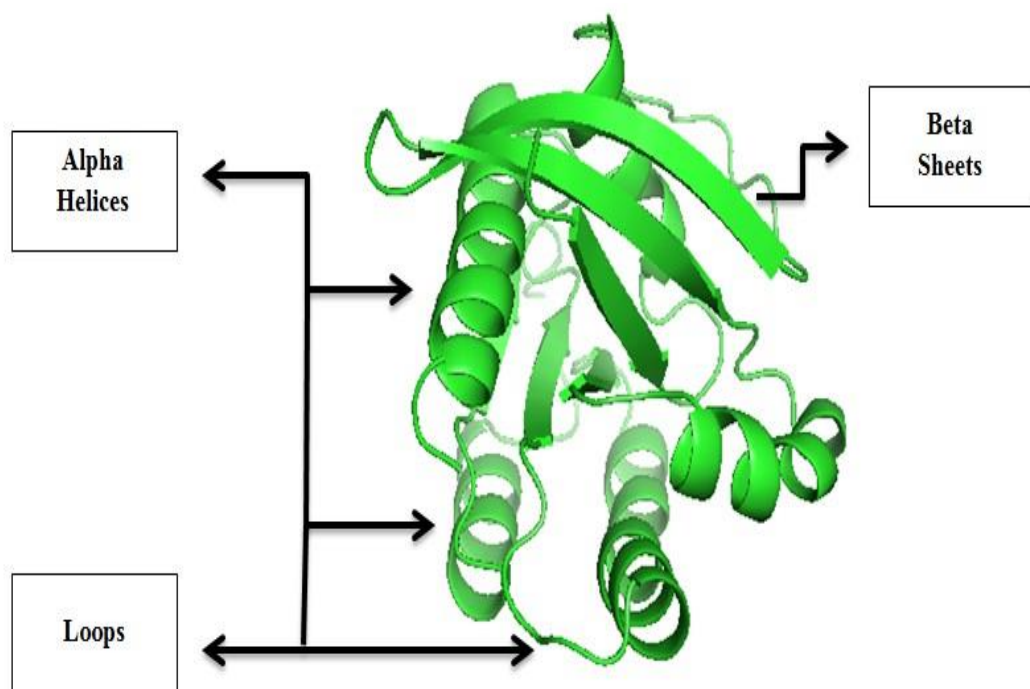
FIGURE 4.22: Refined 3D Structure of *Rap2A* Protein via Pymol Software.

4.12 Protein Model Evaluation

The model quality of a protein was evaluated via the SWISS-MODEL structure assessment server by Ramachandran plot analysis which was used to analyze the amino acid residues, this tool carried out stereochemical analysis of a protein structure by analyzing residues through residues geometry and overall protein structural conformation and validation. QMEAN (quantitative model energy analysis) was used to analyze the quantitative model energy of a protein structure and the quality of a protein.

The ProSA program calculated the overall quality of the protein structure and also recognized the identification method of the protein structure. This model showed two identification methods, one was X-ray crystallography method and the other was the NMR identification method. The Z score calculated was - 6.31 showing that the model structure quality was best as this score was within the range indicating that protein quality was better. On the contrary, if the score is not within range, the structure is considered invalid. The light blue colour represents the X-ray crystallography region while the dark blue colour shows the NMR region. The local model quality graph shows the energy plot of the protein model (Figure 4.23).
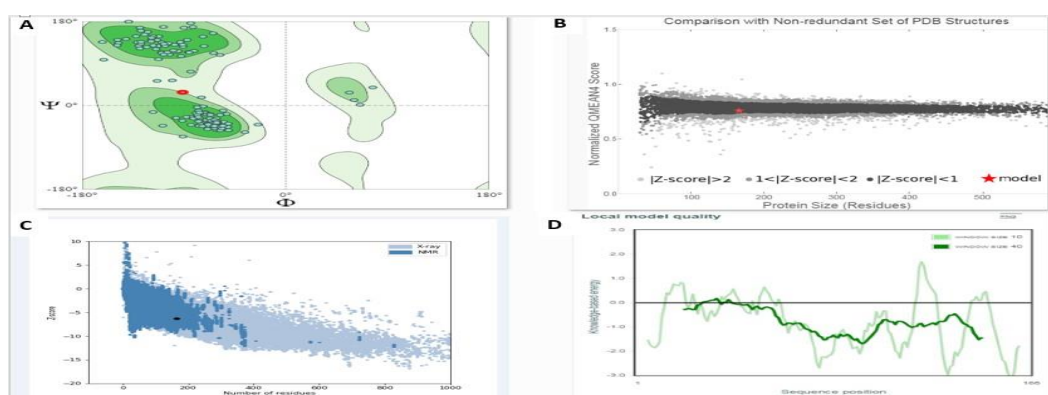
FIGURE 4.23: (A) *Rap2A* protein structure analyzed by Ramachandran plot. (B) QMEAN shows the quality estimation of the protein structure. (C) ProSA web predicts the z score as well as the energy score of the protein model, the darkest blue color shows that the structure belongs to the NMR region while the lighter blue color represents the structure from the X-ray crystallography region. (D) Local model quality graph estimate basically shows which part of the protein model is reliable and which one is not reliable.

4.13   Molecular Docking

For current research studies, the CB-Dock online docking tool was used for the molecular docking process. CB-Dock presented results in five different poses in an interactive 3D visualization. The best pose was chosen based on the lowest vina score (KJ/m^{-1}) (Figure 4.24). In the current study, there were 9 ligands identified in the methanolic extract of *A. carvifolia* through HPLC which were chosen for the molecular docking process that were apigenin, caffeic acid, gallic acid, rhamnetin, rutin, ferulic acid, syringic acid, vanillic acid and quercetin. On the basis of the best vina score, cavity size and grid map score, the four best ligands (apigenin, caffeic acid, gallic acid, rhamnetin Figure 4.24 - 4.27) were selected for protein-ligand interaction and molecular dynamic simulation. Further, one synthetic drug lenvatinib was also used for protein-ligand interaction and molecular dynamic simulation for comparison with the findings of ligand molecules (Figure 4.28). Table 4.7 presents the ligand's vina score, cavity size, and grid map score.
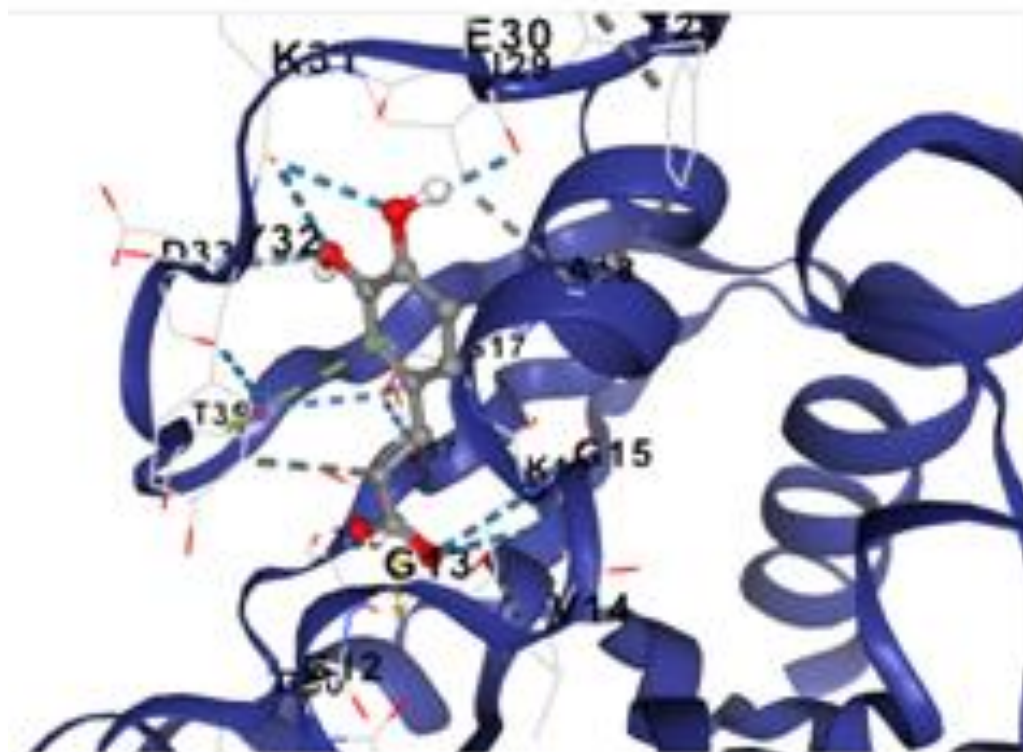
FIGURE 4.24: A. Docking poses of apigenin
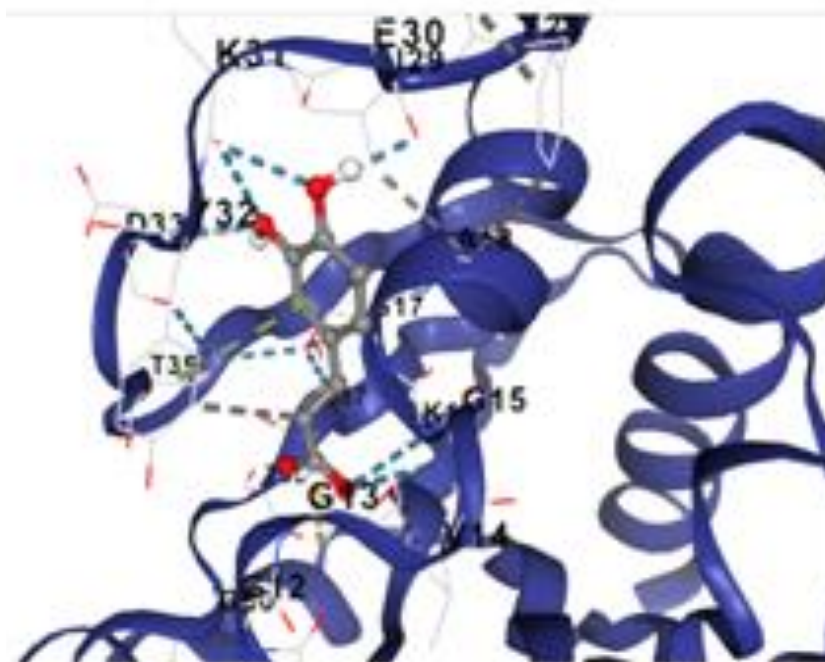
FIGURE 4.25: B. Docking poses of caffeic acid
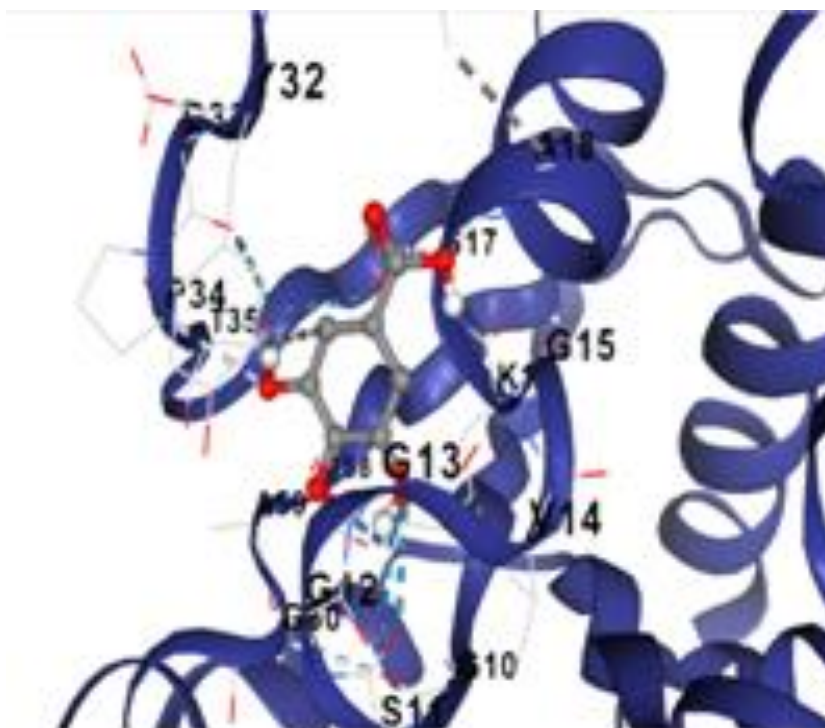
FIGURE 4.26: C. Docking poses of gallic acid
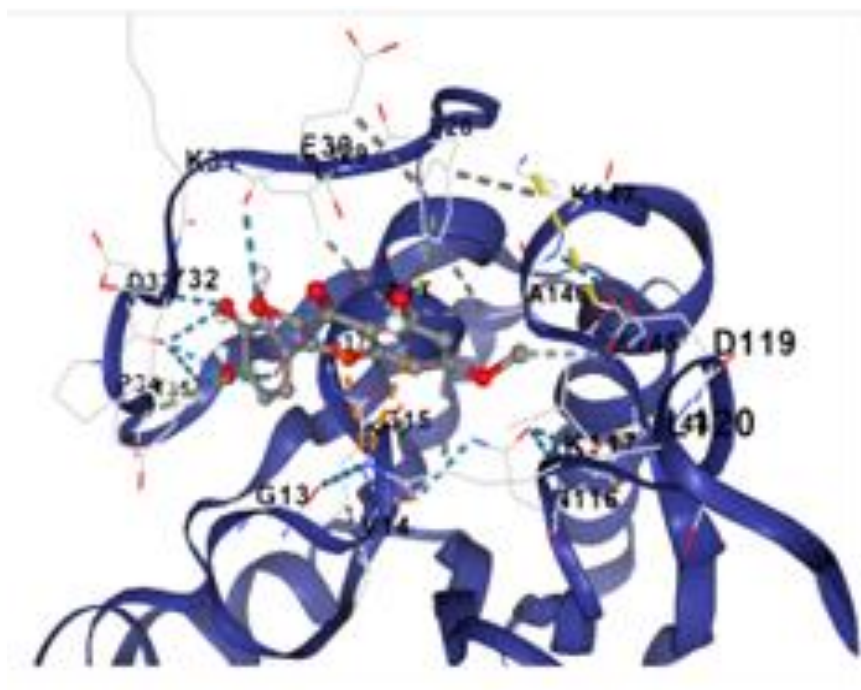
FIGURE 4.27: D. Docking poses of rhamnetin
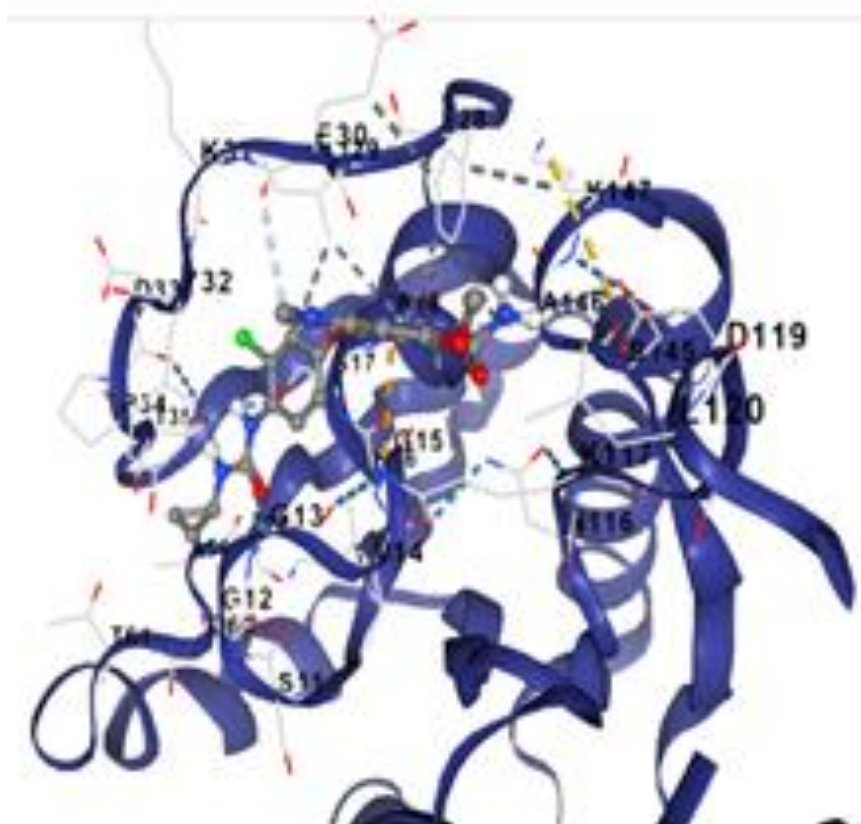
FIGURE 4.28: E. Docking poses of lenvatinib

TABLE 4.7: Docking results of ligands and standard drug against *Rap2A* protein

S. No	Ligands	Vina Score	Cavity Size	Molecular Weight g/mol	Grid Map	Max Energy kcal/mol	Min Energy kcal/mol
01	Apigenin	-9.1	716	270.24	33	14.4726	3.4818
02	Caffeic acid	-7.3	716	180.16	33	1.9678	-4.2202
03	Gallic acid	-6.6	718	170.12	33	11.5108	-1.1879
04	Rhamnetin	-9.5	716	316.26	33	9.9008	0.3216
05	Rutin	-9.5	716	610.52	33	45.7495	6.6328
06	Ferulic acid	-7.6	716	194.18	33	7.3440	1.4950
07	Syringic acid	-6.6	716	198.17	33	8.7418	1.1699
08	Vanillic acid	-6.6	716	168.15	33	8.5008	1.7454
09	Quercetin	-9.4	716	302.23	33	8.6927	3.3080
10	Lenvatinib	-9.2	716	426.9	33	9.7834	-17.0994

4.14 Analysis of Docked Complex through Lig-Plot+

Analysis of docked complexes was done by Ligplot+ protein-ligand interaction software which automatically generated a diagram of protein-ligand interactions. These interactions were modified through hydrophobic and hydrogen bonds. Ligplot+ generated a 2D representation of the protein-ligand complex, which facilitated the rapid analysis of protein complexes and demonstrated informative intermolecular interactions. So, these interactions included hydrophobic interactions, hydrogen bonding and atom accessibilities (Table 4.8). The complex file, in PDB format, was opened in Ligplot+ and the H-bonds and hydrophobic interactions of the docked molecules were examined. The ligpolt+ results of four best poses of selected ligands and protein complexes (apigenin, caffeic acid, gallic acid and rhamnetin) and one synthetic drug complex (lenvatinib) are presented in Figure 4.29 - 4.33.
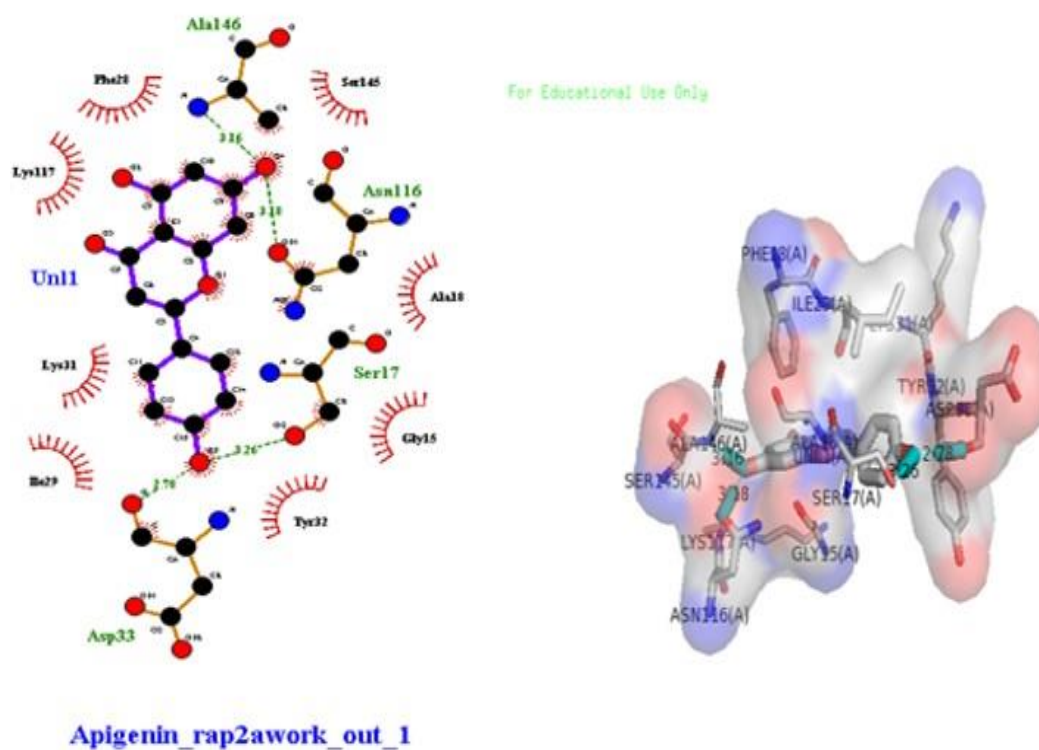
FIGURE 4.29: A. Protein-ligand interaction of *Rap2A* with apigenin via Ligplot Plus.
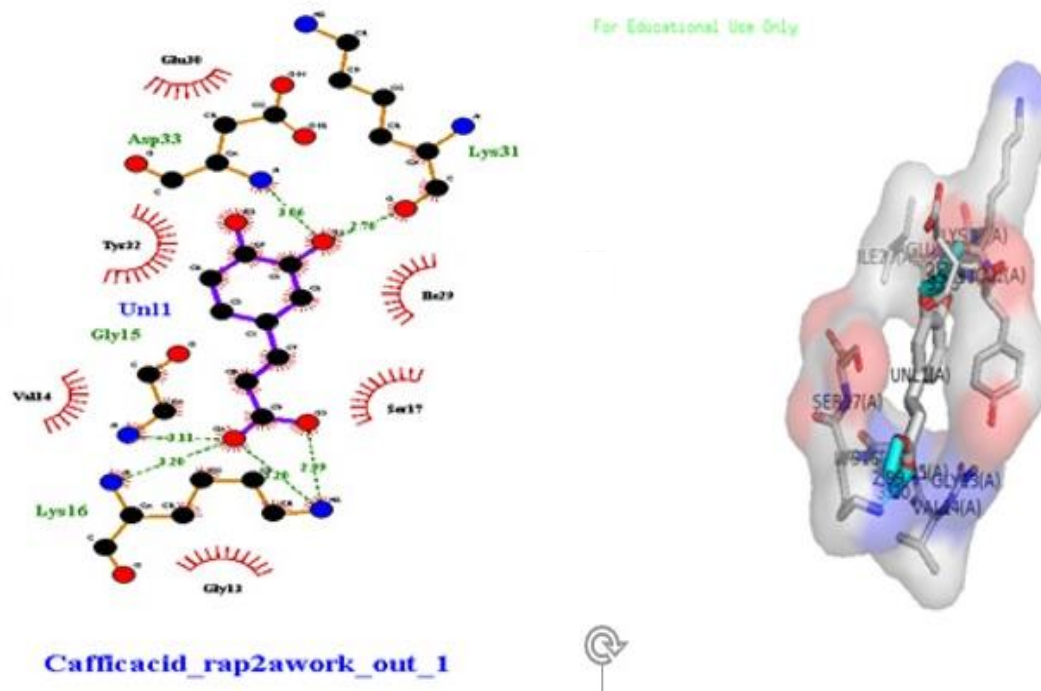
FIGURE 4.30: B. Protein-ligand interaction of *Rap2A* with caffeic acid via Ligplot Plus.
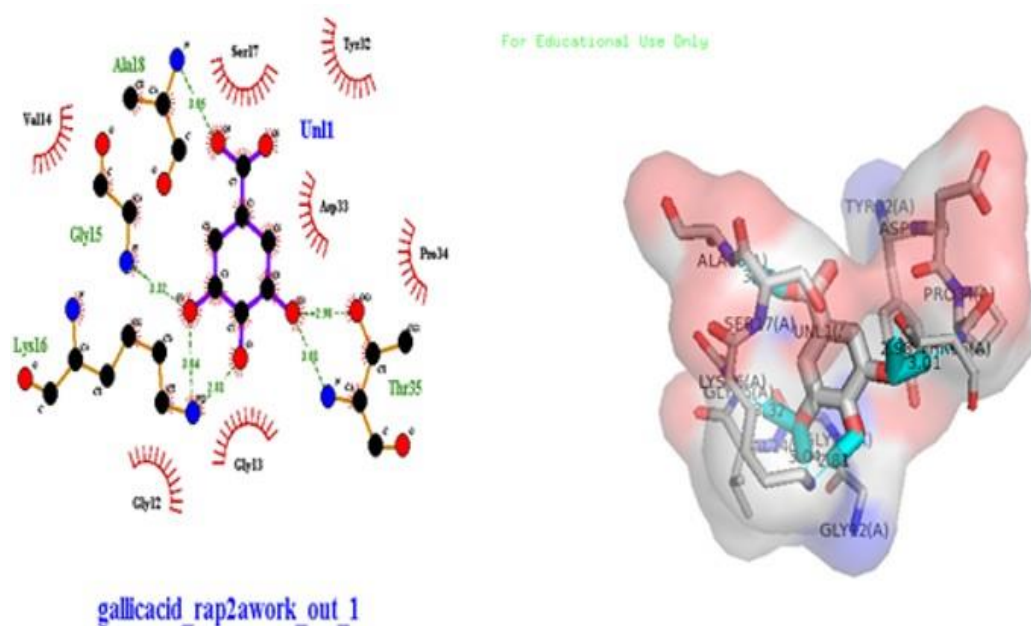
FIGURE 4.31: C. Protein-ligand interaction of *Rap2A* with gallic acid via Ligplot Plus.
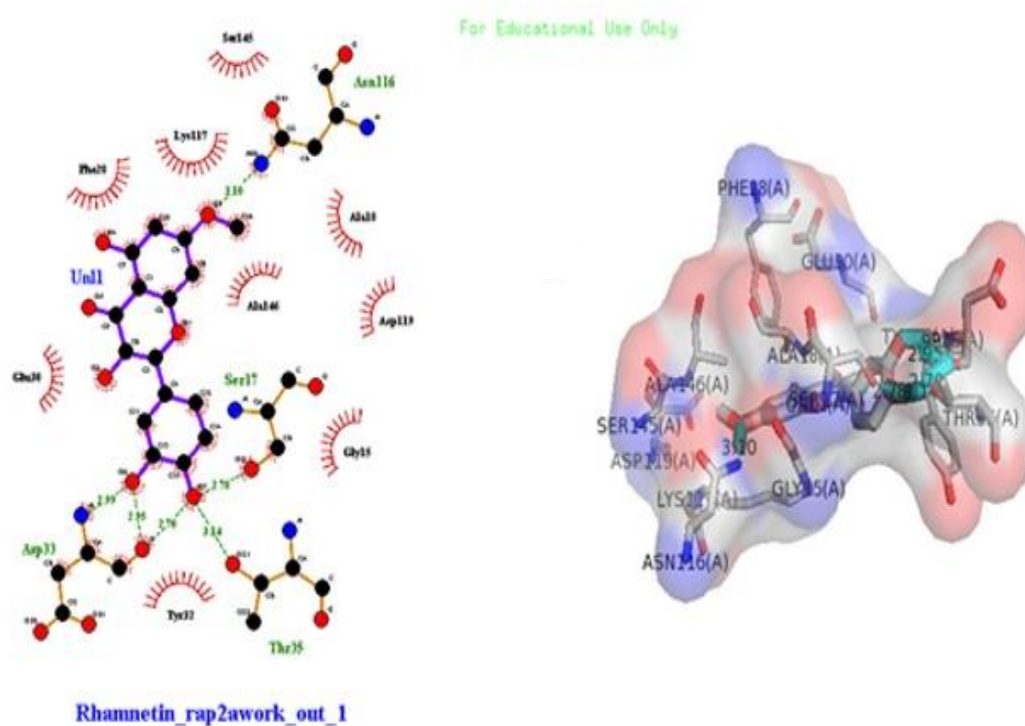
FIGURE 4.32: D. Protein-ligand interaction of rhamnetin with *Rap2A* via Ligplot Plus.
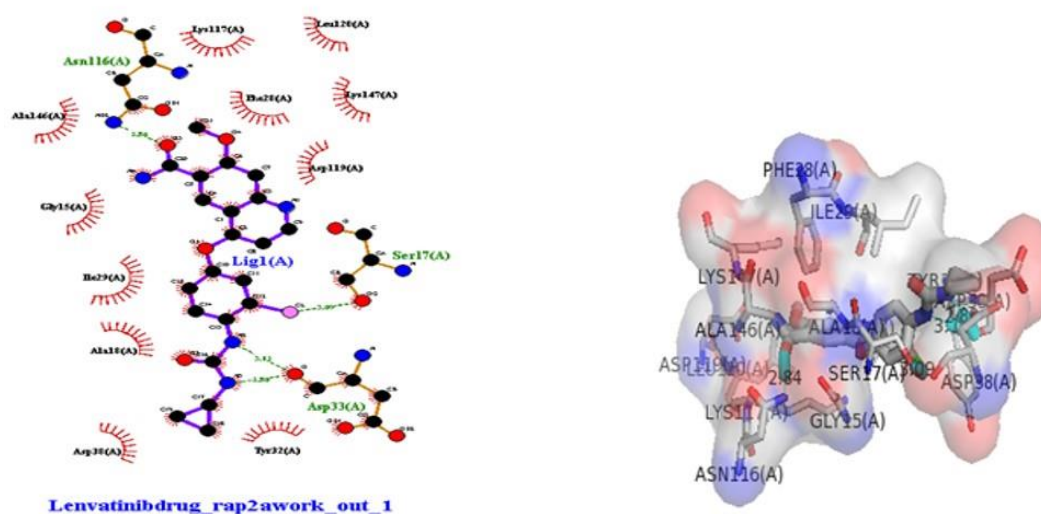
FIGURE 4.33: E. Protein-ligand interaction of *Rap2A* with lenvatinib via Ligplot Plus.

TABLE 4.8: Findings of interaction between four ligands and standard drug molecule with target protein.

S. No	Ligands & Drug	Binding energy	Number of hydrogen bond	Amino acids	HBS distance			Hydrophobic interaction	
01	Apigenin	-9.1	4	4	3.16	3.18	3.26	Ser145	Ala18
					2.78			Gly15	Tyr32
								Ile29	Lys31
								Lys117	Phe28
02	Caffeic acid	-7.3	6	4	3.06	2.78	3.11	Glu30	Tyr32
					3.20	3.20	2.99	Val14	Ile29
								Ser17	Gal14
03	Gallic acid	-6.6	6	4	3.05	3.32	3.04	Ser17	Tyr32
					2.81	2.98	3.01	Asp33	Pro34
								Val14	Gly12
								Gly30	
04	Rhamnetin	-9.5	6	4	3.10	2.99	2.95	Ser145	Lys117
					2.70	2.78	3.14	Phe28	Glu30
								Ala18	Asp119
								Gly15	Ala146
								Tyr32	

TABLE 4.8: Findings of interaction between four ligands and standard drug molecule with target protein.

S. No	Ligands & Drug	Binding energy	Number of hydrogen bond	Amino acids	HBS distance			Hydrophobic interaction	
05	Lenvatinib	-9.2	4	3	3.54	3.09	3.13	Lys117	Asn116
					3.50			Phe28	Ala146
								Lys147	Asp119
								Gly15	Ile29
								Ala18	Tyr32
								Asp38	

4.15 Interpretation of RMSD and RMSF Values in Docking Results

In the current research study, RMSD (Root-mean-square deviation) values in docking results were checked. The RMSD values gave the average deviation between the corresponding ligand and protein molecules. RMSD was used to measure how different a calculated docking pose of a ligand is from its corresponding co-crystallized orientation in the same protein. Pose 2 and 3 was identified as the best pose according to RMSD rules and regulations (Figure 4.34 - 4.35). The range value for RMSD is less than 2 and not greater than 4. RMSD values of all five complexes are given in Table 4.9. The RMSF (root mean square fluctuation) measured the average deviation of protein residues. It examined the area of protein structure that deviated the greatest or leased from their mean structure. Furthermore, the trajectories were further examined for root-mean-square deviation (RMSD) and root-mean-square fluctuation (RMSF), ligand torsion profiles, and protein-ligand interaction profiling with the help of the MD Simulation Interaction Diagram module of the Desmond.
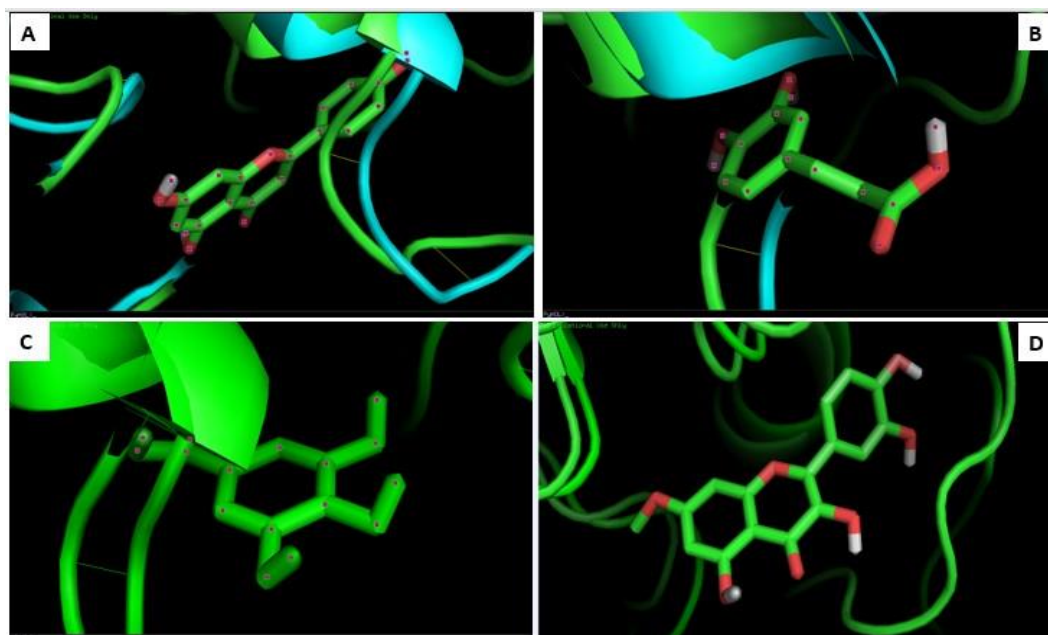
FIGURE 4.34: A. Protein-ligand superimposition with RMSD and RMSF calculations.

This is the best pose and shows the strong interaction of ligands with the targeted protein *Rap2A*. The ribbon-like structure is a protein (*Rap2A*) and in the center sticklike structure is ligand apigenin (A), caffeic acid (B), gallic acid (C), and rhamnetin (D).
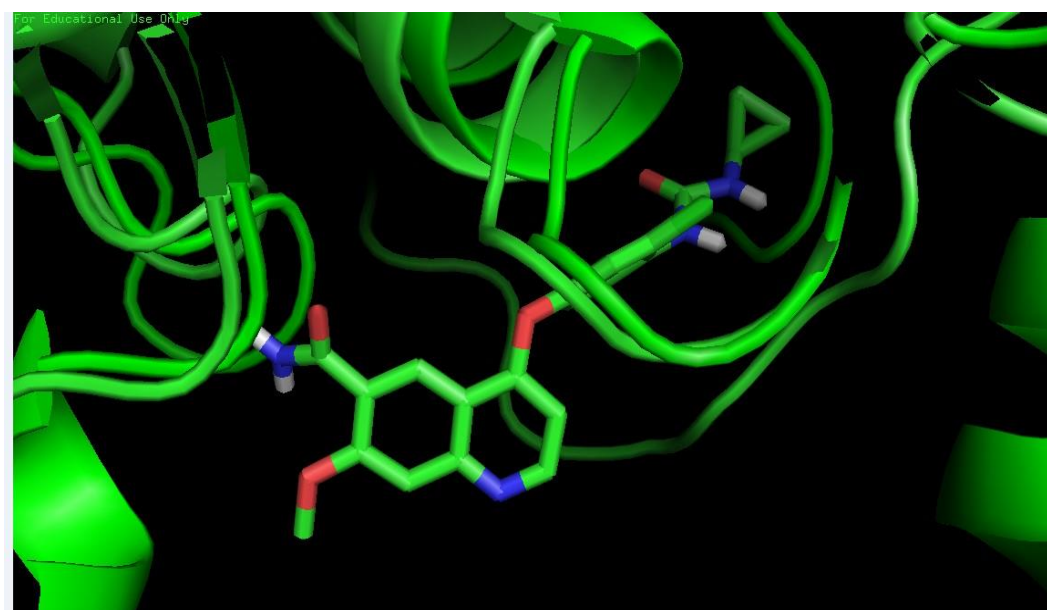
FIGURE 4.35: B: Protein-ligand superimposition with RMSD and RMSF calculations. The green ribbon-like structure is a protein (*Rap2A*) and in the center stick-like structure is the standard drug lenvatinib.

TABLE 4.9: Definitions of Variables: Impact of Successive Round on Investors'
Trust

S. No.	Ligands	Vina Score	RMSD Value Pose 1	RMSD Value Pose 2	RMSD Value Pose 3	RMSD Value Pose 4	RMSD Value Pose 5
01	Apigenin	-9.1	13.952	1.297	13.926	13.926	14.410
02	Caffeic acid	-7.3	13.952	1.297	13.926	13.453	14.410
03	Gallic acid	-6.6	13.952	1.297	13.296	13.453	14.410
04	Rhamnetin	-9.5	13.952	1.297	13.926	13.453	14.410
05	Lenvatinib	-9.2	13.952	1.297	1.297	13.453	14.410

4.16 Molecular Dynamic Simulation

For molecular dynamic simulation, four ligands (apigenin, caffeic acid, gallic acid and rhamnetin) complexes with *Rap2A* protein were selected while on the other hand reference drug (lenvatinib's complex) for comparison was chosen. Simulations of all these complexes were run on different nanoseconds (Figure 4.36 - 4.40). Apigenin simulation was run from 1 nanosecond to 100 ns and the apigenin was found stable till 100 ns. The caffeic acid simulation was not so good because the complex was unstable while performing the simulation. The simulation results of caffeic acid showed that this complex was stable till 20 ns but after that, it was found unstable showing that caffeic acid interaction with *Rap2A* protein is not better than apigenin complex. The gallic acid complex simulation was very poor because after 10 ns it was found unstable and unreliable. While rhamnetin and reference drug did not show simulation as after 1 ns, their complexes showed instability. So, from the overall simulation results of these complexes, it was concluded that apigenin was better than all other studied complexes. According to simulation results, the comparison of lenvatinib (reference drug) with all other ligand complexes was not very appreciable because lenvatinib drug did not show interaction with the targeted protein *Rap2A*. Therefore, the molecular dynamic simulation results of the apigenin complex with *Rap2A* indicated that this complex was far better than other complexes because till 100ns apigenin complex remained stable showing that apigenin interaction with *Rap2A* protein is quite strong.
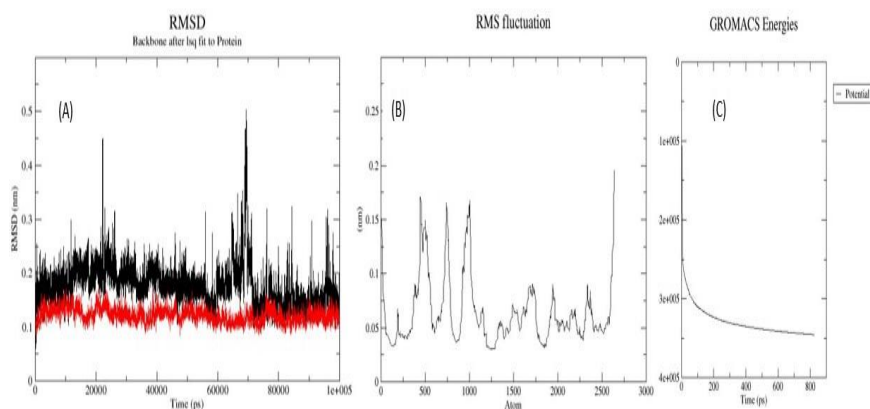
FIGURE 4.36: A. The molecular dynamic simulation results of the apigenin complex with *Rap2A* according to RMSD (A), RMSF (B), and GROMACS (C) calculations.
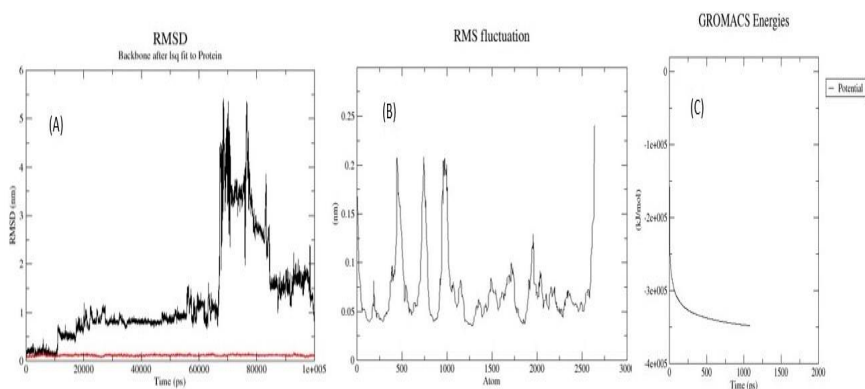
FIGURE 4.37: B. The molecular dynamic simulation results of the caffeic acid complex with *Rap2A*, according to RMSD (A), RMSF (B), and GROMACS (C) calculations.
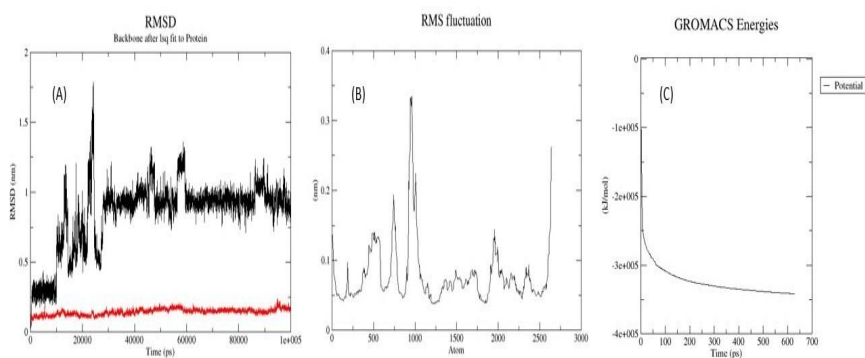
FIGURE 4.38: C. The molecular dynamic simulation results of the gallic acid, according to RMSD (A), RMSF (B), and GROMACS (C) calculations.
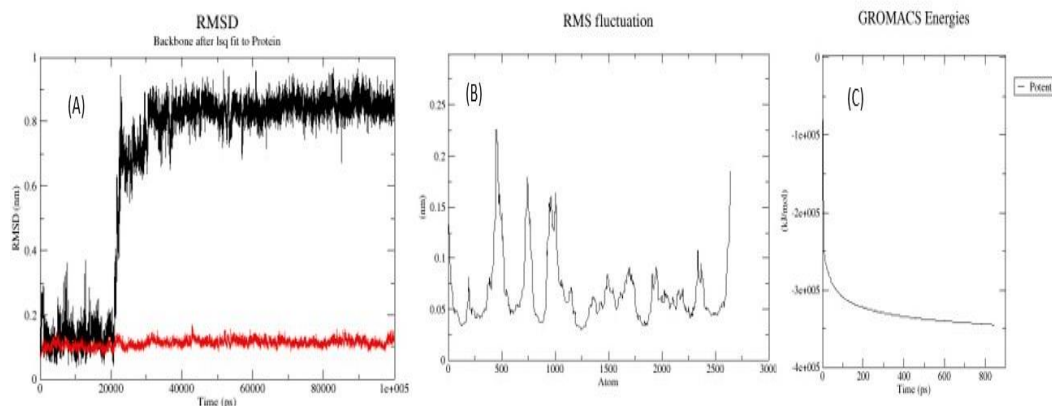
FIGURE 4.39: D. The molecular dynamic simulation results of the rhamnetin, according to RMSD (A), RMSF (B) and GROMACS (C) calculations.
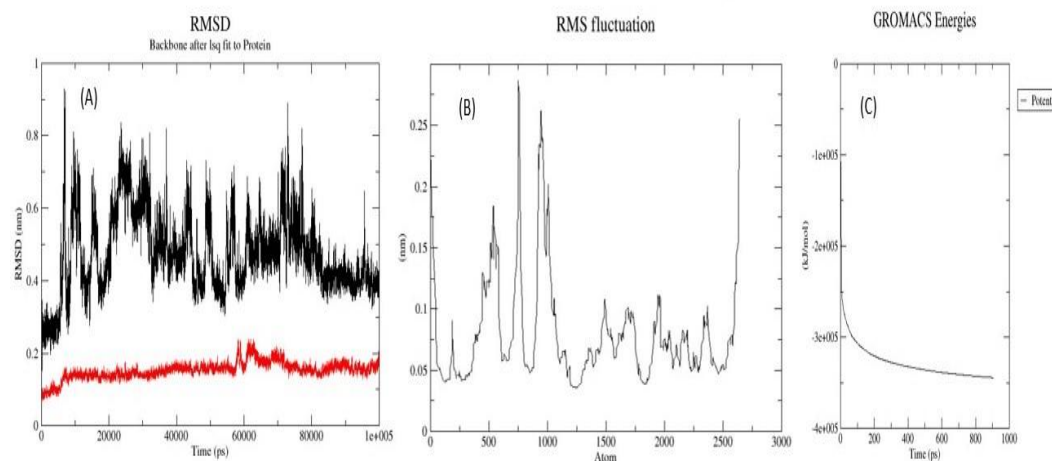
FIGURE 4.40: E. The molecular dynamic simulation results of the reference drug lenvatinib, according to RMSD (A), RMSF (B) and GROMACS (C) calculations.

4.17   ADMET Properties of Ligands

A general "rule of thumb" for the valuation of drug-like properties, known as Lipinski's rule of 5 (Ro5), has been introduced for almost 2 decades. Selected four ligands and one standard drug from the drug bank database followed Lipinski's rule of five (Table 4.10), which is a rule to evaluate drug-likeness or determination of chemical compounds with certain pharmacological and biological activities that would make it a likely orally active drug. According to Lipinski's rule of five, the Log p-value of most drug molecules should be limited to 5, molecular weight

should be less than 500, hydrogen bond acceptor should not be greater than 10 and hydrogen bond donor should be limited to 5.

TABLE 4.10: A. Lipinski's rule of five results of ligands and standard drug

S No	Ligands & Drug	Log p-value	Molecular weight	Hydrogen bond acceptor	Hydrogen bond Donor
01	Apigenin	2.5768	270.24	05	03
02	Caffeic acid	1.1956	180.159	03	03
03	Gallic acid	0.5016	170.12	04	04
04	Rhamnetin	2.291	316.265	07	04
05	Lenvatinib	4.0719	426.86	05	03

Furthermore, the selected ligands were screened for their ADMET (Pharmacokinetic) properties. The potential success of compounds depends on their ADMET properties. PKCSM tool was used to find ADMET properties of ligands. Pharmacokinetic properties including absorption, distribution, metabolism, excretion, and toxicity (ADMET) contribute a vital role in the compound's screening as future drugs. The pharmacokinetic parameters of standard drugs and lead compounds are listed in Table 4.11. In the case of absorption properties, the solubility of water of the reference drug was slightly lower than the apigenin and $CaCO_2$ permeability values of all other 3 lead compounds and the synthetic drug was also less than that of apigenin. Lenvatinib was found to be a P-gp substrate and P-gp I/II inhibitor. Whereas, apigenin showed itself as a p-gp substrate but not the inhibitor of P-gp I and II. Whereas, all other three lead compounds were found neither substrate nor inhibitor (Table 4.11). In the case of distribution properties, BBB permeability of < -1 means no impairment to the brain. The central nervous system permeability for lenvatinib and apigenin was found to be -2 while in the case of other lead compounds like gallic acid, caffeic acid and rhamnetin it was found to be < -3 (Table 4.11). The Fu value of lead compounds was found to be more than lenvatinib which showed apigenin and other lead compounds are more effective than synthetic drug in case of unbound friction in plasma. In the case of metabolism properties, lenvatinib showed itself as a substrate of CYP3A4 isoforms while all four lead

compounds (apigenin caffeic acid, gallic acid rhamnetin) were not predicted as a substrate of these isoforms. Lenvatinib was predicted as an inhibitor of CYP2C9 and CYP3A4 which is the main isoform for drug metabolism while apigenin was found to be a CYP2C19 and CYP1A2 Inhibitor (Table 4.11). While predicting toxicity properties, the predicted value of drug clearance as total clearance of apigenin or other lead compounds was high as compared to synthetic drug. Total clearance is related to bioavailability and is important for determining dosing rates. All compounds stand in the 'No' category for the Renal OCT2 substrate model, which means that they do not interfere with the normal functioning of organic cation transporter 2 which plays a role in the renal clearance of drugs (Table 4.11). Toxicity is the very significant parameter of ADMET properties which consists of 9 models. Maximum tolerated dose helps to set the maximum recommended tolerated dose, which was found to be 0.426 for lenvatinib and 0.328 for apigenin indicating that lenvatinib is ahead in safety than lead compound (Table 4.11). It is evident that lenvatinib showed itself as h ERG II inhibitor. Mostly h ERG I/II inhibitors are withdrawn from the pharmaceutical market. The model named oral rat acute toxicity (LD_{50}) expressed as mol/kg as the amount of drug that can cause the death of 50% of rats (test animals). LD_{50} value of lenvatinib was slightly higher than apigenin while slightly lower than the other 3 lead compounds. Oral rat chronic toxicity (LOAEL) determines the lowest dose of a drug which can produce adverse effects over long duration usage (chronic use) of the drug. LOAEL predicted value of lenvatinib was found to be 1.7 and less than that of apigenin and other 3 lead compounds which showed its potency to be more toxic than studied bioactive compounds. Hepatotoxicity simply indicates the injury to the liver which shows results in two categories yes/no. Lenvatinib was found to be hepatotoxic whereas lead compounds were not. Both lenvatinib and apigenin do not cause any allergic reactions. *T. pyriformis* toxicity is expressed as the negative logarithm of the concentration required to inhibit 50% growth.

TABLE 4.11: ADMET properties of ligands and standard drug.

Properties of Drug-likeliness	Ligands & Drug				
	Apigenin	**Caffeic acid**	**Gallic acid**	**Rhamnetin**	**Lenvatinib**
Water solubility	-3.3289	-2.33	-2.56	-3.213	-3.376
Caco2 permeability	1.007	0.634	-0.081	-0.361	0.031
Intestinal absorption (Human)	93.25%	69.407%	43.374%	80.214%	88.883%
Skin permeability	-2.735	-2.722	-2.735	-2.735	-2.735
P- glycoprotein substrate	Yes	No	No	Yes	Yes
P-glycoprotein I inhibitor	No	No	No	No	Yes
P-glycoprotein II inhibitor	No	No	No	No	Yes
VDss (human)	0.822	-1.098	-1.855	0.419	0.304
Fraction Unbound (human)	0.147	0.529	0.617	0.073	0
BBB permeability	-0.734	-0.647	-1.102	-1.345	-1.342
CNS permeability	-2.061	-2.608	-3.74	-3.235	-2.575
CYP2D6 Substrate	No	No	No	No	No
CYP3A4 Substrate	No	No	No	No	Yes
CYP1A2 Inhibitor	Yes	No	No	yes	No
CYP2C19 Inhibitor	Yes	No	No	No	No
CYP2C9 Inhibitor	No	No	No	No	Yes

TABLE 4.11: ADMET properties of ligands and standard drug.

Properties of Drug-likeliness	Ligands & Drug				
	Apigenin	**Caffeic acid**	**Gallic acid**	**Rhamnetin**	**Lenvatinib**
CYP2D6 Inhibitor	No	No	No	No	No
CYP3A4 Inhibitor	No	No	No	No	Yes
Total clearance	0.566	0.508	0.518	0.473	0.213
Renal OCT2 substrate	No	No	No	No	No
AMES Toxicity	No	No	No	No	No
Max tolerated Dose (human)	0.328	1.145	0.7	0.56	0.426
hERG I inhibitor	No	No	No	No	No
hERG II Inhibitor	No	No	No	No	Yes
Oral Rat acute toxicity (LD50)	2.45	2.383	2.218	2.453	2.227
Oral Rat chronic toxicity (LOAEL)	2.298	2.029	3.06	2.679	1.7
Hepato toxicity	No	No	No	No	Yes
Skin Sensitisation	No	No	No	No	No
T. pyriformis toxicity	0.38	0.293	0.285	3.331	0.309
Minnow toxicity'	2.432	2.246	3.188	1.885	-0.005

4.18 Lead Compound and Synthetic Drug Comparison

The comparison between the anti-cancer drug lenvatinib and the proposed lead compound apigenin was done by comparing the properties like docking values, physiochemical properties, interaction properties, ADMET properties and MD simulations results. So, it was predicted that apigenin is far better than lenvatinib reference drug on the basis of these studied parameters.

Chapter 5

Discussion

The current research work was performed to evaluate the anticancer potential of *A. carvifolia* Buch extract and its silver nanoparticles against liver cancer targeting the *Rap2A* gene along with apoptotic pathway genes and proteins. During this work, a green chemistry approach was utilized for the synthesis of silver nanoparticles using the extract of *A. carvifolia* Buch.

The synthesized nanoparticles and plant extract were tested on the liver cancer cell line HePG2 to determine their antiproliferative potential. Furthermore, to know the impact of *A. carvifolia* and respective silver nanoparticles on the targeted gene *Rap2A*, the expression of this particular gene was determined by real-time qPCR. Moreover, the level of protein of the *Rap2A* gene was also determined in the treated and non-treated cells by the ELISA.

Apart from that, to ensure the apoptotic role of plant extract and synthesized silver nanoparticles, apoptotic pathway genes and proteins (Bax, caspase 3, caspase, 8, and caspase 9) were also studied by the real-time qPCR and ELISA. This study also involved the computational analysis of metabolites identified in the extract of *A. carvifolia* Buch by HPLC against the target gene *Rap2A* by using molecular docking and MD simulation.

The ADMET properties of the metabolites were also determined and compared with the standard drug.

5.1 Identification of *A. carvifolia* Buch

DNA barcoding technique has been broadly used for the identification of species accurately. It consists of stranded short DNA sequences as makers for quick and authentic identification of species. This has also been identified as a renaissance for taxonomic recognition of species and has been extensively adopted in different applications. Recently, DNA barcoding has emerged as a novel tool for species recognition and molecular evolutionary studies. Hence, DNA barcoding is a molecular taxonomic bioinformatics tool which is used for species identification, differentiation and novel species discovery as well. DNA barcoding sequences could be amplified by adopting the universal primers recovered and routinely sequenced for species characterization. DNA reference libraries have been designed globally, that make possible the identification and comparison of barcode sequences of plant species that are not familiar. Therefore, making possible biodiversity preservation, evaluation, and sustainable utilization for different purposes [125].

In molecular biology, DNA barcoding is adopted for classifying different species at the molecular and genetic levels using primers with 500 bp to 700 bp segments. The most commonly used DNA barcoding markers are *ITS, rbcL, psbA-trnH,* and *matK* for plant species due to their significance in biodiversity research and preservation efforts [126]. The chloroplast plays a vital role in various essential biochemical processes including photosynthesis [127]. This has been proved to be the suitable choice for investigating phylogenetic relationships among species because the genome of chloroplast shows a relatively conserved structure in comparison to traditional DNA fragments. So, the features of the chloroplast genome i.e. conserved yet subtly variable make it efficiently utilizable for applications in advancing scientific investigations [128]. This stability of the chloroplast genome is beneficial for species identification providing a consistent basis for this purpose. lower mutation rates exhibiting sequences are vital for accompanying phylogenetic analyses at higher taxonomic levels, while higher mutation rates are central for distinctive analysis of closely related species [129].

In the current research work, for the identification of *A. carvifolia* Buch, DNA was extracted from the shoots by adopting the reported protocol [19]. The seed germination was done on $\frac{1}{2}$ MS media without any growth hormone following the surface sterilization with a sterilizing solution comprising ethanol (70%) and mercuric chloride (0.1%). The seed germination was observed in 6-8 days after cold treatment of 2 days in the dark at 4 °C. Subsequently, grown plantlets of one month were utilized for DNA extraction using the CTAB method. The quality of extracted DNA was tested by UV-vis spectrophotometer after taking absorption at 260/280nm, which showed good quality and quantity. Furthermore, to verify the quality of the DNA, electrophoresis (0.8% agarose gel) was carried out.

Furthermore, *A. carvifolia* was identified by adopting a previously reported methodology which involved initial steps of surface sterilization of seeds and then germination on a specific medium [92]. The optimal germination medium is critical for the optimal growth of the plantlets. Afterward, these plantlets were utilized for the extraction of DNA, following a formerly established protocol [130]. The use of that already reported procedure confirmed the reliability and consistency of the DNA extraction process, paying to the accuracy of the identification methodology in general.

Confirming the reproducibility of the results of PCR over time is reliant upon both the quality and quantity of DNA [130]. There are certain limitations in the extraction of high-quality DNA, one of which is the existence of plant secondary metabolites which adds an extra layer of complexity to the DNA extraction procedures. This causes extra experimentation with different extraction methods for customization to the particular plant species of interest in order to obtain a sufficient quantity of DNA of high quality [131]. Different kinds of methods have been tested previously to combat the difficulties related to obtaining suitable DNA from plants. Thus, in addressing these trials, the DNA extraction procedure applied in the current study appeared as mainly effective. This procedure not only established an advantage in conserving the quality of DNA but also found proficient at generating considerable quantities, paying to the sustainability and accuracy of molecular investigations in medicinal plant research.

In the current study, the DNA, after extraction was amplified using primers specific to the *psbA* and *trnH* genes. PCR was performed on the prepared reaction mixture following the reported methodology [19]. An amplified product of 500 bp was achieved from all samples successfully. As shorter length DNA barcode is recommended to facilitate easy DNA extraction, amplification, and subsequent sequencing. For the validation of amplified DNA, sequencing was done in triplicate through ABI Prism 310 Automated DNA Sequencer, yielding consistent outcomes and thus confirming the existence of nucleotides specific to the species. The CLUSTAL W (function in BioEdit software) was used for identification purposes and comparison of sequences [132].

Furthermore, the validity was done for amplified products which were sequenced using the dideoxy chain termination method. Afterwards, the obtained sequences were matched to the *A. carvifolia* standard *psbA-trnH* sequence accessible on the NCBI web platform. This comparative analysis was a decisive step in approving the precision and dependability of the recognized DNA, aligning with conventional values for molecular identification in botanical research. Previously, the *psbA-trnH* DNA barcode proved to be a suitable gene for the successful discrimination of various almond varieties, along with their related species. The results showed that the *trnH-psbA* plastid gene (1058 bp) was found to be the reliable gene among the tested 14 specimens, suggesting an advanced level of diversity of nucleotides in this explicit area [133]. In the examined poisonous plants, the non-coding *trnH-psbA* intergenic spacer emerges as the most promising candidate. It displays high universality, sequence quality, coverage, and discriminatory capabilities [134].

5.2 Synthesis and Characterization of Nanoparticles

Nanotechnology is one of the newest scientific achievements leading to rising industries with the public and financial interests. This felid is a modern form of material manufacturing by handling and operating material structures on a nanoscale [21].

The major purpose of most nanoscience studies is to manufacture novel resources or to formulate accessible materials. Nanoparticles show better or considerably enhanced properties based on definite characteristics for example morphology, size and distribution. Bulk and atomic structures vary in their characteristics and metal nanoparticles bridge the gap among them with their exclusive physicochemical properties, which are increased surface area, more reactivity, large surface-to-volume ratio, spatial confinement, tunable pore size and particle morphology. The nanoparticles made up of inert metals mainly Au, Ag, Pt and Pd are investigated efficiently in medical applications against various diseases including cancer [135]. At the commercial level, silver metal is extensively used in nanotechnology which contributes 5 hundred tons for the synthesis of silver nanoparticles annually [136]. Silver nanoparticles (AgNPs) have a prominent role in wound healing due to their innate therapeutic properties [137]. They also play a prominent role in therapeutic applications, such as through anticancer, antidiabetic, antioxidant, antimicrobial, and antiviral activities [124].

There has been an increased number of environmental concerns, and in order to address these concerns, nanoparticle production through a green chemistry approach is the main focus. The utilization of eco-friendly, green chemistry approaches is in demand to address the environmental challenges. The attractive physiochemical characteristics of silver nanoparticles are responsible for noteworthy applications in the field of nanomedicine. Since ages, silver has long been known to have effective medicinal properties including antimicrobial properties and has also been utilized for decades to combat various infections. It can be traced from the literature that nanotechnology based nanostructured systems can enhance plant extract's characteristics. This might boost numerous features of the plant extracts such as the efficacy of plant extract, continuous release of its dynamic constituents, decreased dosage with lesser side effects and enhanced efficacy [138]. Green synthesis of nanoparticles using eco-friendly substances is a developing branch in nanotechnology. Recently, inspired by the perception of green chemistry, the biological synthesis of nanoparticles has been focused on utilizing biological entities, such as plants, algae, and microorganisms. It offers many advantages over chemical synthesis, such as being environment-friendly, cost-effectiveness, efficient energy

utilization, and suitability for biomedical and pharmaceutical applications. Plants are considered to be a superior source for the synthesis of nanoparticles as compared to chemical synthesis, as they are eco-friendly and nontoxic [139, 140].

In the current study, silver nanoparticles were synthesized using the extract of *A. carvifolia* Buch at different concentrations of 10, 20, 40, 80 and 160 mg/L to optimize the best concentration for the synthesis of silver nanoparticles by using silver nitrate salt solution (5mM). The colour change from yellowish to dark brown indicated the complete formation of silver nanoparticles. There are reports describing that colour change from yellowish to dark brown is the first indication of silver nanoparticle synthesis. Silver nanoparticles synthesized from *Artemisia sieberi* showed a similar change in colour, where a solution of plant extract and silver nitrate (2μM) turned to dark brown after mixing and complete synthesis of silver nanoparticles [141]. Furthermore, the synthesized nanoparticles in the current study were subjected to characterization by UV-vis spectroscopy for further confirmation of silver nanoparticles and their optical properties. There was observed a strong absorption peak at 450 nm for silver nanoparticles prepared from all concentrations of plant extract. SPR (surface plasmon resonance) is responsible for UV–visible maximum absorption of silver nanoparticles in the range of 400–500 nm. The widening of the peak also indicates that synthesized particles are polydisperse [142]. Previously, silver nanoparticles prepared from extracts of *Artemisia annua* and *Artemisia sieberi* also displayed characteristic absorption peaks at 410 nm and 445 nm respectively by UV-vis spectroscopy [141, 143]. The mechanism behind this is that the absorption and scattering of light is done by the silver nanoparticles with extraordinary efficiency and this is done because of the conduction electrons which are present on the metal surface. These conductance electrons when excited by the specific wavelength light undergo a collective oscillation. This oscillation is known as a surface plasmon resonance (SPR). The absorption and scattering properties of silver nanoparticles can be adjusted by controlling the particle size, shape, and the local refractive index near the particle surface [144].

Besides, the different concentrations of *A. carvifolia* extract (160, 80, 40, 20 and 10 mg/mL) were utilized for the optimization of synthesis of AgNPs. There was

observed a 1.5 times increase in the absorbance of the nanoparticle's suspension with an increase in the concentration of plant extract. The highest absorbance was observed when nanoparticles were prepared with 160 mg/L of plant extract. This increase in the intensity of the AgNP's absorbance has also been observed by other investigators [88]. Whereas, the silver nitrate solution and the *A. carvifolia* plant extract showed no absorbance at 450 nm. The proportion of silver ions to their capping and stabilizing agents determines the extent of silver nanoparticles. Moreover, the reducing agent's concentration and that of the metal itself also hold a vital part in the synthesis of silver nanoparticles. In an earlier report, comparable results were also described in the silver nanoparticles of *Artemisia annua* [145].

Scanning Electron Microscopy (SEM) gave additional understanding into the size and morphology of the green synthesized silver nanoparticles. The nanoparticles were found with a calibrated size of 80 $\pm$6 nm. Furthermore, the shape of silver nanoparticles was found to be icosahedron (polyhedral). It can be observed from the SEM images that silver nanoparticles were found to be a bit agglomerated. The magnetic behaviour of silver nanoparticles might be responsible for this and the larger surface area to volume ratio of nanoparticles also tends to aggregate them for the reduction of their surface energy. Moreover, biocompatible polymers can be coated on the surface of nanoparticles to avoid this process [146].

The functionality and toxicity of nanoparticles on the environment and other organisms is majorly dependent on their size, shape and morphological features. Likewise, the size of nanoparticles might increase their surface area with increased efficacy by enhanced uptake of cells. Different biomolecules and phytocompounds found in plants are responsible for shaping the size and morphology of nanoparticles. The silver nanoparticles of *Artemisia absinthium* were found to have a size of 50 nm with a spherical shape [147]. The silver nanoparticles of *Artemisia annua* were found to be in the range of 49.4 to 88 nm with a spherical shape as well [143].

FTIR was carried out to find the latent natural compounds in *A. carvifolia* Buch plant extract which were involved in the synthesis of nanoparticles. The spectra depicted changes between 800-1500 cm^{-1} which confirmed the involvement of flavonoids, phenolics and lipid-containing oils having aldehydes and ketonic bonds.

Ketones with carbonyl (C–O) stretching vibration were observed at 1000-1140 cm^{-1}. It was confirmed from FTIR investigations, that the amino acid and proteins resulting in carbonyl gatherings have the extra beached capacity to bind with metal, displaying that the proteins might be involved in shaping the metal nanoparticles. Previously, silver nanoparticles of *Artemisia marschalliana* showed similar peaks showing the vibrations of carbonyl (C–O) [148]. Similarly, the =C-O stretching between the 1100-1350 cm^{-1} may go with the lipid's carboxyl groups. Similar findings were observed for nanoparticles of *Artemisia annua* [145]. There was observed change in the range of 1331-1334 cm^{-1} showing the involvement of carboxyl groups in the synthesis of the silver nanoparticle.

The phytochemical analysis of previously reported silver nanoparticles of *A. sieberi* showed the presence of amines, carboxylic groups and alkenes [141]. Another FTIR report of *A. sieberi* silver nanoparticles showed the peaks for hydroxyl groups, alkanes, alkenes, amides, and amines [149]. In addition, the study conducted by Alotibi and Rizwana (2019) revealed that the methanolic extract of *A. sieberi* was rich in the functional groups of OH, CH stretching, C=O stretching, and aromatic skeletal stretches, which agreed with the current results as well [150]. Besides, some other species of the *Artemisia* genus had a similar composition of alkyl halides, alkanes, alkenes, aldehydes, and amide groups, such as *Artemisia maritima*, *Artemisia indica* and *Artemisia vestita* [141].

Additionally, EDS was used to study the elemental composition of silver nanoparticles which showed silver as the major element. Furthermore, the prepared nanoparticles did not exhibit any nitrogen indicating the absence of noticeable traces of ions from the AgNO$_3$ precursor used, which confirms the presence of metallic silver in the sample and evidence of successful reduction of silver ions [95]. Moreover, carbon and oxygen atoms were also found in the EDS spectra confirming the presence of phytochemicals on the silver nanoparticle's surface which act as capping and stabilizing agents of nanoparticles [140]. A similar pattern of EDS spectra was observed in the case of silver nanoparticles of *Artemisia annua*, *Artemisia sieberi* and *Artemisia absinthium* [141, 143, 147]. X-ray crystallography results showed the crystalline nature of silver nanoparticles with identified peaks [38.23 (1

1 1), 44.41 (2 0 0), 64.38 (2 2 0), 77.5 (3 1 1)] at 20 degrees. These findings were found in agreement with the standard ICSD No. 98-018-0878 [96, 124]. A similar XRD pattern was observed for the silver nanoparticles of *Artemisia monosperma* [151].

5.3 Cytotoxicity Analysis of Plant Extract and Nanoparticles

Cancer is a global threat to human lives that occurs due to the uncontrolled growth of abnormally organized tissues [1]. Recently, based on the reported data, the number of newly diagnosed cancer cases reached more than 19 million, which led to 10 million deaths in 2020 [2, 152]. There are various curative treatments available for cancer patients like surgery, radiation and chemotherapy, immunotherapy and hormonal therapy. However, due to a lack of precise and targeted delivery to neoplastic tissues, such approaches cause various side effects [153]. Due to this, there is an urgent need to design alternative novel anticancer therapies to target cancer management. Nanomaterials prepared in a natural way could be adopted as a potential candidate that can ensure targeted drug therapy with minimal side effects [153]. In comparison to free pharmaceuticals, nanomedicines offer a number of advantages, including enhanced selectivity, which lowers systemic toxicity and improves drug penetration into the targeted tissue while delaying the onset of early degradation in the compounds. Metallic nanoparticles (MNPs) have a lot of potential for medicinal applications like cancer treatment. They can be prepared using a simple and basic method using several physicochemical techniques which makes them potential candidates for anticancer medications [96].

To study the cytotoxic potential of silver nanoparticles, samples were tested against liver cancer cell lines HepG2. In this study, four different concentrations of synthesized silver nanoparticles and plant extract (10, 20, 30, 40 and 50 μM) were used to study their cytotoxicity. The percentage of cell viability of HePG2 cells was found to be decreased more at the higher concentration (50 μM) than at the lower

concentration (10 μM). Plant extract and silver nanoparticles showed cytotoxicity in a concentration dependent manner indicating their increased cytotoxicity at higher concentrations. Furthermore, IC$_{50}$ of silver nanoparticles was found 2.57 μM for HepG2 cells, while for plant extract it was 11.57 μM. The statistical significance of the data was also observed.

Previously synthesized silver nanoparticles of *Artemisia marschalliana* were found active when tested against the cells of gastric carcinoma [148]. Another report of synthesized biogenic silver nanoparticles of the copperpod plant showed significant cytotoxicity against MCF7 and HePG2 cell lines [154]. Previously, green synthesized silver nanoparticles have been shown to exhibit anticancer activity against MCF7 and HePG2 cell lines, while, silver oxide nanoparticles were found cytotoxic to HePG2 and Chang liver cells [155]. In another study, maleic-acid and citric acid-capped silver particles were reported to have an inhibitory role against liver cancer cell line (HePG2) [96] and those synthesized by green chemistry approach using extract of *Mentha asiatica* were also found to have similar results against the same liver cancer cell line [95].

According to ISO standards, a reduction of cell viability by more than 30% is considered to indicate cytotoxicity. The fact is that silver nanoparticles induce toxicity because of the generation of ROS and oxidative stress, and it is also reported that toxicity is dependent on the size of the nanoparticles [156]. Another report describes that the development of the immune response by silver nanoparticles is size dependent. In that study, treatment of various sized silver nanoparticles (4, 20, and 70 nm) was given to human macrophages (U-937), and it was observed that nanoparticles which were smallest in size showed the highest proinflammatory activity (by releasing cytokines and inducing oxidative stress) [157].

Apoptosis induced by silver nanoparticles of *Artemisia monosperma* against human breast cancer cells has already been reported with an IC$_{50}$ value of 32 μg/mL, which occurred possibly because of the translocation of the AgNPs within the nucleus and was mediated by ROS generation and mitochondrial dysfunction [151]. AgNPS were also found cytotoxic to decrease the viability of MCF-7, HePG2 and HeLa cells [96]. Moreover, it was revealed that silver colloids treated MCF-7 breast cancer

cells exhibited considerably decreased dehydrogenase activity, causing reduced NADH/NAD+, consequently, reduced mitochondrial membrane potential leads to cell death. Another report elaborated that, phagocytized silver nanoparticles totally block the cell cycle in the S-phase and excite inflammatory signaling through ROS generation, which finally induces the secretion of TNF-α [155].

5.4 Gene Expression and Protein Analysis of *Rap2A*, Bax and Caspases

Hepatocellular carcinoma (HCC) is the most common type of primary liver cancer which is the 6th leading cancer in prevalence and the 4th most common source of cancer-related deaths globally [3]. There are many causes of hepatocellular carcinoma, including chronic liver disease, HBV and HCV infection, and nonalcoholic steatohepatitis [4]. Numerous possible biomarkers have been identified by the latest development of high throughput sequencing data for determining the prognosis of patients [9]. Rap proteins belong to the Ras GTPase binding family having 50 to 60 % similarity of sequence with RAS protein. The variety and accuracy of both proteins are determined through various parts of GEFs and GAP. In human genes, five special genes of the RAP family such as RAP 1A, 1B, 2A, 2B and 2C have been recognized. RAP proteins mainly play a role in cell adhesion, movement and polarity [158]. The result of RAP gene commencement relies on the context-precise contact of the RAP gene with their monitors and downstream effectors.

In the current study, the level of expression of the target gene of liver cancer (*Rap2A*) in silver nanoparticles and plant extract-treated HePG2 cells was found to be significantly decreased as compared to untreated cells indicating its role as an oncogene in liver cancer. The experiment was run with the IC_{50} of plant extract and synthesized silver nanoparticles and it was observed that expression of *Rap2A* gene was decreased more prominently in HePG2 cells treated with synthesized silver nanoparticles than that of plant extract. Previously, the expression of Rap genes in HCC was studied by detailed molecular and clinical features. In that study, there

was observed a strong association of the *Rap2A* gene in HCC by pathway analysis including both metabolic pathways and those related to the cell cycle. Where it was observed that *Rap2A* showed a robust capability to differentiate tumors from normal tissues. The expression of *Rap2A* was related to the modification of its copy numbers and DNA methylation [11].

The cancerous role of the Rap gene has been recognized in various forms of tumors for instance breast, lung, ovary stomach, cervix, prostate, and brain tumors [11]. Estimated indication advocates that Rap proteins also take part in serious functions in HCC and cancer development. Single nucleotide polymorphism in the RaP1A gene (rs494453) has been represented to be linked among high occurrence and reappearance after transplantation of the liver. More advanced action of the NF-κB/RAP1 signaling channel is linked to tumorigenicity in hepatocellular carcinoma [159]. There has been a strong link between liver inflammation and RaP1A expression, which is a risk factor for liver carcinogenesis [12].

Furthermore, the stimulatory effects of synthesized silver nanoparticles and plant extract on the Bax gene up-regulation were also studied. Similarly, the experiment was run with the IC_{50} of plant extract and synthesized silver nanoparticles. Synthesized silver nanoparticles caused more upregulation of the Bax gene in HePG2 cells than that of plant extract. High levels of expression of the Bax gene suggested the role of silver nanoparticles in HePG2 cell apoptosis through an intrinsic apoptotic pathway. In a previous study, similar findings were observed, where silver nanoparticles significantly increased Bax gene expression in the liver cancer cell line. It was also reported that the relative level of the dimerization pattern of the Bax protein shifts the cell to survival or cell death [160]. Moreover, caspase-3, caspase-8 and caspase-9 genes were also evaluated for relative expression to determine the apoptotic role of synthesized silver nanoparticles against treated cells. It was found that silver nanoparticles brought up-regulation of all studied caspase gene expression in HepG2 cells.

Apoptosis is a process of programmed cell death and there are different genes involved in the regulation of this process including upregulation or activation of Bax gene expression and death caspases. BAX (key gene in extrinsic IL-3 mediated

apoptosis cascade), CASP 3 (the chief executioner of programmed cell death in extrinsic and intrinsic signaling cascade), CASP 8 (starter gene in TNF-α apoptosis cascade) and CASP 9 (starter gene in intrinsic apoptosis cascade) genes showed increased expression in HepG2 cells as compared to control group signifying the cytotoxic role of synthesized nanoparticles in the activation of apoptotic pathway.

Furthermore, the level of proteins of all studied genes was also evaluated and similar findings were observed which confirmed the activation of programmed cell death of nanoparticles treated HepG2 cells [160]. The *Rap2A* protein was found to be decreased in plant extract and silver nanoparticles treated cells, whereas the level of Bax and caspase-3, caspase-8 and caspase-9 proteins were found to be increased in the HePG2 cells treated with silver nanoparticles and plant extract. Likewise, synthesized silver nanoparticles caused more downregulation of *Rap2A* protein and more upregulation of apoptotic proteins than plant extract. Caspases are regulators of apoptosis and inflammation, having a critical role in the pathways of cell death. In this study, the synthesized silver nanoparticle's effects were evaluated in the cascades of caspases, as they are the main executioners of apoptosis and cell death pathways in signal transduction [161]. Certain precursors are cleaved by the effector caspases -3/-7 resulting in cell apoptosis. These effector caspases are activated by caspases -8 and -9 [162].

5.5 Phytochemical Analysis of *A. carvifolia* Buch

The genus *Artemisia L.* belonging to the *Asteraceae* family exhibits efficient and therapeutic implications. Plants of this group are frequently found in the moderate sectors of the northern hemisphere with an inadequate number of species in the southern hemisphere of the globe [163]. It contains approximately 500 species of both herbs and shrubs and is a different genus of the Anthemideae tribe [163, 164]. The financial significance of numerous plants of *Artemisia* species is because of their consumption as aesthetics, feedstuff, fodder, therapeutics, and soil binder,

although some species are allergic and toxic weeds [163]. The artemisia genus is reported to have medicinal properties including antioxidant, anti-inflammatory, and antimicrobial with numerous anti-cancer compounds present in it [17]. *Artemisia carvifolia* Buch has been reported to have antidiabetic, antimalarial and anticancer properties. It has also been reported to have phytoconstituents including flavonoids, artemisinin and derivatives with anticancer properties [18–20].

The absorption spectra and retention time of 9 standard polyphenols including ferulic acid, apigenin, caffeic acid, syringic acid, rutin, gallic acid, vanillic acid, rhamnetin and quercetin were used to study the HPLC profile of methanolic extract of *A. carvifolia.* The highest concentration found was that of rhamnetin which was 1.65 μg/mg. The second highest concentration found was that of apigenin (1.39 μg/mg) while the lowest concentration found was that of quercetin (0.12 μg/mg). Previously, polyphenols or flavonoids have been spotted in various *Artemisia* species [100, 165]. Formerly some of the flavonoids in *Artemisia carvifolia* plant extract were detected [18, 19] but rhamnetin and ferulic acid were detected first time in this plant extract this time.

Earlier research has identified flavonoids or polyphenols in various *Artemisia* species such as *A. absinthium* [166], *A. abrotanum* [167, 168], *A. arborescens* [169], *A. annua* [100, 170], *A. asiatica* [171], *A. capillaris* [171], *A. afra* [172]. When *A. dubia* dried plant material of both control and transformed were subjected to phytochemical analysis, the results showed that the transformed plant material produced more flavonoids and phenolic compounds than the untransformed shoots and roots [173].

Numerous chromatographic methods i.e. gas chromatography (GC), paper chromatography (PC), capillary electrophoresis (CE), thin-layer chromatography (TLC), and high-performance liquid chromatography (HPLC), have been used to determine flavonoids [174]. The two most popular techniques for characterizing and quantifying known flavonoids are mass spectrometry (MS) and high-performance liquid chromatography (HPLC) combined with DAD/PDA detectors [175]. The identification and separation of nonvolatile substances can be accomplished with high selectivity and sensitivity using the simple HPLC method, which eliminates

the need for additional derivatization steps. This is the most desirable method for identifying specific flavonoids in all their matrices, including foods, medicines, biological samples, and beverages, due to its availability, flexibility, and variety of separation columns and coupling detectors [174].

Typically, heated reflux extraction techniques are used to extract flavonoids from a variety of solvents, including water, acetone, methanol, ethanol, or a combination of these solvents. In order to extract polyphenols from plant samples, they must be freeze dried, air dried, or oven dried. In a study, plant extracts of *Dryopteris erythrosora* that were first dried in the air before being dried in an oven showed the highest level of total flavonoid content when compared to plant extracts that were dried in an oven directly [176].

HPLC coupled with DAD is a beneficial tool for quantifying suitable polyphenols, actually this approach by its mobile phase allows perfect separation of compounds. The compounds are determined via a comparison of retention time [177]. HPLC, ESI, and MS are more sensitive analytical tools and very competent approaches for the characterization of low and high molecular weight metabolites including phenolic and non-phenolic compounds [178]. Usually, phenolic acids and flavonoids are determined among the phytochemicals of medicinal plants by adopting HPLC with a DAD detector. It was reported that the HPLC technique was utilized to estimate some of these phenolics in *Moringa oleifera* by using gradient acetonitrile and methanol [179, 180]. In the current research work, successful quantitative and qualitative analyses of flavonoids and their derivatives were carried out using the HPLC system along with ultraviolet detector which proved to be an optimal and valid technique for the detection and quantification of flavonoids.

5.6 Computational Analysis

Naturally occurring compounds and their related drugs are being consumed these days to cure almost 87 % of human diseases as well as various microbial diseases, cancer, and immunological disorders. It has been revealed that nearly 25 % of approved drugs globally are acquired from plants. In various developing

countries approximately 80 % population uses drugs obtained through plants for health-related problems [181]. The drug designing process includes computational methods of virtual screening which uses huge databases of molecular structures, designed by computational techniques. By this approach, it is possible to recognize molecules more susceptible to binding to the molecular drug targets typically a protein or enzyme receptor [60, 182, 183]. Furthermore, it also includes classical molecular dynamic simulations which are initiated from an atomistic depiction of the system and permit studying its deterministic evolution over time by Newton's laws of motion. Molecular dynamic simulation is an atomistic strategy offering the opportunity of using computationally intensive every atom's simulation methods that may be clear like an atomic microscope. MDS permits accessing atomic motion at a femtosecond time scale, therefore, permits *In-silco* studies of protein dynamics that agree with the mainly detailed experimental studies [184].

The primary structure of *Rap2A* protein was retrieved and physiochemical properties were analyzed by ProtParam Expasy. Afterwards, *Rap2A* protein with pdb id 2rap was selected from the Protein Data Bank (PDB) and the 3D structure of *Rap2A* was downloaded in pdb format. The small G protein *Rap2A* has been crystallized in complex with GDP and GTP'S. The *Rap2A* GTP complex is the first structure of a small G protein. The *Rap2A*-GTP complex (PDB 3RAP) is the most similar model in PDB to Rap1B-GTP, but despite the almost perfect conservation of switch I and switch II, the models show marked differences [114].

For refining the protein structure pymol software was used. Ramachandran plot was used for the evaluation of protein model quality. This tool carried out stereochemical analysis of a protein structure by analyzing residues through residues geometry and overall protein structural conformation and validation [185]. QMEAN (quantitative model energy analysis) was used to analyze the quantitative model energy of a protein structure and the quality of a protein. [186]. The ProSA program calculated the overall quality of the protein structure and also recognized the identification method of the protein structure. This model showed two identification methods, one was the X-ray crystallography method and the other was the NMR identification method. The Z score calculated was -6.31 showing that the model structure quality

was best as this score is within the range indicating better protein quality. But if the score is not within range, the structure is considered invalid. The light blue colour represents the X-ray crystallography region while the dark blue colour shows the NMR region [187].

The physicochemical properties of the protein, the composition comprising of type of amino acid, their ratio, the net charge of the protein, and its stability index play a vital role in determining the structure as well as the function of a protein [188]. Furthermore, the fundamental unit of protein structure and function are protein domains which are local, dense units of structure, whose interior is hydrophobic and exterior is hydrophilic. The domains form a final globular-like state with no further ability to be subdivided in terms of structure. These functional domains work either independently or in cooperation with neighboring domains. Proteins' specific function is based on the specific domains of that particular protein which makes it different from others. Hence, the identification of protein domains is fundamental for the classification of proteins and establishing their functions as well as for the prediction of protein structure design [189].

The structure of proteins plays an integral part in determining their functions. PDB is the main library for determining the 3D structure of biological macro-molecules including proteins at atomic level. This database provides everlasting and skillful resources for structural biologists to archive and explore their work, present mechanisms for reproducibility ensuring the biomolecular structures and also facilitates widely to researchers across scientific disciplines [190]. The structure of macromolecules obtained through PDB is validated by the Ramachandran plot which is the main quality metrics utilized in the authentication of the protein's atomic model's quality. Validation is considered an integral part of obtaining 3D models of macromolecules either through X-ray crystallography, or cryoelectronic microscopy as well as for the interpretation of the model's quality obtained through PDB [191].

The PubChem database was used for downloading the 2D structures and infor-mation of identified ligands of *A. carvifolia* i.e. apigenin, caffeic acid, gallic acid,

rhamnetin, rutin, ferulic acid, syringic acid, vanillic acid and quercetin, and standard drug lenvatinib [192]. The energy minimization of ligands was carried out by ChemPro software chem12 as a preliminary step in the preparation of ligands for docking as unstable ligands present unpredictable vina scores in docking results. For current research studies, the CB-Dock online docking tool was used for the molecular docking process [193]. Based on the best vina score, cavity size and grid map score, the four best ligands (apigenin, caffeic acid, gallic acid, rhamnetin) were selected for protein-ligand interaction and molecular dynamic simulation along with lenvatinib as a standard drug.

Molecular docking is adopted widely for studying the binding affinity, interactions and biological activity of peptides proteins and other macromolecules which is a key tool in computer-assisted drug designing and structural molecular biology. The purpose here is to predict the predominant binding mode(s) of a ligand with a protein of known three-dimensional structure. Successful docking methods search high-dimensional spaces effectively and use a scoring function that correctly ranks candidate dockings. Docking can be used to perform virtual screening on large libraries of compounds, rank the results, and propose structural hypotheses of how the ligands inhibit the target, which is invaluable in lead optimization [194].

In the current research study, RMSD (Root-mean-square deviation) values in docking results were checked. The RMSD values gave the average deviation between the corresponding ligand and protein molecules. RMSD was used to measure how different a calculated docking pose of a ligand is from its corresponding co-crystallized orientation in the same protein [195]. Pose 2 was identified as the best pose according to RMSD rules and regulations. The range value for RMSD is less than 2 and not greater than 4. The RMSF (root mean square fluctuation) measured the average deviation of protein residues. It examined the area of protein structure that deviated the greatest or leased from their mean structure. Furthermore, the trajectories were further examined for root-mean-square deviation (RMSD) and root-mean-square fluctuation (RMSF), ligand torsion profiles, and protein-ligand interaction profiling with the help of the MD Simulation Interaction Diagram module of the Desmond [196].

For molecular dynamic simulation, four ligands (apigenin, caffeic acid, gallic acid and rhamnetin) complexes with *Rap2A* protein were selected while on the other hand reference drug (lenvatinib's complex) for comparison was chosen. Simulations of all these complexes were run on different nano seconds. Apigenin simulation was run from 1 nano second to 100 ns and the apigenin was found stable till 100ns. Caffeic acid simulation was not so good because the complex was unstable while performing the simulation. The simulation results of caffeic acid showed that this complex was stable till 20ns but after that it was found unstable showing that caffeic acid interaction with *Rap2A* protein is not better than apigenin complex. The gallic acid complex simulation was very poor because after 10 ns it was found unstable and unreliable. While rhamnetin and reference drug did not show simulation as after 1 ns, their complexes showed instability. So, from over all simulation results of these complexes, it was concluded that apigenin is better than all other studied complexes. According to simulation results, the comparison of lenvatinib (reference drug) with all other ligand complexes was not much appreciable because lenvatinib drug did not show interaction with the targeted protein *Rap2A*. Therefore, the molecular dynamic simulation results of the apigenin complex with *Rap2A* indicated that this complex was far better than other complexes because till 100 ns apigenin complex remained stable showing that apigenin interaction with *Rap2A* protein is quite strong.

Molecular dynamic simulation has evolved as the most powerful method to investigate and analyze biomolecular dynamics, with the introduction of high-end processing capacity in the simulation that can be performed between micro second to nano second that can accurately describe the dynamics of any system. For molecular dynamic stimulation, many force fields such as GROMACS [197], AMBER and CHARMM are the extensively used methods, which may offer exact information on the movement and flexibility of protein complexes, that contribute to the interaction of dynamics with protein ligands complexes [198].

Selected four ligands and one standard drug from the drug bank database followed Lipinski's rule of five, which is a rule to evaluate drug-likeness or determination of chemical compounds with certain pharmacological and biological activities that

would make it a likely orally active drug. According to Lipinski's rule of five, the Log p-value of most drug molecules should be limited to 5, molecular weight should be less than 500, hydrogen bond acceptor should not be greater than 10 and hydrogen bond donor should be limited to 5. A general "rule of thumb" for the valuation of drug-like properties, known as Lipinski's rule of 5 (Ro5), has been introduced for almost 2 decades [199].

Furthermore, the selected ligands were screened for their ADMET (Pharmacokinetic) properties. The potential success of compounds depends on their ADMET properties. PKCSM tool was used to find ADMET properties of ligands. Pharmacokinetic properties including absorption, distribution, metabolism, excretion, and toxicity (ADMET) play a critical role in the screening of compounds as drug candidates. In the case of absorption properties, the water solubility of the reference drug was slightly less than the apigenin and $CaCO_2$ permeability values of all other 3 lead compounds and the synthetic drug was also less than that of apigenin. The Fu value of lead compounds was found to be more than lenvatinib which showed apigenin and other lead compounds are more effective than synthetic drug in case of unbound friction in plasma. While predicting toxicity properties, the predicted value of drug clearance as total clearance of apigenin or other lead compounds was high as compared to synthetic drug. Total clearance is related to bioavailability and is important for determining dosing rates. Toxicity is the very significant parameter of ADMET properties which consists of 9 models. Maximum tolerated dose helps to set the maximum recommended tolerated dose, which was found to be 0.426 for lenvatinib and 0.328 for apigenin indicating that lenvatinib is ahead in safety than lead compound. LOAEL predicted value of lenvatinib was found to be 1.7 and less than that of apigenin and other 3 lead compounds which showed its potency to be more toxic than studied bioactive compounds. Hepatotoxicity simply indicates the injury to the liver which shows results in two categories yes/no. Lenvatinib was found to be hepatotoxic whereas lead compounds were not. Both lenvatinib and apigenin do not cause any allergic reactions. *T. pyriformis* toxicity is expressed as the negative logarithm of the concentration required to inhibit 50% growth. The main aim of our research was to determine the pharmacokinetic profile of four *A.*

carvifolia metabolites and one synthetic drug by adopting PKCSM and SwissAME computational techniques.

The comparison between an anti-cancer drug for liver cancer (lenvatinib) and the proposed lead compound apigenin was done by comparing properties like docking values, physiochemical properties, interaction properties, ADMET properties and simulation results. So, it was predicted that apigenin is so far batter then lenvatinib reference drug on the basis of these studied parameters. In recent years, this potential compound apigenin has been recognized as a health-promoting drug because of its poor intrinsic toxicity and discrete activities on normal versus cancer cells due to its anti-oxidant as well as anti-inflammatory activities [200]. Apigenin has demonstrated broad antitumor impacts against a multitude of cancers, such as melanoma, osteosarcoma, breast, colorectal, liver, lung, and prostate cancers. It is found that this potent molecule induces cell apoptosis/autophagy and modulation of the cell cycle to suppress tumor cell proliferation [201].

Thus, in the current study, the extract of *Artemisia carvifolia* Buch was found effective in downregulating the *Rap2A* gene in the liver cancer cell line HePG2. There was observed a significant decrease in the expression of the *Rap2A* gene and protein in a treated cell line, along with the increased level of apoptotic genes and proteins as compared to untreated cells [202]. Thus, the *Rap2A* gene can be a potential drug target and apigenin can be a potential drug candidate for liver cancer as proposed by the current study.

Chapter 6

Conclusion

The world is facing the challenge of liver cancer which is one of the main reasons of death worldwide. In Pakistan, this disease is increasing and may show the most widespread tumor in adult men. Therapeutic plants play a helpful part in the treatment of cancers and other illnesses. *Artemisia* species has therapeutic and efficient implications against various diseases. Medicinal plants and plant-based medicines are being used in healthcare since ancient times. There has been tremendous research worldwide to establish their medicinal properties and many have led to the development of valuable drugs and medicines.

Nanotechnology has gained significant importance in the current era for enhancing the efficacy and therapeutic potential of medicinal plant extracts and metabolites present in them. The aim of the present research work was to analyze the *A. carvifolia* Buch extract and respective silver nanoparticles for efficacy against liver cancer cell line HepG2. Furthermore, it also aimed to screen the extract of this plant for the presence of important metabolites specifically the flavonoids and to test those metabolite's interaction with *Rap2A* protein by molecular docking and molecular dynamic simulation. Moreover, the ADMET properties of these metabolites were also determined. This is the first-ever report describing the synthesis and efficacy of silver nanoparticles of *A. carvifolia* Buch against liver cancer.

Observations of the current study are important to throw light on the efficacy of *A. carvifolia* Buch plant extract and its AgNps where a green chemistry approach was utilized that led to the successful development of AgNps because of stabilizing agents in *A. carvifolia* Buch plant extract. The *A. carvifolia* Buch plant extract and respective silver nanoparticles were found effective drug candidates against liver cancer targeting the *Rap2A* gene. Amazingly, silver nanoparticles displayed significant cytotoxic potential against liver cancer cell lines.

Rap2A gene expression and protein level were found to be down-regulated in the liver cancer cell line after treatment with silver nanoparticles and plant extract. Furthermore, the apoptotic role of synthesized silver nanoparticles and plant extract was confirmed by higher gene expression of apoptotic pathway genes and proteins including Bax, caspase 3, caspase 8 and caspase 9. The efficacy of synthesized silver nanoparticles was found more than the plant extract. Thus, the current study also provides evidence for using the *Rap2A* gene as a potential drug target for the treatment of liver cancer.

Moreover, polyphenols including ferulic acid, apigenin, caffeic acid, syringic acid, rutin, gallic acid, vanillic acid, rhamnetin and quercetin were also studied in the HPLC profile of methanolic extract of *A. carvifolia*. The detected metabolites of *A. carvifolia* were used for the molecular docking against *Rap2A* protein to determine its capability to be used as a potential drug target for liver cancer. After the complete protein model evaluation along with detailed analysis of binding scores, physiochemical properties, interaction and ADMET properties, RMSD and RMSF interpretation, and Molecular Dynamics Simulations, the four best ligands named apigenin, caffeic acid, gallic acid, and rhamnetin were identified as hit compounds inhibiting *Rap2A* protein. Eventually, apigenin was identified as a lead compound out of these four compounds based on the findings. Based on all the above-mentioned parameters, it was concluded that apigenin could be a better anticancer drug candidate against liver cancer having the efficient ability to inhibit the *Rap2A* gene which can be a new drug target for liver cancer. Moreover, apigenin was

also found better in comparison to the synthetic drug lenvatinib, against liver cancer suggesting its anticancer potential against liver cancer.

6.1 Future Recommendation

The current study provides evidence for using the *Rap2A* gene as a potential drug target for the treatment of liver cancer. However, further studies are needed to be done in this regard for confirmation in animal models. Future recommendations of the current study are given below:

1. The anti-cancerous potential of *A. carvifolia* Buch against liver cancer can be tested by producing its metallic nanoparticles of different metals i.e. Au, Cu, Fe Zn etc.

2. Gene targets of metallic nanoparticles and extracts other than the *Rap2A* gene can explored.

3. A new possible inhibitor for the Rap gene signaling cascade can be explored by targeting other metabolites present in this plant extract.

4. New cancer biomarkers in human liver cancer can be studied belonging to the same gene family other than the *Rap2A* gene.

5. Animal models and clinical trials should be performed to confirm the *Rap2A* gene as a potential biomarker for liver cancer diagnosis and treatment.

6. The *Rap2A* gene can be explored for its potential as an oncogene in other tumors as well.

7. *A. carvifolia* extract and its nanoparticles can be studied for efficacy against other cancers as well.

8. Other apoptotic markers can be studied to further confirm the efficacy of *A. carvifolia* extract and respective nanoparticles as apoptotic agents.

9. Other analytical techniques i.e. GC-MS or LC-MS can be performed to determine the presence of other metabolites in the extract of *A. carvifolia* Buch.

10. Detailed mechanism of action of *A. carvifolia* Buch and respective nanoparticles can be explored by targeting further gene and protein targets.

Bibliography

[1] H. H. Math, K. N. Shashiraj, R. S. Kumar, M. Rudrappa, M. P. Bhat, D. S. Basavarajappa, A. I. Almansour, K. Perumal, and S. Nayaka, "Investigation of in vitro anticancer and apoptotic potential of biofabricated silver nanoparticles from cardamine hirsuta (l.) leaf extract against caco-2 cell line," *Inorganics*, vol. 11, no. 8, p. 322, 2023.

[2] B. S. Chhikara and K. Parang, "Global cancer statistics 2022: the trends projection analysis," *Chemical Biology Letters*, vol. 10, no. 1, pp. 451–451, 2023.

[3] F. Bray, J. Ferlay, I. Soerjomataram, R. L. Siegel, L. A. Torre, and A. Jemal, "Global cancer statistics 2018: Globocan estimates of incidence and mortality worldwide for 36 cancers in 185 countries," *CA: a cancer journal for clinicians*, vol. 68, no. 6, pp. 394–424, 2018.

[4] H. Zhang, J. Zhu, L. Xi, C. Xu, and A. Wu, "Validation of the toronto hepatocellular carcinoma risk index for patients with cirrhosis in china: a retrospective cohort study," *World Journal of Surgical Oncology*, vol. 17, pp. 1–9, 2019.

[5] A. B. Hafeez Bhatti, F. S. Dar, A. Waheed, K. Shafique, F. Sultan, N. H. Shah *et al.*, "Hepatocellular carcinoma in pakistan: national trends and global perspective," *Gastroenterology Research and practice*, vol. 2016, pp. 1–10, 2016.

[6] B. Zhai and X.-Y. Sun, "Mechanisms of resistance to sorafenib and the corresponding strategies in hepatocellular carcinoma," *World journal of hepatology*, vol. 5, no. 7, p. 345, 2013.

[7] D. Jain and P. Janmeda, "Exposure, formation, and various available treatments to combat hepatocellular carcinoma: A comprehensive review," *The Applied Biology & Chemistry Journal (TABCJ)*, vol. 4, no. 2, pp. 69–83, 2023.

[8] I. Lurje, Z. Czigany, J. Bednarsch, C. Roderburg, P. Isfort, U. P. Neumann, and G. Lurje, "Treatment strategies for hepatocellular carcinoma-a multidisciplinary approach," *International journal of molecular sciences*, vol. 20, no. 6, p. 1465, 2019.

[9] D. A. Wheeler, L. R. Roberts, C. G. A. R. Network *et al.*, "Comprehensive and integrative genomic characterization of hepatocellular carcinoma," *Cell*, vol. 169, no. 7, p. 1327, 2017.

[10] G. M. Bokoch, "Biology of the rap proteins, members of the ras superfamily of gtp-binding proteins." *Biochemical Journal*, vol. 289, no. Pt 1, p. 17, 1993.

[11] S. Kumari, M. Arora, J. Singh, L. K. Kadian, R. Yadav, S. S. Chauhan, and A. Chopra, "Molecular associations and clinical significance of raps in hepatocellular carcinoma," *Frontiers in Molecular Biosciences*, vol. 8, p. 677979, 2021.

[12] X. Zheng, W. Zhao, P. Ji, K. Zhang, J. Jin, M. Feng, F. Wang, S. Zheng, and X. Wang, "High expression of rap2a is associated with poor prognosis of patients with hepatocellular carcinoma," *International journal of clinical and experimental pathology*, vol. 10, no. 9, p. 9607, 2017.

[13] R. H. Khokhar, A. A. Jamali, and S. Rind, "Hepatocellular carcinoma in patients suffering from chronic hepatitis b versus co-infection of hepatitis b and d virus," *Journal of Islamabad Medical & Dental College*, vol. 6, no. 4, pp. 203–207, 2017.

[14] L. Zhang, H.-b. Duan, and Y.-s. Yang, "Knockdown of rap2b inhibits the proliferation and invasion in hepatocellular carcinoma cells," *Oncology Research*, vol. 25, no. 1, p. 19, 2017.

[15] P. R. Choudhury, A. D. Talukdar, D. Nath, P. Saha, and R. Nath, "Traditional folk medicine and drug discovery: prospects and outcome," *Advances in Pharmaceutical Biotechnology: Recent Progress and Future Applications*, vol. 2020, pp. 3–13, 2020.

[16] S. Narendiran, D. Janani, M. Keerthana, K. Nivethitha, S. Nirmala Devi, S. Padmavathy, T. Supraja, H. Sayeedur Rahman, R. Velvizhi, N. Swathi *et al.*, "Comparative studies on in-vitro phytochemicals analysis and larvicidal efficacy of medicinal plant extracts against culex quinquefasciatus," *Int. J. Life. Sci. Scienti. Res*, vol. 2, no. 6, pp. 742–748, 2016.

[17] H. Forouhandeh, V. Tarhriz, M. Zadehkamand, and P. Asgharian, "Anti-proliferative activity of artemisia marschalliana on cancerous cell lines," *BMC Complementary Medicine and Therapies*, vol. 23, no. 1, p. 119, 2023.

[18] E. Dilshad, H. Ismail, I.-u. Haq, R. M. Cusido, J. Palazon, K. Ramirez-Estrada, and B. Mirza, "Rol genes enhance the biosynthesis of antioxidants in artemisia carvifolia buch," *BMC Plant Biology*, vol. 16, pp. 1–9, 2016.

[19] A. N. Khan and E. Dilshad, "Enhanced antioxidant and anticancer potential of artemisia carvifolia buch transformed with rol a gene," *Metabolites*, vol. 13, no. 3, p. 351, 2023.

[20] E. Dilshad, H. Ismail, M. A. Khan, R. M. Cusido, and B. Mirza, "Metabolite profiling of artemisia carvifolia buch transgenic plants and estimation of their anticancer and antidiabetic potential," *Biocatalysis and agricultural biotechnology*, vol. 24, p. 101539, 2020.

[21] A. Ebrahiminezhad, S. Taghizadeh, A. Berenjian, F. Heidaryan Naeini, and Y. Ghasemi, "Green synthesis of silver nanoparticles capped with natural carbohydrates using ephedra intermedia," *Nanoscience & Nanotechnology-Asia*, vol. 7, no. 1, pp. 104–112, 2017.

[22] M. Thiruvengadam, G. Rajakumar, and I.-M. Chung, "Nanotechnology: current uses and future applications in the food industry," *3 Biotech*, vol. 8, pp. 1–13, 2018.

[23] V. T. Sabe, T. Ntombela, L. A. Jhamba, G. E. Maguire, T. Govender, T. Naicker, and H. G. Kruger, "Current trends in computer aided drug design and a highlight of drugs discovered via computational techniques: A review," *European Journal of Medicinal Chemistry*, vol. 224, p. 113705, 2021.

[24] P. V. Bharatam, "Computer-aided drug design," *Drug discovery and development: From targets and molecules to medicines*, vol. 2021, pp. 137–210, 2021.

[25] A. S. Butt, Z. Abbas, and W. Jafri, "Hepatocellular carcinoma in pakistan: where do we stand?" *Hepatitis monthly*, vol. 12, no. 10 HCC, p. e6023, 2012.

[26] Y. Liu and L. Liu, "Changes in the epidemiology of hepatocellular carcinoma in asia," *Cancers*, vol. 14, no. 18, p. 4473, 2022.

[27] M. C. Plaz Torres, G. Bodini, M. Furnari, E. Marabotto, P. Zentilin, M. Strazzabosco, and E. G. Giannini, "Surveillance for hepatocellular carcinoma in patients with non-alcoholic fatty liver disease: universal or selective?" *Cancers*, vol. 12, no. 6, p. 1422, 2020.

[28] D. Suresh, A. N. Srinivas, and D. P. Kumar, "Etiology of hepatocellular carcinoma: special focus on fatty liver disease," *Frontiers in Oncology*, vol. 10, p. 601710, 2020.

[29] H. Razavi, "Global epidemiology of viral hepatitis," *Gastroenterol Clin North Am*, vol. 49, no. 2, pp. 179–189, 2020.

[30] M. M. Elizalde, L. Tadey, J. F. Quarleri, R. H. Campos, and D. M. Flichman, "Biological characterization of hepatitis b virus genotypes: their role in viral replication and antigen expression," *Frontiers in microbiology*, vol. 12, p. 758613, 2021.

[31] J. A. Marrero, L. M. Kulik, C. B. Sirlin, A. X. Zhu, R. S. Finn, M. M. Abecassis, L. R. Roberts, and J. K. Heimbach, "Diagnosis, staging, and management of hepatocellular carcinoma: 2018 practice guidance by the american association for the study of liver diseases," *Hepatology*, vol. 68, no. 2, pp. 723–750, 2018.

[32] A. Isidan, A. Yenigun, D. Soma, E. Aksu, K. Lopez, Y. Park, A. Cross-Najafi, P. Li, D. Kundu, M. G. House *et al.*, "Development and characterization of human primary cholangiocarcinoma cell lines," *The American Journal of Pathology*, vol. 192, no. 9, pp. 1200–1217, 2022.

[33] M. Tufail and C. Wu, "Exploring the burden of cancer in pakistan: an analysis of 2019 data," *Journal of Epidemiology and Global Health*, vol. 13, no. 2, pp. 333–343, 2023.

[34] S. Ashtari, M. A. Pourhoseingholi, A. Sharifian, and M. R. Zali, "Hepatocellular carcinoma in asia: Prevention strategy and planning," *World journal of hepatology*, vol. 7, no. 12, p. 1708, 2015.

[35] J. Zhang, G. Chen, P. Zhang, J. Zhang, X. Li, D. Gan, X. Cao, M. Han, H. Du, and Y. Ye, "The threshold of alpha-fetoprotein (afp) for the diagnosis of hepatocellular carcinoma: A systematic review and meta-analysis," *PLoS One*, vol. 15, no. 2, p. e0228857, 2020.

[36] R. R. Plentz and N. P. Malek, "Early detection of hepatocellular carcinoma: how to screen and follow up patients with liver cirrhosis according to the german s3 guideline?" *Diagnostics*, vol. 5, no. 4, pp. 497–503, 2015.

[37] S. Qin *et al.*, "Guidelines on the diagnosis and treatment of primary liver cancer (2011 edition)." *Chinese clinical oncology*, vol. 1, no. 1, pp. 10–10, 2012.

[38] S. Man, C. Luo, M. Yan, G. Zhao, L. Ma, and W. Gao, "Treatment for liver cancer: From sorafenib to natural products," *European journal of medicinal chemistry*, vol. 224, p. 113690, 2021.

[39] S. Daher, M. Massarwa, A. A. Benson, and T. Khoury, "Current and future treatment of hepatocellular carcinoma: an updated comprehensive review," *Journal of clinical and translational hepatology*, vol. 6, no. 1, p. 69, 2018.

[40] A. X. Zhu, "Development of sorafenib and other molecularly targeted agents in hepatocellular carcinoma," *Cancer: Interdisciplinary International Journal of the American Cancer Society*, vol. 112, no. 2, pp. 250–259, 2008.

[41] A. X. Zhu, L. S. Blaszkowsky, D. P. Ryan, J. W. Clark, A. Muzikansky, K. Horgan, S. Sheehan, K. E. Hale, P. C. Enzinger, P. Bhargava *et al.*, "Phase ii study of gemcitabine and oxaliplatin in combination with bevacizumab in patients with advanced hepatocellular carcinoma," *Journal of Clinical Oncology*, vol. 24, no. 12, pp. 1898–1903, 2006.

[42] A. A. Abdelgalil, H. M. Al-Kahtani, and F. I. Al-Jenoobi, "Erlotinib," vol. 45, pp. 93–117, 2020.

[43] A. X. Zhu, K. Stuart, L. S. Blaszkowsky, A. Muzikansky, D. P. Reitberg, J. W. Clark, P. C. Enzinger, P. Bhargava, J. A. Meyerhardt, K. Horgan *et al.*, "Phase 2 study of cetuximab in patients with advanced hepatocellular carcinoma," *Cancer: Interdisciplinary International Journal of the American Cancer Society*, vol. 110, no. 3, pp. 581–589, 2007.

[44] A. Villanueva, D. Y. Chiang, P. Newell, J. Peix, S. Thung, C. Alsinet, V. Tovar, S. Roayaie, B. Minguez, M. Sole *et al.*, "Pivotal role of mtor signaling in hepatocellular carcinoma," *Gastroenterology*, vol. 135, no. 6, pp. 1972–1983, 2008.

[45] M. Heuer, T. Benkoe, V. R. Cicinnati, G. M. Kaiser, G. Sotiropoulos, H. Baba, J. Treckmann, C. Broelsch, and A. Paul, "Effect of low-dose rapamycin on tumor growth in two human hepatocellular cancer cell lines," in *Transplantation proceedings*, vol. 41, no. 1.   Elsevier, 2009, pp. 359–365.

[46] H. Huynh, K. Pierce Chow, K. C. Soo, H. C. Toh, S. P. Choo, K. F. Foo, D. Poon, V. C. Ngo, and E. Tran, "Rad001 (everolimus) inhibits tumour growth in xenograft models of human hepatocellular carcinoma," *Journal of cellular and molecular medicine*, vol. 13, no. 7, pp. 1371–1380, 2009.

[47] H. Huang, J. Di, D. Qu, Z. Gao, Y. Zhang, and J. Zheng, "Role of rap2 and its downstream effectors in tumorigenesis," *Anti-Cancer Agents in Medicinal Chemistry (Formerly Current Medicinal Chemistry-Anti-Cancer Agents)*, vol. 15, no. 10, pp. 1269–1276, 2015.

[48] P. Y. Yip, "Phosphatidylinositol 3-kinase-akt-mammalian target of rapamycin (pi3k-akt-mtor) signaling pathway in non-small cell lung cancer," *Translational lung cancer research*, vol. 4, no. 2, p. 165, 2015.

[49] C.-K. Looi, L.-W. Hii, S. C. Ngai, C.-O. Leong, and C.-W. Mai, "The role of ras-associated protein 1 (rap1) in cancer: bad actor or good player?" *Biomedicines*, vol. 8, no. 9, p. 334, 2020.

[50] M. Islam, S. Jones, and I. Ellis, "Role of akt/protein kinase b in cancer metastasis," *Biomedicines*, vol. 11, no. 11, p. 3001, 2023.

[51] J.-X. Wu, D.-G. Zhang, J.-N. Zheng, and D.-S. Pei, "Rap2a is a novel target gene of p53 and regulates cancer cell migration and invasion," *Cellular signalling*, vol. 27, no. 6, pp. 1198–1207, 2015.

[52] C. Nössing and K. M. Ryan, "50 years on and still very much alive:'apoptosis: a basic biological phenomenon with wide-ranging implications in tissue kinetics'," *British Journal of Cancer*, vol. 128, no. 3, pp. 426–431, 2023.

[53] R. Jan *et al.*, "Understanding apoptosis and apoptotic pathways targeted cancer therapeutics," *Advanced pharmaceutical bulletin*, vol. 9, no. 2, p. 205, 2019.

[54] R. S. Wong, "Apoptosis in cancer: from pathogenesis to treatment," *Journal of experimental & clinical cancer research*, vol. 30, pp. 1–14, 2011.

[55] D. Nn, "Cell death: critical control points," *Cell*, vol. 116, pp. 205–219, 2004.

[56] S. Orrenius, P. Nicotera, and B. Zhivotovsky, "Cell death mechanisms and their implications in toxicology," *Toxicological sciences*, vol. 119, no. 1, pp. 3–19, 2011.

[57] I. M. Ghobrial, T. E. Witzig, and A. A. Adjei, "Targeting apoptosis pathways in cancer therapy," *CA: a cancer journal for clinicians*, vol. 55, no. 3, pp. 178–194, 2005.

[58] O. Oyebode, N.-B. Kandala, P. J. Chilton, and R. J. Lilford, "Use of traditional medicine in middle-income countries: a who-sage study," *Health policy and planning*, vol. 31, no. 8, pp. 984–991, 2016.

[59] M. J. Abad, L. M. Bedoya, L. Apaza, and P. Bermejo, "The artemisia l. genus: a review of bioactive essential oils," *Molecules*, vol. 17, no. 3, pp. 2542–2566, 2012.

[60] D. Bisht, D. Kumar, D. Kumar, K. Dua, and D. K. Chellappan, "Phytochemistry and pharmacological activity of the genus artemisia," *Archives of Pharmacal Research*, vol. 44, no. 5, pp. 439–474, 2021.

[61] S. Z. Taghizadeh Rabe, M. Mahmoudi, A. Ahi, and S. A. Emami, "Antiproliferative effects of extracts from iranian artemisia species on cancer cell lines," *Pharmaceutical biology*, vol. 49, no. 9, pp. 962–969, 2011.

[62] E. Dilshad, "Genetic transformation of artemisia carvifolia buch with rol genes for enhancement of secondary metabolites," p. 03, 2016.

[63] S. Ramanathan, S. C. Gopinath, M. M. Arshad, P. Poopalan, and V. Perumal, "Nanoparticle synthetic methods: strength and limitations," pp. 31–43, 2021.

[64] V. Pareek, A. Bhargava, R. Gupta, N. Jain, and J. Panwar, "Synthesis and applications of noble metal nanoparticles: a review," *Advanced Science, Engineering and Medicine*, vol. 9, no. 7, pp. 527–544, 2017.

[65] N. Baig, I. Kammakakam, and W. Falath, "Nanomaterials: A review of synthesis methods, properties, recent progress, and challenges," *Materials Advances*, vol. 2, no. 6, pp. 1821–1871, 2021.

[66] S. Ghosh, R. Ahmad, M. Zeyaullah, and S. K. Khare, "Microbial nanofactories: synthesis and biomedical applications," *Frontiers in Chemistry*, vol. 9, p. 626834, 2021.

[67] Y. Bao, J. He, K. Song, J. Guo, X. Zhou, and S. Liu, "Plant-extract-mediated synthesis of metal nanoparticles," *Journal of Chemistry*, vol. 2021, pp. 1–14, 2021.

[68] O. Pryshchepa, P. Pomastowski, and B. Buszewski, "Silver nanoparticles: Synthesis, investigation techniques, and properties," *Advances in Colloid and Interface Science*, vol. 284, p. 102246, 2020.

[69] H. Mirzaei and M. Darroudi, "Zinc oxide nanoparticles: Biological synthesis and biomedical applications," *Ceramics International*, vol. 43, no. 1, pp. 907–914, 2017.

[70] M. Roshani, A. Rezaian-Isfahni, M. H. Lotfalizadeh, N. Khassafi, M. H. J. N. Abadi, and M. Nejati, "Metal nanoparticles as a potential technique for the diagnosis and treatment of gastrointestinal cancer: a comprehensive review," *Cancer Cell International*, vol. 23, no. 1, p. 280, 2023.

[71] A. Ali, H. Zafar, M. Zia, I. ul Haq, A. R. Phull, J. S. Ali, and A. Hussain, "Synthesis, characterization, applications, and challenges of iron oxide nanoparticles," *Nanotechnology, science and applications*, pp. 49–67, 2016.

[72] A. Hamad, K. S. Khashan, and A. Hadi, "Silver nanoparticles and silver ions as potential antibacterial agents," *Journal of Inorganic and Organometallic Polymers and Materials*, vol. 30, no. 12, pp. 4811–4828, 2020.

[73] D. N. Păduraru, D. Ion, A.-G. Niculescu, F. Mu?at, O. Andronic, A. M. Grumezescu, and A. Bolocan, "Recent developments in metallic nanomaterials for cancer therapy, diagnosing and imaging applications," *Pharmaceutics*, vol. 14, no. 2, p. 435, 2022.

[74] A. Farzin, S. A. Etesami, J. Quint, A. Memic, and A. Tamayol, "Magnetic nanoparticles in cancer therapy and diagnosis," *Advanced healthcare materials*, vol. 9, no. 9, p. 1901058, 2020.

[75] K. Baryeh, M. Attia, J. C. Ulloa, and J. Y. Ye, "Magnetic nanoparticle-based hybrid materials in the biomedical field: Fundamentals and applications," in *Magnetic Nanoparticle-Based Hybrid Materials*. Elsevier, 2021, pp. 387–423.

[76] L. Pinzi and G. Rastelli, "Molecular docking: shifting paradigms in drug discovery," *International journal of molecular sciences*, vol. 20, no. 18, p. 4331, 2019.

[77] H. Oshima, S. Re, and Y. Sugita, "Prediction of protein–ligand binding pose and affinity using the grest+ fep method," *Journal of Chemical Information and Modeling*, vol. 60, no. 11, pp. 5382–5394, 2020.

[78] I. M. Ibrahim, D. H. Abdelmalek, M. E. Elshahat, and A. A. Elfiky, "Covid-19 spike-host cell receptor grp78 binding site prediction," *Journal of infection*, vol. 80, no. 5, pp. 554–562, 2020.

[79] J. Fan, A. Fu, and L. Zhang, "Progress in molecular docking," *Quantitative Biology*, vol. 7, pp. 83–89, 2019.

[80] J. L. Morrison, R. Breitling, D. J. Higham, and D. R. Gilbert, "A lock-and-key model for protein–protein interactions," *Bioinformatics*, vol. 22, no. 16, pp. 2012–2019, 2006.

[81] D. E. Koshland Jr, "The key–lock theory and the induced fit theory," *Angewandte Chemie International Edition in English*, vol. 33, no. 23-24, pp. 2375–2378, 1995.

[82] Y. Chen and D. Zhi, "Ligand–protein inverse docking and its potential use in the computer search of protein targets of a small molecule," *Proteins: Structure, Function, and Bioinformatics*, vol. 43, no. 2, pp. 217–226, 2001.

[83] D. B. Kitchen, H. Decornez, J. R. Furr, and J. Bajorath, "Docking and scoring in virtual screening for drug discovery: methods and applications," *Nature reviews Drug discovery*, vol. 3, no. 11, pp. 935–949, 2004.

[84] A. Haredi Abdelmonsef, R. Dulapalli, T. Dasari, L. Souda Padmarao, T. Mukkera, and U. Vuruputuri, "Identification of novel antagonists for rab38 protein by homology modeling and virtual screening," *Combinatorial chemistry & high throughput screening*, vol. 19, no. 10, pp. 875–892, 2016.

[85] Y. Tang, W. Zhu, K. Chen, and H. Jiang, "New technologies in computer-aided drug design: Toward target identification and new chemical entity discovery," *Drug discovery today: technologies*, vol. 3, no. 3, pp. 307–313, 2006.

[86] S. Decherchi and A. Cavalli, "Thermodynamics and kinetics of drug-target binding by molecular simulation," *Chemical Reviews*, vol. 120, no. 23, pp. 12 788–12 833, 2020.

[87] K. Al-Khafaji and T. T. Tok, "Molecular dynamics simulation, free energy landscape and binding free energy computations in exploration the anti-invasive activity of amygdalin against metastasis," *Computer Methods and Programs in Biomedicine*, vol. 195, p. 105660, 2020.

[88] M. J. Abraham, T. Murtola, R. Schulz, S. Páll, J. C. Smith, B. Hess, and E. Lindahl, "Gromacs: High performance molecular simulations through multi-level parallelism from laptops to supercomputers," *SoftwareX*, vol. 1, pp. 19–25, 2015.

[89] Z. Jing, C. Liu, S. Y. Cheng, R. Qi, B. D. Walker, J.-P. Piquemal, and P. Ren, "Polarizable force fields for biomolecular simulations: Recent advances and applications," *Annual Review of biophysics*, vol. 48, pp. 371–394, 2019.

[90] R. Lazim, D. Suh, and S. Choi, "Advances in molecular dynamics simulations and enhanced sampling methods for the study of protein systems," *International journal of molecular sciences*, vol. 21, no. 17, p. 6339, 2020.

[91] E. Dilshad, H. Ismail, W. Kayani, and B. Mirza, "Optimization of conditions for genetic transformation and in vitro propagation of artemisia carvifolia buch," *Curr Synth Syst Biol*, vol. 4, no. 1, pp. 1–5, 2016.

[92] E. Dilshad, R. M. Cusido, K. R. Estrada, M. Bonfill, and B. Mirza, "Genetic transformation of artemisia carvifolia buch with rol genes enhances artemisinin accumulation," *PLoS One*, vol. 10, no. 10, p. e0140266, 2015.

[93] A. Turaki, B. Ahmad, U. Magaji, U. Abdulrazak, B. Yusuf, and A. Hamza, "Optimised cetyltrimethylammonium bromide (ctab) dna extraction method of plant leaf with high polysaccharide and polyphenolic compounds for downstream reliable molecular analyses," *African Journal of Biotechnology*, vol. 16, no. 24, pp. 1354–1365, 2017.

[94] M. Ali, B. Kim, K. D. Belfield, D. Norman, M. Brennan, and G. S. Ali, "Green synthesis and characterization of silver nanoparticles using artemisia absinthium aqueous extract-a comprehensive study," *Materials Science and Engineering: C*, vol. 58, pp. 359–365, 2016.

[95] I. Bashir, M. A. Khan, E. Dilshad, B. Siyo, E. Hussain, and I. Ali, "Antioxidant and anticancer silver nanoparticles of mentha asiatica aerial part extract: A novel study," *Inorganic and Nano-Metal Chemistry*, pp. 1–7, 2021.

[96] E. Dilshad, M. Bibi, N. A. Sheikh, K. F. Tamrin, Q. Mansoor, Q. Maqbool, and M. Nawaz, "Synthesis of functional silver nanoparticles and microparticles with modifiers and evaluation of their antimicrobial, anticancer, and antioxidant activity," *Journal of functional biomaterials*, vol. 11, no. 4, p. 76, 2020.

[97] K. N. Shashiraj, A. Hugar, R. S. Kumar, M. Rudrappa, M. P. Bhat, A. I. Almansour, K. Perumal, and S. Nayaka, "Exploring the antimicrobial, anticancer, and apoptosis inducing ability of biofabricated silver nanoparticles using lagerstroemia speciosa flower buds against the human osteosarcoma (mg-63) cell line via flow cytometry," *Bioengineering*, vol. 10, no. 7, p. 821, 2023.

[98] P. R. Griffiths, "Fourier transform infrared spectrometry," *Science*, vol. 222, no. 4621, pp. 297–302, 1983.

[99] C. Raj, A. Agarwal, G. Bharathy, B. Narayan, and M. Prasad, "Cyberbullying detection: Hybrid models based on machine learning and natural language processing techniques," *Electronics*, vol. 10, no. 22, p. 2810, 2021.

[100] E. Dilshad, S. Zafar, H. Ismail, M. T. Waheed, R. M. Cusido, J. Palazon, and B. Mirza, "Effect of rol genes on polyphenols biosynthesis in artemisia annua and their effect on antioxidant and cytotoxic potential of the plant," *Applied Biochemistry and Biotechnology*, vol. 179, pp. 1456–1468, 2016.

[101] A. Van Tonder, A. M. Joubert, and A. D. Cromarty, "Limitations of the 3-(4, 5-dimethylthiazol-2-yl)-2, 5-diphenyl-2h-tetrazolium bromide (mtt) assay

when compared to three commonly used cell enumeration assays," *BMC research notes*, vol. 8, pp. 1–10, 2015.

[102] C. A. Heid, J. Stevens, K. J. Livak, and P. M. Williams, "Real time quantitative pcr." *Genome research*, vol. 6, no. 10, pp. 986–994, 1996.

[103] M. W. Pfaffl, "A new mathematical model for relative quantification in real-time rt–pcr," *Nucleic acids research*, vol. 29, no. 9, pp. e45–e45, 2001.

[104] S. Aydin, "A short history, principles, and types of elisa, and our laboratory experience with peptide/protein analyses using elisa," *Peptides*, vol. 72, pp. 4–15, 2015.

[105] A. Atapour, H. Khajehzadeh, M. Shafie, M. Abbasi, S. Mosleh-Shirazi, S. R. Kasaee, and A. M. Amani, "Gold nanoparticle-based aptasensors: A promising perspective for early-stage detection of cancer biomarkers," *Materials Today Communications*, vol. 30, p. 103181, 2022.

[106] K. Shah and P. Maghsoudlou, "Enzyme-linked immunosorbent assay (elisa): the basics," *British journal of hospital medicine*, vol. 77, no. 7, pp. C98–C101, 2016.

[107] B. V. Rao, G. N. Sowjanya, A. Ajitha, and V. U. M. Rao, "A review on stability indicating hplc method development," *World journal of pharmacy and pharmaceutical sciences*, vol. 4, no. 8, pp. 405–423, 2015.

[108] S. Theodoridis, A. Stefanaki, M. Tezcan, C. Aki, S. Kokkini, and K. E. Vlachonasios, "Dna barcoding in native plants of the labiatae (lamiaceae) family from chios island (greece) and the adjacent çeşme-karaburun peninsula (turkey)," *Molecular Ecology Resources*, vol. 12, no. 4, pp. 620–633, 2012.

[109] G. Klebe, "Virtual ligand screening: strategies, perspectives and limitations," *Drug discovery today*, vol. 11, no. 13-14, pp. 580–594, 2006.

[110] A. Kerflani, K. S. Larbi, A. Rabahi, A. Bouchoucha, S. Zaater, and S. Terrachet-Bouaziz, "Novel palladium (ii) complexes with iminocoumarin ligands: Synthesis, characterisation, electrochemical behaviour, dft calculations

and biological activities, admet study and molecular docking," *Inorganica Chimica Acta*, vol. 529, p. 120659, 2022.

[111] G. M. Morris and M. Lim-Wilby, "Molecular docking," *Molecular modeling of proteins*, pp. 365–382, 2008.

[112] P. Bhardwaj, G. Biswas, N. Mahata, S. Ghanta, and B. Bhunia, "Exploration of binding mechanism of triclosan towards cancer markers using molecular docking and molecular dynamics," *Chemosphere*, vol. 293, p. 133550, 2022.

[113] S. Surabhi and B. Singh, "Computer aided drug design: an overview," *Journal of Drug delivery and Therapeutics*, vol. 8, no. 5, pp. 504–509, 2018.

[114] X.-Y. Meng, H.-X. Zhang, M. Mezei, and M. Cui, "Molecular docking: a powerful approach for structure-based drug discovery," *Current computer-aided drug design*, vol. 7, no. 2, pp. 146–157, 2011.

[115] G. Zhang, S. Guo, H. Cui, and J. Qi, "Virtual screening of small molecular inhibitors against dpre1," *Molecules*, vol. 23, no. 3, p. 524, 2018.

[116] W. Chen, L. Chen, Q. Dai *et al.*, "impt-fdnpl: identification of membrane protein types with functional domains and a natural language processing approach," *Computational and Mathematical Methods in Medicine*, vol. 2021, 2021.

[117] Y. Liu, M. Grimm, W.-t. Dai, M.-c. Hou, Z.-X. Xiao, and Y. Cao, "Cb-dock: A web server for cavity detection-guided protein–ligand blind docking," *Acta Pharmacologica Sinica*, vol. 41, no. 1, pp. 138–144, 2020.

[118] Y. Cao and L. Li, "Improved protein–ligand binding affinity prediction by using a curvature-dependent surface-area model," *Bioinformatics*, vol. 30, no. 12, pp. 1674–1680, 2014.

[119] A. C. Wallace, R. A. Laskowski, and J. M. Thornton, "Ligplot: a program to generate schematic diagrams of protein-ligand interactions," *Protein engineering, design and selection*, vol. 8, no. 2, pp. 127–134, 1995.

[120] N. Singh, C. Sudandiradoss, and J. Abraham, "Screening of furanone in cucurbita melo and evaluation of its bioactive potential using in silico studies," *Interdisciplinary Sciences: Computational Life Sciences*, vol. 8, pp. 395–402, 2016.

[121] M. M. Copeland, H. N. Do, L. Votapka, K. Joshi, J. Wang, R. E. Amaro, and Y. Miao, "Gaussian accelerated molecular dynamics in openmm," *The Journal of Physical Chemistry B*, vol. 126, no. 31, pp. 5810–5820, 2022.

[122] D. Van Der Spoel, E. Lindahl, B. Hess, G. Groenhof, A. E. Mark, and H. J. Berendsen, "Gromacs: fast, flexible, and free," *Journal of computational chemistry*, vol. 26, no. 16, pp. 1701–1718, 2005.

[123] A. Boze, "Winscp 2.0 beta," *Information Technology and Libraries*, vol. 21, no. 4, pp. 190–192, 2002.

[124] S. K. Nagaraja, S. K. Niazi, A. Bepari, R. A. Assiri, and S. Nayaka, "Leonotis nepetifolia flower bud extract mediated green synthesis of silver nanoparticles, their characterization, and in vitro evaluation of biological applications," *Materials*, vol. 15, no. 24, p. 8990, 2022.

[125] J. Yu, X. Wu, C. Liu, S. Newmaster, S. Ragupathy, and W. J. Kress, "Progress in the use of dna barcodes in the identification and classification of medicinal plants," *Ecotoxicology and Environmental Safety*, vol. 208, p. 111691, 2021.

[126] M. Li, H. Cao, P. P.-H. BUT, and P.-C. SHAW, "Identification of herbal medicinal materials using dna barcodes," *Journal of Systematics and Evolution*, vol. 49, no. 3, pp. 271–283, 2011.

[127] H. Neuhaus and M. Emes, "Nonphotosynthetic metabolism in plastids," *Annual review of plant biology*, vol. 51, no. 1, pp. 111–140, 2000.

[128] C.-K. Liu, J.-Q. Lei, Q.-P. Jiang, S.-D. Zhou, and X.-J. He, "The complete plastomes of seven peucedanum plants: comparative and phylogenetic analyses for the peucedanum genus," *BMC Plant Biology*, vol. 22, no. 1, p. 101, 2022.

[129] B. Heinze, "A database of pcr primers for the chloroplast genomes of higher plants," *Plant methods*, vol. 3, pp. 1–7, 2007.

[130] I. Ahmed, M. Islam, W. Arshad, A. Mannan, W. Ahmad, and B. Mirza, "High-quality plant dna extraction for pcr: an easy approach," *Journal of applied genetics*, vol. 50, pp. 105–107, 2009.

[131] E. V. Mavrodiev, C. Dervinis, W. M. Whitten, M. A. Gitzendanner, M. Kirst, S. Kim, T. J. Kinser, P. S. Soltis, and D. E. Soltis, "A new, simple, highly scalable, and efficient protocol for genomic dna extraction from diverse plant taxa," *Applications in plant sciences*, vol. 9, no. 3, p. e11413, 2021.

[132] S. Chen, X. Yin, J. Han, W. Sun, H. Yao, J. Song, and X. Li, "Dna barcoding in herbal medicine: retrospective and prospective," *Journal of Pharmaceutical Analysis*, 2023.

[133] A. H. Hassan, "Dna barcode trnh-psba is a promising candidate gene for efficient identification of bitter and sweet almond and related species," *Egyptian Journal of Desert Research*, vol. 73, no. 1, pp. 265–281, 2023.

[134] I. Bruni, F. De Mattia, A. Galimberti, G. Galasso, E. Banfi, M. Casiraghi, and M. Labra, "Identification of poisonous plants by dna barcoding approach," *International Journal of Legal Medicine*, vol. 124, pp. 595–603, 2010.

[135] T. Efferth, "Willmar schwabe award 2006: antiplasmodial and antitumor activity of artemisinin-from bench to bedside," *Planta medica*, vol. 73, no. 04, pp. 299–309, 2007.

[136] C. Larue, H. Castillo-Michel, S. Sobanska, L. Cécillon, S. Bureau, V. Barthès, L. Ouerdane, M. Carrière, and G. Sarret, "Foliar exposure of the crop lactuca sativa to silver nanoparticles: evidence for internalization and changes in ag speciation," *Journal of hazardous materials*, vol. 264, pp. 98–106, 2014.

[137] V. P. Veeraraghavan, N. D. Periadurai, T. Karunakaran, S. Hussain, K. M. Surapaneni, and X. Jiao, "Green synthesis of silver nanoparticles from aqueous extract of scutellaria barbata and coating on the cotton fabric for antimicrobial

applications and wound healing activity in fibroblast cells (l929)," *Saudi journal of biological sciences*, vol. 28, no. 7, pp. 3633–3640, 2021.

[138] M. K. Dewi, A. Y. Chaerunisaa, M. Muhaimin, and I. M. Joni, "Improved activity of herbal medicines through nanotechnology," *Nanomaterials*, vol. 12, no. 22, p. 4073, 2022.

[139] G. Singhal, R. Bhavesh, K. Kasariya, A. R. Sharma, and R. P. Singh, "Biosynthesis of silver nanoparticles using ocimum sanctum (tulsi) leaf extract and screening its antimicrobial activity," *Journal of nanoparticle Research*, vol. 13, pp. 2981–2988, 2011.

[140] E. K. Kambale, C. I. Nkanga, B.-P. I. Mutonkole, A. M. Bapolisi, D. O. Tassa, J.-M. I. Liesse, R. W. Krause, and P. B. Memvanga, "Green synthesis of antimicrobial silver nanoparticles using aqueous leaf extracts from three congolese plant species (brillantaisia patula, crossopteryx febrifuga and senna siamea)," *Heliyon*, vol. 6, no. 8, 2020.

[141] F. Al-Otibi, N. A. Alshammry, R. I. Alharbi, M. N. Bin-Jumah, and M. M. AlSubaie, "Silver nanoparticles of artemisia sieberi extracts: Chemical composition and antimicrobial activities," *Plants*, vol. 12, no. 11, p. 2093, 2023.

[142] M. Sastry, K. Mayya, and K. Bandyopadhyay, "ph dependent changes in the optical properties of carboxylic acid derivatized silver colloidal particles," *Colloids and Surfaces A: Physicochemical and Engineering Aspects*, vol. 127, no. 1-3, pp. 221–228, 1997.

[143] A. Aghajanyan, L. Gabrielyan, R. Schubert, and A. Trchounian, "Silver ion bioreduction in nanoparticles using artemisia annua l. extract: Characterization and application as antibacterial agents," *AMB Express*, vol. 10, pp. 1–9, 2020.

[144] S. I. Rasmagin and L. A. Apresyan, "Analysis of the optical properties of silver nanoparticles," *Optics and Spectroscopy*, vol. 128, pp. 327–330, 2020.

[145] N. Khatoon, R. Ahmad, and M. Sardar, "Robust and fluorescent silver nanoparticles using artemisia annua: Biosynthesis, characterization and

antibacterial activity," *Biochemical engineering journal*, vol. 102, pp. 91–97, 2015.

[146] R. Abbasi, G. Shineh, M. Mobaraki, S. Doughty, and L. Tayebi, "Structural parameters of nanoparticles affecting their toxicity for biomedical applications: a review," *Journal of Nanoparticle Research*, vol. 25, no. 3, p. 43, 2023.

[147] A. Balciunaitiene, P. Viskelis, J. Viskelis, P. Streimikyte, M. Liaudanskas, E. Bartkiene, P. Zavistanaviciute, E. Zokaityte, V. Starkute, M. Ruzauskas *et al.*, "Green synthesis of silver nanoparticles using extract of artemisia absinthium l., humulus lupulus l. and thymus vulgaris l., physico-chemical characterization, antimicrobial and antioxidant activity," *Processes*, vol. 9, no. 8, p. 1304, 2021.

[148] S. Salehi, S. A. S. Shandiz, F. Ghanbar, M. R. Darvish, M. S. Ardestani, A. Mirzaie, and M. Jafari, "Phytosynthesis of silver nanoparticles using artemisia marschalliana sprengel aerial part extract and assessment of their antioxidant, anticancer, and antibacterial properties," *International journal of nanomedicine*, pp. 1835–1846, 2016.

[149] S. H. Salmen, N. M. Alkammash, T. A. Alahmadi, and S. Alharbi, "Characterization and antibacterial activity of silver nanoparticles biosynthesized using leaves extract of artemisia sieberi and calotropis procera," *Rev. Chim*, vol. 72, pp. 76–82, 2021.

[150] F. Al Otibi and H. Rizwana, "Chemical composition, ftir studies, morphological alterations, and antifungal activity of leaf extracts of artemisia sieberi from saudi arabia." vol. 21, pp. 1241–1248, 2019.

[151] E. S. Al-Sheddi, N. Alsohaibani, N. bin Rshoud, M. M. Al-Oqail, S. M. Al-Massarani, N. N. Farshori, T. Malik, A. A. Al-Khedhairy, and M. A. Siddiqui, "Anticancer efficacy of green synthesized silver nanoparticles from artemisia monosperma against human breast cancer cells," *South African Journal of Botany*, vol. 160, pp. 123–131, 2023.

[152] P. Maleki, F. Nemati, A. Gholoobi, A. Hashemzadeh, Z. Sabouri, and M. Darroudi, "Green facile synthesis of silver-doped cerium oxide nanoparticles and

investigation of their cytotoxicity and antibacterial activity," *Inorganic Chemistry Communications*, vol. 131, p. 108762, 2021.

[153] A. Santhosh, S. Sandeep, H. Manukumar, B. Mahesh, and N. K. Swamy, "Green synthesis of silver nanoparticles using cow urine: Antimicrobial and blood biocompatibility studies," *JCIS Open*, vol. 3, p. 100023, 2021.

[154] B. Pannerselvam, D. Thiyagarajan, A. Pazhani, K. P. Thangavelu, H. J. Kim, and S. K. Rangarajulu, "Copperpod plant synthesized agnps enhance cytotoxic and apoptotic effect in cancer cell lines," *Processes*, vol. 9, no. 5, p. 888, 2021.

[155] V. Karunagaran, K. Rajendran, and S. Sen, "Optimization of biosynthesis of silver oxide nanoparticles and its anticancer activity," *International Journal of Nanoscience*, vol. 16, no. 05n06, p. 1750018, 2017.

[156] W. Florkiewicz, D. Malina, K. Pluta, K. Rudnicka, A. Gajewski, E. Olejnik, B. Tyliszczak, and A. Sobczak-Kupiec, "Assessment of cytotoxicity and immune compatibility of phytochemicals-mediated biosynthesised silver nanoparticles using cynara scolymus," *IET nanobiotechnology*, vol. 13, no. 7, pp. 726–735, 2019.

[157] N. Ninan, N. Goswami, and K. Vasilev, "The impact of engineered silver nanomaterials on the immune system," *Nanomaterials*, vol. 10, no. 5, p. 967, 2020.

[158] Z. Meng, Y. Qiu, K. C. Lin, A. Kumar, J. K. Placone, C. Fang, K.-C. Wang, S. Lu, M. Pan, A. W. Hong *et al.*, "Rap2 mediates mechanoresponses of the hippo pathway," *Nature*, vol. 560, no. 7720, pp. 655–660, 2018.

[159] S.-J. Mo, X. Hou, X.-Y. Hao, J.-P. Cai, X. Liu, W. Chen, D. Chen, and X.-Y. Yin, "Eya4 inhibits hepatocellular carcinoma growth and invasion by suppressing nf-κb-dependent rap1 transactivation," *Cancer Communications*, vol. 38, pp. 1–15, 2018.

[160] E. Ahmadian, S. M. Dizaj, E. Rahimpour, A. Hasanzadeh, A. Eftekhari, J. Halajzadeh, H. Ahmadian *et al.*, "Effect of silver nanoparticles in the

induction of apoptosis on human hepatocellular carcinoma (hepg2) cell line," *Materials Science and Engineering: C*, vol. 93, pp. 465–471, 2018.

[161] J. Chai, C. Du, J.-W. Wu, S. Kyin, X. Wang, and Y. Shi, "Structural and biochemical basis of apoptotic activation by smac/diablo," *Nature*, vol. 406, no. 6798, pp. 855–862, 2000.

[162] S. Kasibhatla and B. Tseng, "Why target apoptosis in cancer treatment?" *Molecular cancer therapeutics*, vol. 2, no. 6, pp. 573–580, 2003.

[163] H. Krishnamachari and V. Nithyalakshmi, "Phytochemical analysis and antioxidant potential of cucumis melo seeds," *Int J Life Sci Scienti Res*, vol. 3, pp. 863–867, 2017.

[164] K. S. Bora and A. Sharma, "The genus artemisia: a comprehensive review," *Pharmaceutical biology*, vol. 49, no. 1, pp. 101–109, 2011.

[165] S. Zafar, E. Dilshad, H. Ismail, C. B. Rizvi, and B. Mirza, "Rol genes enhance content of artemisinin and other secondary metabolites in shennong hybrid of artemisia annua," *Chinese Herbal Medicines*, vol. 11, no. 2, pp. 209–215, 2019.

[166] S. Kordali, A. Cakir, A. Mavi, H. Kilic, and A. Yildirim, "Screening of chemical composition and antifungal and antioxidant activities of the essential oils from three turkish artemisia species," *Journal of agricultural and food chemistry*, vol. 53, no. 5, pp. 1408–1416, 2005.

[167] P. Remberg, L. Björk, T. Hedner, and O. Sterner, "Characteristics, clinical effect profile and tolerability of a nasal spray preparation of artemisia abrotanum l. for allergic rhinitis," *Phytomedicine*, vol. 11, no. 1, pp. 36–42, 2004.

[168] H. Tunón, W. Thorsell, A. Mikiver, and I. Malander, "Arthropod repellency, especially tick (ixodes ricinus), exerted by extract from artemisia abrotanum and essential oil from flowers of dianthus caryophyllum," *Fitoterapia*, vol. 77, no. 4, pp. 257–261, 2006.

[169] Y. Mazur and A. Meisels, "The isolation of 5-hydroxy-3, 6, 7, 3', 4'-pentamethoxyflavone from artemisia arborescens," *B Res Coun Israel, 5A*, pp. 67–69, 1955.

[170] J. Han, M. Ye, X. Qiao, M. Xu, B.-r. Wang, and D.-A. Guo, "Characterization of phenolic compounds in the chinese herbal drug artemisia annua by liquid chromatography coupled to electrospray ionization mass spectrometry," *Journal of pharmaceutical and biomedical analysis*, vol. 47, no. 3, pp. 516–525, 2008.

[171] M.-J. Kim, D.-H. Kim, H.-K. Na, T. Y. Oh, C.-Y. Shin, and Y.-J. Surh, "Eupatilin, a pharmacologically active flavone derived from artemisia plants, induces apoptosis in human gastric cancer (ags) cells," *Journal of environmental pathology, toxicology and oncology*, vol. 24, no. 4, 2005.

[172] N. Liu, F. Van der Kooy, and R. Verpoorte, "Artemisia afra: a potential flagship for african medicinal plants?" *South African Journal of Botany*, vol. 75, no. 2, pp. 185–195, 2009.

[173] B. H. Kiani, N. Ullah, I.-u. Haq, and B. Mirza, "Transgenic artemisia dubia wall; showed altered phytochemistry and pharmacology," *Journal of Bioresource Management*, vol. 2, no. 1, p. 2, 2015.

[174] K. Billowria, R. Ali, N. K. Rangra, R. Kumar, and P. A. Chawla, "Bioactive flavonoids: A comprehensive review on pharmacokinetics and analytical aspects," *Critical Reviews in Analytical Chemistry*, pp. 1–15, 2022.

[175] A. Jurinjak Tušek, D. Šamec, and A. Šalić, "Modern techniques for flavonoid extraction-to optimize or not to optimize?" *Applied Sciences*, vol. 12, no. 22, p. 11865, 2022.

[176] X. Zhang, X. Wang, M. Wang, J. Cao, J. Xiao, and Q. Wang, "Effects of different pretreatments on flavonoids and antioxidant activity of dryopteris erythrosora leave," *PloS one*, vol. 14, no. 1, p. e0200174, 2019.

[177] A. P. G. da Silva, P. C. Spricigo, E. Purgatto, S. M. de Alencar, S. F. Sartori, and A. P. Jacomino, "Chemical composition, nutritional value and bioactive

compounds in six uvaia accessions," *Food Chemistry*, vol. 294, pp. 547–556, 2019.

[178] M. Leporini, R. Tundis, V. Sicari, T. M. Pellicanò, A. Dugay, B. Deguin, and M. R. Loizzo, "Impact of extraction processes on phytochemicals content and biological activity of citrus× clementina hort. ex tan. leaves: New opportunity for under-utilized food by-products," *Food research international*, vol. 127, p. 108742, 2020.

[179] L. Mizzi, C. Chatzitzika, R. Gatt, and V. Valdramidis, "Hplc analysis of phenolic compounds and flavonoids with overlapping peaks," *Food technology and biotechnology*, vol. 58, no. 1, pp. 12–19, 2020.

[180] A. Thomas, A. Kanakdhar, A. Shirsat, S. Deshkar, and L. Kothapalli, "A high performance thin layer chromatographic method using a design of experiment approach for estimation of phytochemicals in extracts of moringa oleifera leaves," *Turkish Journal of Pharmaceutical Sciences*, vol. 17, no. 2, p. 148, 2020.

[181] P. E. Duffy and T. K. Mutabingwa, "Artemisinin combination therapies," *The Lancet*, vol. 367, no. 9528, pp. 2037–2039, 2006.

[182] K. S. Bora and A. Sharma, "The genus artemisia: a comprehensive review," *Pharmaceutical biology*, vol. 49, no. 1, pp. 101–109, 2011.

[183] S. Zeb, A. Ali, W. Zaman, S. Zeb, S. Ali, F. Ullah, and A. Shakoor, "Pharmacology, taxonomy and phytochemistry of the genus artemisia specifically from pakistan: a comprehensive review," *Pharmaceutical and Biomedical Research*, vol. 4, no. 4, pp. 1–12, 2019.

[184] G. Lian, F. Li, Y. Yin, L. Chen, and J. Yang, "Herbal extract of artemisia vulgaris (mugwort) induces antitumor effects in hct-15 human colon cancer cells via autophagy induction, cell migration suppression and loss of mitochondrial membrane potential." *Journal of BU ON.: official journal of the Balkan Union of Oncology*, vol. 23, no. 1, pp. 73–78, 2018.

[185] M. Varadi and S. Velankar, "The impact of alphafold protein structure database on the fields of life sciences," *Proteomics*, vol. 23, no. 17, p. 2200128, 2023.

[186] M. Alam, K. Abbas, M. Ali, S. Kamal, and S. Bhagia, "An in-silico study encompassing virtual screening and adme/t properties of phytochemicals present in leaf extract of trapa natans in relevance to sodium taurocholate co-transporting polypeptide involved in hepatitis b," *Journal of Pharmacognosy and Phytochemistry*, vol. 12, no. 1, pp. 641–652, 2023.

[187] Y. Shen and A. Bax, "Synergism between x-ray crystallography and nmr residual dipolar couplings in characterizing protein dynamics," *Structural Dynamics*, vol. 10, no. 4, pp. e40 901–e40 910, 2023.

[188] T. L. Nham Tran, A. F. Miranda, A. Mouradov, and B. Adhikari, "Physicochemical characteristics of protein isolated from thraustochytrid oilcake," *Foods*, vol. 9, no. 6, p. 779, 2020.

[189] Y. Wang, H. Zhang, H. Zhong, and Z. Xue, "Protein domain identification methods and online resources," *Computational and structural biotechnology journal*, vol. 19, pp. 1145–1153, 2021.

[190] "Protein data bank: the single global archive for 3d macromolecular structure data," *Nucleic acids research*, vol. 47, no. D1, pp. D520–D528, 2019.

[191] O. V. Sobolev, P. V. Afonine, N. W. Moriarty, M. L. Hekkelman, R. P. Joosten, A. Perrakis, and P. D. Adams, "A global ramachandran score identifies protein structures with unlikely stereochemistry," *Structure*, vol. 28, no. 11, pp. 1249–1258, 2020.

[192] S. Kim, J. Chen, T. Cheng, A. Gindulyte, J. He, S. He, Q. Li, B. A. Shoemaker, P. A. Thiessen, B. Yu *et al.*, "Pubchem 2023 update," *Nucleic acids research*, vol. 51, no. D1, pp. D1373–D1380, 2023.

[193] Y. Liu, X. Yang, J. Gan, S. Chen, Z.-X. Xiao, and Y. Cao, "Cb-dock2: Improved protein–ligand blind docking by integrating cavity detection, docking

and homologous template fitting," *Nucleic acids research*, vol. 50, no. W1, pp. W159–W164, 2022.

[194] M. Shoaib, A. Singh, S. Gulati, and S. Kukreti, "Mapping genomes by using bioinformatics data and tools," pp. 245–278, 2021.

[195] H. Shim, H. Kim, J. E. Allen, and H. Wulff, "Pose classification using three-dimensional atomic structure-based neural networks applied to ion channel–ligand docking," *Journal of chemical information and modeling*, vol. 62, no. 10, pp. 2301–2315, 2022.

[196] G. M. Ferreira, T. Kronenberger, A. K. Tonduru, R. D. C. Hirata, M. H. Hirata, and A. Poso, "Sars-cov-2 mpro conformational changes induced by covalently bound ligands," *Journal of Biomolecular Structure and Dynamics*, vol. 40, no. 22, pp. 12 347–12 357, 2022.

[197] N. Aho, P. Buslaev, A. Jansen, P. Bauer, G. Groenhof, and B. Hess, "Scalable constant ph molecular dynamics in gromacs," *Journal of Chemical Theory and Computation*, vol. 18, no. 10, pp. 6148–6160, 2022.

[198] R. A. Renganathan and V. R. Rai, "Molecular docking and molecular dynamics evaluation of aspergillus sp., itaconic acid isolated from garcinia indica for anticancer potential," *Biointerface Research in Applied Chemistry*, vol. 13, no. 3, p. 247, 2022.

[199] T. K. Karami, S. Hailu, S. Feng, R. Graham, and H. J. Gukasyan, "Eyes on lipinski's rule of five: A new "rule of thumb" for physicochemical design space of ophthalmic drugs," *Journal of ocular pharmacology and therapeutics*, vol. 38, no. 1, pp. 43–55, 2022.

[200] S. Gupta, F. Afaq, and H. Mukhtar, "Selective growth-inhibitory, cell-cycle deregulatory and apoptotic response of apigenin in normal versus human prostate carcinoma cells," *Biochemical and biophysical research communications*, vol. 287, no. 4, pp. 914–920, 2001.

[201] M. Ghanbari-Movahed, S. Shafiee, J. T. Burcher, R. Lagoa, M. H. Farzaei, and A. Bishayee, "Anticancer potential of apigenin and isovitexin with focus

on oncogenic metabolism in cancer stem cells," *Metabolites*, vol. 13, no. 3, p. 404, 2023.

[202] S. Javid and E. Dilshad, "Artemisia carvifolia buch silver nanoparticles downregulate the rap2a gene in liver cancer," *Scientific Reports*, vol. 13, no. 1, p. 21553, 2023.